An Investigation and Evaluation of Photosynthetic and Respiratory Measurements as Determined from pCO_2 Changes of Incubated Culture and Lake Water Samples

by

John Mark Davies

A Thesis

Submitted to the Faculty of Graduate Studies

in Partial Fulfilment of the Requirements

for the Degree of

MASTER OF SCIENCE

Department of Botany

University of Manitoba

Winnipeg, Manitoba, Canada

THE UNIVERSITY OF MANITOBA

FACULTY OF GRADUATE STUDIES

*****

COPYRIGHT PERMISSION PAGE

AN INVESTIGATION AND EVALUATION OF PHOTOSYNTHETIC AND RESPIRATORY MEASUREMENTS AS DETERMINED FROM pCO_2 CHANGES OF INCUBATED CULTURE AND LAKE WATER SAMPLES

BY

JOHN MARK DAVIES

A Thesis/Practicum submitted to the Faculty of Graduate Studies of The University of Manitoba in partial fulfillment of the requirements of the degree of

MASTER OF SCIENCE

Abstract

A new method for measuring net community primary productivity and dark respiration was examined using steady state cultures and tested under field conditions. The method is based on measuring changes of pCO_2 in the head-space of a sealed incubation bottle by gas chromatography over the course of an incubation. At the end of the incubation the sample is acidified and the total DIC in the bottle is determined. Using the defined relationships between pCO_2, DIC, and alkalinity (Park 1969) DIC is calculated for each sampling time with the assumption that alkalinity change is not significant.

Nitrogen-limited, phosphorous-limited, and nitrogen and phosphorous limited cultures of *Chlamydomonas reinhardtii* were grown in chemostats, and subsamples were incubated using the pCO_2 method. Principle component analysis was used to evaluate expected rates of photosynthesis based on changes in particulate carbon with pCO_2 measured rates. The relationship was not significantly different from 1:1; however the intercept was significantly different from zero. This may be attributable to an unexplained DOC fraction, changes in the physiological status of algae under different nutrient regimes, or possibly bacterial or fungal contamination. Culture studies and field measurements supported the assumption that alkalinity changes did not significantly affect the relationship between algal growth

rates and pCO_2 measured growth.

Field measurements were conducted at the Experimental Lakes Area (ELA), Northwestern Ontario. Photosynthesis-irradiance curves were generated for all but two dates. It was found that the method was sensitive enough to measure productivity at most ELA lakes. It was concluded that the pCO_2 method did not have sufficient sensitivity to measure productivity in Lake 373, an ultra-oligotrophic lake (less than 1 μChl*a*/L). Respiration rates were often positive leading to the postulation that either the incubations were not long enough or possibly there was dark carbon fixation.

Although not rigorously examined, comparisons between ^{14}C and pCO_2 in culture work suggest that ^{14}C underestimates net productivity. Cultures had high respiration rates (50%) so the underestimation by ^{14}C was not unexpected (Jesperson, 1994). Direct comparison of ^{14}C and pCO_2 were not conducted at ELA, however, extrapolated ^{14}C P_m^B rates from the ELA data base suggested that ^{14}C over-estimated, under-estimated and measured NPP.

In Perspective

A science of land health needs, first of all, a base datum of normality, a picture of how healthy land maintains itself as an organism. (Aldo Leopold)

When we think, we do not just think: we think with ideas ... it is the transmission of ideas which enables man to choose between one thing and another.
More education can help us only if it produces more wisdom. (E.F. Schumacher)

Acknowledgments

I am indebted to the scientific community within the Freshwater Institute for facilitating an unique learning environment. It was through my interactions with the spectra of specialists, which has traditionally made the institute an exceptional place, that I was able to appreciate and understand many concepts in freshwater ecology. I cannot name you all!

Dr. R.E.Hecky, my advisor, is an exemplary example of a committed scientist who has an exceptional devotion to his work and the people he works with. I still find his insight and understanding of scientific problems remarkable. He also demonstrated a willingness to make personal sacrifices for what he believes in and for the people he worked with. I feel privileged to have been his student.

Of the many people whose advise I sought, Len Hendzel never tired of my questions especially regarding culturing techniques. He was a valuable source of information with respect to the physiological status of algal cultures.

My committee as a whole provided me with the tools to conduct this research and kept me on track. Ray Hesslein, who, despite an ever increasing hectic schedule, has always made time to discuss the mechanics of gas chromatographs and data that I generated. His insight undoubtedly saved me many hours of frustration. Gordon Robinson had helpful editing suggestions, and Carol Kelly provided a thorough

understanding of the pCO_2 method. Carol Kelly and Akira Furutani also initiated field studies before I began my study. This allowed me to start my research with a better understanding of potential limitations and the inherent problems of the method.

Everett Fee provided me with "psparms", the program used to generate photosynthesis-irradiance curves, and re-wrote the program so that it accepted negative values.

The Department of Fisheries and Oceans Freshwater Institute funded this project through LRTAP V and NSERC grant 311-1719-03 to R.E.Hecky.

Table of Contents

Table of Contents, continued Page

List of Tables

List of Figures

List of Figures, continued

List of Appendices

Background

General

Throughout human existence the importance of aquatic ecosystems has been paramount to the success of our species. They have provided valuable sources of water, food, and recreation. The base of the autochthonous food web within these ecosystems is comprised of plants, and because lakes often have large pelagic zones, planktonic algae can be a vital component of the food chain. In recent years it has become clear that increased human activity on the planet and the direct use of this valuable resource for human initiatives has altered the state of aquatic ecosystems. A non-inclusive list of such activities, affecting algal growth and ecosystems as a whole, includes the addition of nutrients from human waste and factories, acid from industrial and automobile emissions, heavy metals, and physical disturbance to habitats. These effects have greatly altered specific lakes and rivers, which for the human consumer and the organisms naturally inhabiting these environments is most often detrimental. Thus, the study and understanding of aquatic ecosystems has become a vital component of responsible governments in addition to the traditional studies carried out at an academic level within universities. The growing concern over these systems helped prompt the International Biological Programme (IBP) in the 1960's and 1970's and continues today with various

governments and international programs such as International Geosphere Biosphere Programme and the Global Environmental Facility.

In order to gauge how disturbances affect ecosystems it is necessary to have a clear definition of the component parts and their interactions with each other. Species composition has proven to be a useful indicator since distinct conditions will tend to favour specific species. Interactions within the food chain have also proven to be very important. Such interactions include the energetics (ie. the rates of formation and subsequent rates of transfer of biochemical energy) between trophic levels. Primary productivity has received a significant amount of attention and research since primary producers ultimately provide the food and chemical energy for dissimilatory biochemical transformation for all other organisms (Le Cren and Lowe-McConnell, 1980).

Primary productivity is defined as the conversion of radiant or chemical energy into biochemical energy by photosynthetic or chemosynthetic organisms (Steemann-Nielson, 1963; Odum, 1983; Platt *et al.* 1984). However, because of its predominance in the global carbon budget only radiant energy (photosynthesis) is considered in most aquatic studies. In aquatic ecosystems planktonic algae can constitute a significant source of carbon, therefore, understanding the dynamics of algal growth is vital for

understanding the energetics of an ecosystem.

Three inter-related components of planktonic photosynthesis, gross phytoplankton photosynthesis (GPP), net phytoplankton photosynthesis (NPP), and respiration (R), must be considered when interpreting productivity measurements. GPP is the total amount of CO_2 fixed into organic carbon, corresponding to the amount of radiant energy converted into biochemical energy. Respiration represents the breakdown of organic carbon to CO_2, an energy producing process. NPP is the difference between GPP and respiration. These terms are often expressed in the equation: GPP - R = NPP. Ryther (1956) argues that net photosynthesis is of the most ecological significance because it represents a tangible quantity of organic matter that is added to the environment and available to other organisms, while Odum (1983) suggests that the ratio of R to GPP is one of the most important quantities in ecology. Thus, each of these values represent an important variable which is needed in order to accurately understand and interpret the energetics of aquatic ecosystems (Steemann-Nielson and Hansen, 1959).

Productivity refers to the rate of accumulation of biomass over time. It does not necessarily relate to the standing biomass in phytoplankton communities. Agricultural production is, perhaps, the most familiar concept when discussing productivity; however, this is a special case.

Since agriculture is directed towards the goal of producing a crop, the total plant biomass accumulated at harvest, over the time it took to reach maturity from seeding can be used as a "productivity" measure. Any factors which remove biomass during the growing season (example: insects, disease, etc.) would lower such estimates. Because modern farms have effective mechanisms for controlling these variables the losses are often minimized. However, in aquatic ecosystems algae are subject to significant removal rates through heavy grazing pressure and planktonic algae are subject to dispersive water currents and sinking (Ryther, 1956). To maintain their population numbers algae must have rapid growth rates - on the order of hours to days (Goldman *et al.* 1979; Bender *et al.* 1987). Therefore since the growth rate of algae is often unknown, and may be different for each species, the measurement of standing biomass is an insufficient means of determining primary productivity for algal communities.

The domination of radiant energy as the source for biochemical energy prompted researchers to use the rate of photosynthesis as an estimate of productivity. By convention productivity measurements are expressed in terms of carbon incorporation over time because "the uptake of carbon is equivalent, mole for mole, to the production of organic carbon, and hence represents one of the most direct approaches to the measurement of primary production"

(Ryther, 1956). Thus, the stoichiometric relationship of the photosynthetic reaction has been of great importance for the determination of primary productivity:

$$6CO_2 + 6H_2O \rightleftharpoons C_6H_{12}O_6 + 6O_2. \quad (1)$$

Currently, the most common methods for measuring primary productivity are based on the uptake of ^{14}C (in oligotrophic systems) or in more productive systems the stoichiometric evolution of O_2 (Vollenweider, 1974). Although other methods have been used, such as the measurement of changes in DIC (dissolved inorganic carbon) either directly (Schindler and Fee, 1973) or by using the defined relationships between DIC, pCO_2 (partial pressure of CO_2), pH, and alkalinity (Park, 1969) they have not become universally accepted by limnologists due to lack of sensitivity. Researchers have also attempted indirect means for measuring primary productivity such as measuring chlorophyll concentrations and the radio-labelling of chlorophyll (Redalje and Laws, 1981). These chlorophyll-based methods require assumptions to be made about the stoichiometric relationships between carbon incorporated in biomass and chlorophyll mass or synthesis.

At the present time the most common measurements of primary productivity are based upon methods that do not provide researchers with a means of directly measuring net productivity as net carbon fixation or phytoplankton growth (Peterson, 1980). Thus, it is desirable to have a method

which can provide these parameters so that measurements of productivity are easier to interpret and are more meaningful.

Several methods have been developed in order to estimate photosynthesis so that the productivity of planktonic algae can be evaluated. Initial estimates of productivity were made by measuring decreases of *in situ* nutrient concentrations (Atkins, 1922, 1923). The first rigorous method, the oxygen method, was introduced by Gaarder and Gran in 1927. A theoretically more sensitive method, the ^{14}C-uptake method introduced by Steemann-Nielson (1952), has become a standard method for measuring productivity. However, several problems (as discussed below) have been encountered in the interpretation of the results obtained by these methods so researchers have attempted to define new ways of estimating productivity. These include using chlorophyll *a* labelling (Redalje and Laws, 1981; Redalje 1983), applying more rigorous standards to measurements of changes in nutrient concentrations (Keller, 1989), and monitoring decreases of *in situ* O_2 over an extended period of time (eg. a season) (Schulenberger and Reid, 1981). The following reviews of the more important methodologies are presented to appreciate some of the difficulties that have been encountered with productivity methods used to date and provide an understanding for the need for new ways to measure productivity.

Oxygen Methods

The first rigorous measurements of primary productivity involved the detection of oxygen concentrations in sample bottles (illuminated and dark) before and after incubation at a range of *in situ* depths (Gaarder and Gran, 1927). A stoichiometric relationship between the amount of oxygen produced and carbon fixed must be assumed; for example equation 1. This method has proven useful to researchers investigating primary productivity in aquatic environments and is still employed to this date in more productive waters. It allows the determination of net oxygen evolution at various light intensities in addition to net oxygen consumption in dark bottles. Thus, in theory, the gross community productivity, net productivity, and respiration can all be determined. However, high background oxygen concentrations and unknown photosynthetic quotients have limited the usefulness of oxygen methods as a simple and interpretable means of measuring productivity. Background concentrations of oxygen are high in most surface waters and the atmosphere relative to changes that occur during short incubations. The high oxygen concentration can mask small changes from photosynthesis and respiration and restricts this method to more productive areas. Also the accurate determination of a conversion factor to the amount of carbon consumed (photosynthetic quotient, PQ) or evolved (respiratory quotient, RQ) has limited the ability of

researchers to create a universal means of comparing data obtained from samples taken at different times and from different locations.

In an attempt to solve the problem of sensitivity associated with Gaarder and Gran's original technique, several approaches have been devised, most of which utilize stable oxygen isotopes. Early physiological studies were the first to use stable oxygen isotopes. Mehler and Brown (1952) dissolved $^{34}O_2$ ($^{18}O^{16}O$) in water samples containing isolated chloroplasts. They measured changes in partial pressure of the oxygen isotopes with a mass spectrometer. Photosynthetic and respiratory rates were then determined by attributing the increase of $^{32}O_2$ ($^{16}O_2$ originating from $H_2{}^{16}O$) to photosynthesis and the decrease of $^{34}O_2/^{32}O_2$ to respiration. Such methods determined that are well suited for culture studies but are not as practical in the field (Bender *et al.* 1987; Grande *et al.* 1989). Theoretically this method should provide researchers with a way of measuring light-dependent respiration, however, the flow of oxygen between the respiratory and photosynthetic apparatuses is not completely understood.

Several other authors have described methods which trace oxygen during photosynthesis. Grande *et al.* (1982) describes a method that is technically more practical for field analysis. A sample is spiked with water that has been tagged with ^{18}O ($H_2{}^{18}O$). After the incubation period an

estimate of gross primary production can be made from the amount of $^{18}O_2$ at the end of the incubation. Technically, this method has the same problem as the radio-carbon technique in terms of interpretation of results (the net/gross photosynthesis argument described below, under the ^{14}C method). However, Grande *et al.* argue that, because background concentrations of oxygen are on the order of 200 times greater than the particulate organic carbon pool (POC) and the incubation period is less than the turnover rate of the cell, once $^{18}O_2$ is outside of the cell an insignificant amount will be utilized for respiratory activities. Kana (1990) offers another variation of stable-oxygen isotope methods. It is based on the assumption that once $^{36}O_2$ is added to a sample its progressive dilution due to photosynthetically produced $^{32}O_2$ can be used to estimate net photosynthesis while the depletion of $^{36}O_2$ in proportion to the relative concentrations of oxygen isotopes provides a measure of respiration.

One of the distinct advantages of stable-oxygen isotope methods is that they provide a means of measuring light-dependent respiration (photo-respiration), however, several assumptions are made when interpreting oxygen methods. These assumptions have limited the ability of researchers to interpret the results in the most meaningful manner. The methods assume that the cycling of oxygen between the photosynthetic and dark respiratory mechanisms within cells

is minimal and that there is insignificant discrimination of the slightly larger isotopes.

Since it is the incorporation of carbon into cellular material which is used as a standard for growth, all oxygen methods are measuring a by-product and must be related to the amount of carbon incorporated on a mole per mole basis ($\Delta O_2/\Delta C$). This ratio is known as the photosynthetic quotient (PQ). According to the stoichiometric relationship of the simple photosynthetic equation with a simple sugar as the end product ($C_6H_{12}O_6$) the PQ should be equal to one. However, when algal composition is examined the PQ's are generally greater than one indicating the cellular material is, on average, more highly reduced than carbohydrate (for example, fatty acids). A relatively wide range of PQ's, from 0.5 to 3.5, have been reported, (Williams and Robertson, 1991). One of the important determining factors of PQ's has been found to involve nitrogen assimilation (Turpin *et al.* 1988). If nitrate is the nitrogen source it must be reduced from an oxidation state of +5 to -3. This conversion of nitrate to ammonia competes with carbon assimilation for reducing power and results in the production of two molecules of oxygen (Lara *et al.* 1987) thereby increasing the PQ to 1.30 for producing mean cellular C:N:P (assuming Redfield Ratios; Stumm and Morgan, 1981). The production of specific cellular metabolites affects the PQ, for example the production of saturated

fatty acids (which approaches the empirical formula CH_2) will result in high values for PQ, whereas lower PQ values will result from the production of more oxidized metabolites such as glycolate. Both the accuracy and interpretability of these methods is decreased due to the added complication of having to use PQ's to relate values obtained using oxygen techniques to actual biomass produced.

Carbon Methods

Radio-carbon uptake constitutes the most common method of estimating productivity. This method is currently considered the most precise and practical means of measuring low-rates of photosynthesis in the field because individual atoms are labelled and subsequently measured. Despite this, radio-carbon measurements are impossible to interpret in terms of gross and net photosynthesis thus making ecological interpretations difficult. The manner in which cells are labelled is not completely understood (Smith and Platt, 1984) and there is no direct means of estimating respiration. It has been found to be one of the least responsive methods to environmental perturbations when expressed in terms of carbon uptake per unit chlorophyll (Fee *et al.* 1989). Despite these disadvantages, ^{14}C-uptake usage has become a measure of *itself* in aquatic biology and a huge database has accumulated since its inception in 1952. Radio-carbon uptake measurements are combined with other ecological indicators that together are used to describe a

particular ecosystem. Some researchers are content with ^{14}C measurements as a measure in itself of productivity or at least as a relative indicator of it. It is felt that as long as common methodology is employed these estimates are comparable. However, if sensitive methods can be employed that enable researchers to calculate GPP, NPP, and R the interpretation of data will more accurately reflect carbon flows within the ecosystem being studied and provide additional information with which to evaluate the allocation of fixed CO_2 within ecosystems.

Despite the theoretical sensitivity and precision that can be obtained, the problems associated with ^{14}C have limited the utility of the method since there has never been consensus on whether ^{14}C results represent net or gross photosynthesis (Ryther, 1956; Steemann-Nielson and Hansen, 1959; Peterson, 1980; William and Goldman, 1981; Dring and Jewson, 1982; Harris and Piccinin, 1983 and many others). The difficulties of interpreting ^{14}C data ultimately reflect a poor understanding of carbon flow through cells. Knowledge of the fate of recent photosynthate is paramount to interpreting the results of ^{14}C data. If recently fixed ^{14}C is entirely retained within the cell while a separate cellular carbon pool sustains respiration then ^{14}C measurements will reflect gross photosynthesis; however, if ^{14}C is immediately respired in proportion to carbon mass then it will begin to approximate net photosynthesis. It is

also likely that patterns of carbon flow are highly variable over time reflecting the nutrient state and environmental stresses of the cell.

Jesperson (1994) summarizes three carbon-flow models of photosynthesizing algal cells which have been suggested in the literature: 1) algal cells consist of one carbon pool but there is little direct interaction within the cells between the photosynthetic and respiratory pathways; 2) algal cells have one well mixed carbon pool, with a significant amount of interaction between the photosynthetic and respiratory pathways; and 3) algal cells consist of various compartments, such as the two carbon pools (four compartment model) proposed by Smith and Platt (1984).

The first model proposes that short incubations predict gross photosynthesis whereas the second model initially measures gross but moves towards net photosynthesis as the incubation proceeds. The rate that it would move towards net would be dependent on the ratio of respiration to GPP. The two-compartmental model is a hybrid between the first two as it has both an exchanging pool which carries out the photosynthetic and respiratory processes and a synthetic pool which is not involved actively in exchange. The advantage of the Smith and Platt model is that the relative sizes of the two pools (consisting of the actively exchanging pool and the synthetic pool) are not constant, so that, depending on the relative size of each pool it can

account for observations over a wide range. This model is then bounded, at least theoretically, by 100% of the cell carbon being in the synthetic pool (model 1) or 100% of the cell carbon is being in the actively exchanging pool (model 2). Unfortunately the relative distribution of carbon in each pool is often unknown in natural systems so that the utility of this model for ecological interpretations is limited. Because it is a radio-isotope that is added in concentrations above natural levels ^{14}C always generates net uptake values for carbon, even at zero production. Since cellular specific activity is well below the specific radioactivity of added ^{14}C, it is difficult to interpret the movement of ^{14}C in the carbon pools of a cell. All algal species in the community and their carbon pools will have their own turnover time until steady state is achieved.

In an attempt to interpret ^{14}C results researchers have compared other methods of measuring productivity concurrent with photosynthetic rates determined from ^{14}C. In these studies it has been found that, despite the long-standing rule stating ^{14}C measurements lie somewhere between gross and net production, many authors have found that it can both over-estimate and underestimate net production (William and Goldman, 1981; Richardson *et al.* 1984; Hoflslagare *et al.* 1985; Ahlgren, 1988, 1991; Jespersen, 1994; and others). None of these studies has identified a simple quantitative or consistent measure that allows researchers to relate ^{14}C

directly to net or gross productivity. However, understanding the problems helps to identify where the limitations of this method lie.

Of the factors identified by researchers, the relative rate of respiration (R/GPP) has been identified as being vital to the interpretation of ^{14}C measurements (Richardson, 1984; Jesperson, 1994; Williams and Lefevre, 1996). The rate of respiration is part of the problem associated with understanding carbon flow patterns in cells. Jespersen (1994) found that overestimation of net photosynthesis by ^{14}C was dependent upon the ratio of ^{12}C respiration to ^{12}C net photosynthesis. When the ratio of respiration to net photosynthesis was low, ^{14}C provided a good estimate of net photosynthesis. Higher respiration rates caused ^{14}C estimates to be closer to gross photosynthesis. Theoretically, if the relationship between ^{14}C-uptake and net photosynthesis was only dependent upon respiration rates (Richardson *et al.* 1984) and respiration effected the radio-labelled pool immediately, then ^{14}C would be closer to gross photosynthesis when respiration rates are low and closer to net when the respiration rates are high. Jesperson's study was consistent with those of other researchers (Peterson, 1980), despite not following the theoretical relationship between ^{14}C-uptake and respiration. Thus, despite the important role that respiration seems to have on the labelling of cells, the path of carbon flow within cells

remains unknown so that no correction factor can be applied even if respiration rates were measurable.

Several other variables important to the interpretation of ^{14}C estimates of productivity remain unresolved. There are differences in methodologies, for example filter collection of samples after incubation and subsequent clearance by fuming with HCl (Vollenweider, 1974) versus the bubbling technique (Schindler *et al.* 1972; Wessels and Birnbaum, 1979). The latter method provides a means of measuring "excreted" carbon (dissolved organic carbon, DOC) that may or may not be in steady state with the ^{14}C label. Without universal methodology, values from different labs need more careful interpretation when they are compared. Despite the common use of ^{14}C, to date the author is unaware of research that addresses direct measurements of the fractionation of ^{14}C by Rubisco (ribulose-1,5-bisphosphate carboxylase/oxygenase) or any other part of the carbon acquisition and fixing processes. The correction factor (1.06) is assumed to be extrapolated from measurements using ^{13}C assuming a kinetic relationship. Since enzymatic processes do not always maintain kinetic relationships this assumption may not be true.

The major advantages of the ^{14}C method are its ease of use and its sensitivity (at least theoretically), since it traces atoms. As has been demonstrated by numerous comparison studies, the relationship between algal growth in

cultures and that estimated by ^{14}C vary for reasons not completely understood at this time. Variables that have been suggested depend on interpretations of other chemical factors such as carbon availability (Ahlgren, 1991) or physiological variables (Goldman *et al.* 1979) which are difficult, impractical, or impossible to measure in natural populations thus limiting the utility of the ^{14}C method.

Use of Chlorophyll for Estimating Productivity

Since it is the chlorophyll molecule that is ultimately involved in the conversion of inorganic carbon to organic carbon there is a potential relationship, at least theoretically, between the light intensity, the concentration of chlorophyll, and the amount of carbon fixed (Ryther and Yentsch, 1957). Although it has become standard to measure chlorophyll concentrations in aquatic ecosystems, it is not considered valid to directly relate these measurements to photosynthesis. The packaging of chlorophyll and its concentration have been found to change significantly under different light conditions (Welschmeyer and Lorenzen, 1984; Falkowski *et al.* 1985; Goericke and Welschmeyer, 1992). Chlorophyll is not always active and it can be associated with non-living material (Ryther and Yentsch, 1957).

Chlorophyll is often used to interpret production rates obtained from other methods and is expressed in units of mg C per mg Chl *a*. Several models have been proposed for

describing productivity throughout the water column (see Jassby and Platt, 1976; Fee 1990). Bannister (1974) argues that the quantum yield (O_2 evolved or C incorporated per μmol of photons absorbed) of chlorophyll remains relatively constant and is an important variable for the description of productivity terms. Other researchers, however, have suggested that measurements of chlorophyll can be used more directly to measure productivity.

More recently, chlorophyll methods have been used for the direct measurement of productivity (Redalje and Laws, 1981). Such methods use chlorophyll as a "representative" molecule for stoichiometric estimates of cell growth and involve the labelling of chlorophyll *a* (chl *a*) with ^{14}C during an incubation period. Chl *a* is then isolated and the specific activity determined. Growth rates and carbon biomass can be determined assuming that the specific activity of the carbon in chl *a* is the same as that for the carbon in the whole cell. Redalje and Laws (1981) and Welschmeyer and Lorenzen (1984) both found that this occurred when incubation periods lasted 6 to 12 hours. Chlorophyll has been observed to undergo rapid turnover times (Grumbach *et al.* 1978), however, this will not affect growth rate and biomass calculations as long as the specific activity of the chl *a* and cell carbon remain equal (Redalje, 1983). Goericke and Welschmeyer (1993) note that the specific activity of chl a and cell carbon will only remain

equal when the sample being studied is in a state of balanced growth (i.e. chlorophyll and carbon have the same turnover time).

Because growth is unbalanced at any particular time during natural daily cycles, periods of luxury consumption or storage of nutrients, and during photoadaptation, it is recommended that incubation periods should be 24 hours. Having such long incubation periods goes against the general scientific view that incubation periods should be kept as short as possible to avoid other artifacts (for example, bacterial growth) effecting the measurements. Samples are placed in artificial environments (bottles) and are therefore not subjected to the natural forces (currents moving algae in the water column, as well as distributing nutrients to or waste away from cells).

Chlorophyll is being used as a representative molecule for the stoichiometric determination of growth rates, therefore the ratio between carbon and chlorophyll must remain constant. However, this ratio is sensitive to light and nutrient status. Objections have been made within the scientific community with respect to the assumptions of this method. Jespersen *et al.* (1992) argue that in order for the specific activity of chl *a* to equal the specific activity of carbon in the rest of the cell, the cell carbon would have to be one well mixed pool. Again, as with the ^{14}C method, understanding carbon flow through cells seems to be

necessary for the assumptions of this method to be acceptable. Jespersen *et al.* specify that such methods are indicative of chlorophyll synthesis and turnover times, which do not necessarily relate to production of biomass.

Net Chemical Uptake

Another approach which has been used to measure productivity is to examine the net budget of nutrients consumed or O_2 evolved in an isolated system over time. Some of the first productivity measurements were estimated in this manner (eg Atkins, 1922; 1923 - following declines in nitrate and phosphate) as well as more recent attempts to measure the seasonal build-up of oxygen trapped in the subsurface layer of the ocean beneath a temperature density cap (Schulenberger and Reid, 1981). Such approaches to measuring productivity are, in essence, batch cultures that do not allow for flows to enter or leave the system and may be one of the best ways to estimate net production in recent and stable stratified systems. Such field experiments may seem attractive since they are direct measurements and do not involve incubations in small closed vessels and they provide a means of measuring net productivity over longer periods, however, some objections to the significance of such studies have been made (Platt, 1984). Such applications require special hydrographical conditions and assume that gains or losses to sedimentation, diffusion, turbulent mixing, grazing, or currents are either minimal or

can be accurately estimated. Lower sensitivity of such chemical methods has also traditionally favoured the more sensitive indirect method of radio-isotopes for short incubation periods and none of these methods generate community respiration rates.

Introduction to pCO_2 Method

Attempts to find a method for determining productivity that is both sensitive and interpretable have led some researchers to use the relationship between four other variables for measuring changes in DIC: pCO_2, DIC, pH, and carbonate alkalinity. When any combination of two is known then one can solve for H_2CO_3, HCO_3^-, and CO_3^{2-} (Park, 1969). Kelly and others (unpublished) recently postulated a sensitive method that allows for the direct determination of changes in DIC during sample incubation periods using gas chromatography to measure changes in pCO_2. After incubations are completed and pCO_2 is measured, samples are acidified to convert all the DIC to CO_2. Final alkalinity is calculated from the final CO_2 concentration and the final DIC. Initial alkalinity, which is assumed to equal the final alkalinity, is used to calculate the initial DIC from the measured pCO_2.

Theoretically the pCO_2 method for measuring primary productivity has several advantages over methods currently used. First, it offers a means of directly measuring CO_2 uptake. Secondly, no assumptions are made about carbon flow-pattern through cells and the recycling of labelled carbon atoms. Thirdly, the method measures net photosynthesis and dark respiration, which are directly relevant to biomass production, energy storage and carbon utilization in the ecosystem. This method is therefore

relatable to whole system carbon budgets (eg. Ramlal *et al.* 1994). This eliminates questionable assumptions about PQ or RQ's that are currently used to estimate net and gross photosynthesis obtained from oxygen methods. It also avoids using radioactive materials, noxious chemicals, and expensive equipment. The many theoretical advantages of the pCO_2 method warrant an investigation to determine the validity of assumptions about alkalinity change and its applicability to field measurements.

The first part of this study concentrates on testing two components of the pCO_2 method. First, the accuracy of carbon-uptake measurements was examined (net photosynthesis) using low growth axenic steady state cultures. This allowed the comparison of uptake measurements obtained by pCO_2 to be compared to the known carbon budget of the algal culture. Secondly, the major assumption in the calculations of the pCO_2 method, that alkalinity does not significantly change during the incubation period, was examined by using the known nutrient budget of the culture. Simultaneous ^{14}C and pCO_2 measurements were conducted on one set of cultures to compare the pCO_2 method with a standard method used in limnological studies.

One litre chemostats were used to obtain cultures with constant growth rates. Three target nutrient regimes were selected; nitrogen and phosphorous-limited (40μM nitrogen:2μM phosphorous), phosphorous-limited (500μM

nitrogen:2μM phosphorous), and nitrogen-limited (40μM nitrogen:10μM phosphorous). Each culture was grown at three growth rates and each culture was duplicated. Once cultures were in steady state 250mL was withdrawn, filtered and analyzed for inorganic and organic nutrients (NO_3^-, NH_4^+, PO_4^{3-}, DIC, DOC, and POC). The remainder of the culture was allocated to five glass serum-stoppered bottles, three light and two dark bottles (Figure 1). The serum-stoppered bottles were then incubated at the same irradiance as the culture for two hours. Partial pressure of CO_2 (pCO_2) in the head-space was measured every twenty minutes using a gas chromatograph. At the end of the incubation, samples in the serum-stoppered bottles were acidified to convert all inorganic carbon into CO_2, and the pCO_2 was measured to determine final DIC.

The second part of this study involved field experiments conducted at the Experimental Lakes Area (ELA). Experiments were conducted in a flatbed incubator (Fee *et al.* 1989) using the same serum-stoppered bottles described above. Lake samples were allocated to bottles and incubated across a light gradient in order to obtain photosynthesis-irradiance curves. The field study allowed further evaluation of the method by appreciating field logistics, applicability of the pCO_2 method, and sensitivity limitations. Routine productivity measurements (^{14}C) conducted at the research station also provided a means of

comparing the two methods.

Materials and Methods

Culturing

Chlamydomonas reinhardtii, Dangeard (Freshwater Institute culture #3), was used for culturing experiments. C. *reinhardtii* was suitable because it is a thoroughly studied alga with known growth requirements and a well-documented life history. It originated from the University of Texas (culture #89) and was obtained from the Indiana collection (culture #89) in the late 1960's. It has been maintained in axenic culture at the Freshwater Institute since February 1971. Axenic culturing techniques were used to ensure sterility during the experiments.

A variation of WC medium (Guillard and Lorenzen, 1972), WC' (Healey, 1985), was used as a growth medium (Appendix 1). The medium used deviated slightly from the WC' recipe, with the following modifications: K_2HPO_4 was replaced by KH_2PO_4, no organic buffer was added, and the initial pH was set at 7.5. The concentration of phosphorous in P-limited cultures was 2μM while nitrogen was 500μM. For N-limited chemostats the nitrogen concentration was reduced to 40μM and the concentration of phosphorous was 10μM. In cultures where N and P were both meant to be present at limiting concentrations nitrogen was reduced to 40μM and phosphorous to 2μM. Distilled-deionized water, Super-Q, (Millipore Corp. Bedford MA.) was used for making medium.

Medium was mixed in a large container that was acid-

washed and triple-rinsed with distilled water. All glassware and tubing that the media or cultures contacted was acid-washed (either placed in an acid bath of 5% HCl or filled with 5% HCl for a minimum of four hours) and triple rinsed with distilled water. Once made, 4L of media was dispensed into one of several 8L Pyrex boro-silicate aspirator bottle reservoirs with silicon tubing attached (Masterflex®, Cole-Parmer Instrument Company; Size 14) to the basal openings.

The reservoirs, with media, were autoclaved (121°C and 20psi) for sixty minutes. KH_2PO_4 and trace elements were each autoclaved separately in test tubes for twenty minutes and added to the media reservoirs at least a week after autoclaving. It was necessary to autoclave the phosphorous and trace elements separately as a precipitate rapidly formed (within two or three days) if all the constituents were autoclaved together. Analysis of this media and the corresponding precipitate led to the conclusion that both iron and phosphorous were precipitating. It was found that the precipitate contained higher concentrations of both phosphorous (13.6μmol/L) and iron (9.5μmol/L) whereas there was less phosphorous (0.3μmol/L) and iron (6.6μmol/L) than expected in the media. The finding of an iron phosphate precipitate is in agreement with various studies in the literature (for example, Dalton *et al.* 1983).

Chemostats were large glass test tubes (diameter of

65mm with an internal volume of 1500mL). The tops were closed with neoprene rubber stoppers (VWR Scientific, size 13) through which passed five pieces of boro-silicate glass tubing of varying lengths. Two of the glass tubes ended immediately below the rubber stopper and functioned as the media port and the inoculation port. Two longer lengths of glass tubing extended to the bottom of the test tube and functioned as the sampling tube and the aeration tube. The fifth tube was the overflow tube, the bottom of which was placed at the one-litre mark (Figure 2). All open ends of glass tubing were covered with aluminum foil before the chemostats were autoclaved.

All culturing experiments were conducted at 20°C in a climate-controlled culture room. Inoculum was grown in 50mL Erlenmeyer flasks containing autoclaved WC' media (2μM phosphorus and 40μM nitrogen). Approximately 8mL of inoculum was aseptically injected from a sterile syringe into the chemostat through a septum covering the inoculation tube. The media reservoirs were aseptically connected to the chemostats and partially filled with approximately 100mL of media. The inoculated chemostats were left to grow until they showed signs of becoming green before the media pumps (Cole-Parmer Instruments Co. 7425 N. Oak Park Ave., Chicago IL 60648) were turned on. Three pumps were set to deliver approximately 100, 200, and 300 mL per day with corresponding dilution rates of 0.1, 0.2, and 0.3 per day

for each of the three nutrient ratios. The chemostats, once up to volume, were then usually left for several weeks until they approximated steady state growth.

The chemostats were bubbled with air (CO_2 ca. 0.035% v/v) which was treated by bubbling it through two aspirator bottles filled with distilled water, and a third containing 1N H_2SO_4. This helped clean the air and saturate it with water to reduce the amount of evaporation from the chemostat. The sulphuric acid was used to remove ammonia in the air stream. Before entering the chemostat the air was passed through a test tube filled with sterile cotton-wool. Outflow from the chemostats was collected in beakers covered with parafilm, leaving only a small hole for air to escape. Actual dilution rates were determined by measuring the volume of effluent over time.

The light source was a bank of four 40W Vita Light® (Duro-Test®) fluorescent tubes (K=5500) placed on one side of the cultures. Several layers of cheesecloth were placed between the light bulbs and the cultures to attenuate the light. The chemostats received a photon flux of $100\mu mol \cdot m^{-2} \cdot s^{-1}$ as determined with a spherical light sensor (Biospherical Instruments Inc. Model QSL-100, San Diego, CA).

Media reservoirs were aseptically replaced when necessary. It was found that cultures reached steady state after approximately three to four weeks. At this time daily

samples were withdrawn through the sampling tube into a test-tube. The sample volume removed (ca. 20mL) was documented and added to the effluent volume. Optical densities were measured at 750nm using a Bausch & Lomb, Spectronic 100 spectrometer, and pH readings (Corning, pH meter 130) were taken. The samples were counted using a haemocytometer (Neubauer Improved; la fontaine, 0.100mm deep x 0.0025mm^2). Each sample from the chemostats was subsampled eighteen times. Samples were vortexed for one minute before the first subsample was counted and subsequently for ten seconds between counts. Cell counting was conducted as outlined by Guillard (1973). One-way analysis of variance (ANOVA) was conducted between the subsamples taken on each day. When the calculated F-value was less than F-critical over five consecutive days the cultures were considered to be in steady-state. Optical densities were also measured (absorption at 750nm in a spectrophotometer), if there was a trend in any one direction or a large variation (>10%) the cultures were considered to not be in steady state.

Gas Chromatography Analysis - Determination of pCO_2

An M200 gas chromatograph (Microsensor Technology Inc.) was used to determine the pCO_2 in the head-space of the incubation bottles for the first set of incubations and the field study. The gas chromatograph (G.C.) has a built in vacuum pump so that it draws in its own samples. Samples

were collected through a 5cm side opening Luer-lock syringe needle which had the Luer-lock end of the needle removed. The needle was joined to a 0.75m length of PEEK tubing (Scientific Products and Equipment Ltd.) with an internal diameter of 254μm (0.010" - an internal volume of 0.038mL). This was fitted to the G.C.'s external 10μ filtering assembly. In addition a teflon-coated filter (Gelman Sciences, PTFE Membrane Filter, 1μ) was placed within the G.C.'s external filtering assembly in front of the 10μ filter. The G.C. was equipped with a HAYESEP A column and a thermal conductivity detector. Sampling time was set at 10s and the injection time at 200msec. Each time a bottle was sampled two samples were taken (total time for both samples equalled 20s), the first to flush the tube and the second one was used to determine the concentration of CO_2. A Hewlett Packard (HP 3392A) integrator was used to obtain areas under the peaks. The areas were converted to ppm by analyzing two sets of standards obtained from calibrated gas cylinders at the following concentrations: 203ppm, 350ppm, 1010ppm, 3390ppm, 5800ppm, and 19900ppm (Linde, Union Carbide specialty gases).

A Carle® (Li-Cor) G.C. was used to determine the pCO_2 for the second set of incubations. It was equipped with a HAYESEP A column, a methanizer, and a flame ionization detector. Pressure-Lok® syringes (0.5mL, Dynatech Precision Sampling Corp.) were used for injecting both the standards

and samples (injection volume of 0.25mL). A Hewlett Packard integrator (HP 3396 Series II) was used for generating areas. Standard samples were taken from pressurized bottles, however, before injecting the syringes were opened to the atmosphere for approximately two seconds to allow them to equilibrate to atmospheric pressure. When unknown samples were measured, the needle of the syringe penetrated the septum of the injection port before it was unlocked.

For a more complete description of the differences between the two G.C.'s refer to Appendix 2.

Chemostat Incubations

When a culture was considered to be in steady state 250mL was drawn out of the chemostat for chemical analysis. Fifty or 60mL of this sample (depending on the density of the culture) was filtered through muffled (500°C for sixteen hours) 2.4cm GF/C filters (Whatman). Filters were analyzed for chlorophyll, particulate organic carbon, nitrogen, and phosphorous (POC, PON, and POP respectively). The filtrate was analyzed for nitrate (NO_3^-), nitrite (NO_2^-), ammonium (NH_4^+), total dissolved nitrogen (TDN), total dissolved phosphorous (TDP), dissolved inorganic carbon (DIC), dissolved organic carbon (DOC), pH, conductivity, and alkalinity. Chemical analysis was conducted at the Canadian Department of Fisheries and Oceans Freshwater Institute's chemistry lab (Winnipeg, MB) following the analytical procedures as outlined by Stainton *et al.* (1977).

The remaining 750mL of chemostat culture was dispensed, via the sampling line, into 160mL serum-stopper bottles. Approximately 130mL of culture was placed into each of three light bottles and two dark bottles. The volume of each bottle (to one-hundredth of a mL) had previously been determined by weighing each bottle empty with a serum stopper and reweighing each bottle filled with distilled water and the same serum stopper. A balance calibrated to 0.01g (Sartorius) was used. The stoppers initially used were red rubber stoppers from medical vacutainers (Becton Dickinson). However, it was found that water often became trapped on the inside surface increasing the chance that it would be drawn into the MTI G.C., so subsequent experiments used stoppers with a flat teflon-coated inner surface that were clamped onto the bottles with aluminum rings (Wheaton Scientific Co.). Once filled with culture the exact volume of each partition (liquid partition and head-space partition) was determined by weighing the bottles empty and weighing the bottles full. It was assumed that 1g of culture equalled 1mL. The samples, in the bottles, were bubbled with the same air source as used in the chemostats through hypodermic needles (18½ gauge) in order to eliminate CO_2 contamination from the room. Bottles were successively stoppered and sampled immediately for initial pCO_2. Atmospheric pressure was recorded at this time with a mercury barometer (Fisher Scientific 02-383, 1995).

Temperature was assumed to equal 20°C for the first set of incubations, however, there was slight variability within the sample chamber so a thermometer (Fisher Scientific 15-000A, 1995) was used to record the temperature (±0.1°C) for the second set of incubations.

The pCO_2 measurements were taken every twenty minutes (except in one chemostat where the interval was changed to fifteen minutes during the run) for two hours. During an incubation bottles were gently rotated (125rpm) on an orbital shaker (New Brunswick Scientific Co. Inc.) placed so the light bottles received the same photon-flux as the culture had in the chemostat ($100\mu mol \cdot m^{-2} \cdot s^{-1}$). Once the final pCO_2 sample was taken bottles were immediately acidified with 200μL (Gilmont® micro-syringe) of concentrated phosphoric acid to drive the pH below 4.0. After acidification the bottles were shaken vigorously (300rpm) for three minutes and then left undisturbed for ten minutes in order to equilibrate CO_2 between the liquid and gas partitions. Acidified pCO_2 was determined in order to calculate final DIC. Two control bottles, consisting of culture effluent which had been autoclaved in sealed serum-stopper bottles and subsequently equilibrated to culture-room temperature, were incubated with each run in the second set of chemostats.

The DIC for each sampling time was calculated from the final pCO_2 and DIC measurements, assuming that the

bicarbonate alkalinity did not change significantly during the incubation. An outline of the calculations can be found in Appendix 3. These calculations were incorporated into a spreadsheet (Quattro Pro 6.0 for Windows). The first point (DIC at time zero) was never included in the analysis of the data. This practice was adopted because it was found that the CO_2 in the head-space was often not equilibrated with that in the liquid. Regression analysis was performed on the remaining points (DIC at each sampling time). The slope generated from the regression analysis was the uptake/production rate of CO_2 by the algae.

Field Incubations

Collection of samples - Integrated samples were collected from the centre-buoy of the acidified lake 302S and lakes 227, 240, 303, 373, and 979 in the Experimental Lakes Area, Appendix 4 (Cleugh and Hauser, 1971; Brunskill and Schindler, 1971). Integration depths were 3m for lakes 302S, 239, 240, and 373. Shallower integrations of 1m and 1.5m respectively were used for lakes 303 and 979, since the depth at the centre-buoy was less than 3m. Samples were collected in 2.5L Nalgene containers covered with opaque PVC tubing. Two tubes were placed through a rubber stopper that was fitted into the top of the Nalgene container. One tube extended to the bottom of the bottle and the second one terminated on the inside of the stopper serving as an exit for air. Outside the bottle the second tube was suspended

above the first by a metal cage clamped onto the bottle. This allowed the entry rate of water into the Nalgene container to be independent of depth (Fee *et al.* 1989).

Treatment of samples - Samples were analyzed at the ELA immediately after they had been collected. In a darkened room subsamples of lake water, that had been acutely shaken, were siphoned into acid washed (soaked in 5% HCl for at least four hours and then rinsed three times with distilled water) serum-stopper bottles (internal volume ca. 160mL) until the bottles were overflowing. The volume of each bottle (to 0.01mL) had previously been determined. When full, bottles were immediately closed with teflon-covered flat stoppers (Wheaton). A needle was placed through the stopper before it was put on in order to expel excess lake water displaced by the stopper. The stopper was secured by clamping an aluminum ring around the lip of the bottle. The bottles (9 light, 3 dark, and 2 controls filled with dH_2O) were placed in a water bath set to approximately the same temperature as the integrated lake water sample (with a difference less than 2°C) until they reached the same temperature as the water bath. Temperature was monitored with mercury thermometers calibrated to 0.1°C (Fisher Scientific 15-000A, 1995). One thermometer was placed in the water bath and a second was placed in a serum-stoppered bottle containing lake sample. When the samples equilibrated to the temperature of the water bath, the

bottles were injected with ca. 30mL of air obtained from a cylinder of compressed air (Liquid Carbonic). Excess water was displaced through a second needle. The samples were then shaken at 250rpm for three minutes and left in the dark for one hour in the water bath to equilibrate the CO_2 between the gas and liquid partitions.

Incubations were carried out in a similar manner to those currently used for ^{14}C-uptake (Shearer *et al.* 1985). The incubation chamber was made of opaque PVC plastic with a clear plexiglass side at one end. The light source (150 Watt high-pressure sodium bulb) was placed next to the plexiglass end. Water set at approximately *in situ* temperature filled the chamber to a level below the lip of the incubation bottles. Ice was used to maintain a constant temperature (±0.3°C) for the duration of the experiment. Light measurements were made with a spherical quantum sensor(Biospherical Instruments Inc. Model QSL-100, San Diego, CA).

Incubations - the initial gas sample was removed immediately before the bottles were placed in the incubator. Subsequent samples were taken every hour for a total of five hours. The first values were used for generating CO_2 uptake and release rates since, unlike the culturing experiments, the CO_2 in the bottles was given sufficient time to equilibrate. Immediately after the final reading had been taken 200μL of concentrated phosphoric acid was injected

into the bottles. The bottles were shaken for three minutes at 250rpm and placed back in the water bath for approximately one hour to equilibrate. A final pCO_2 measurement was taken. The bottles were then dried externally, weighed, emptied, dried internally and re-weighed. The volume of the sample and the head-space in each bottle was then determined.

Chlorophyll determination for field incubations - 200mL of water from the Nalgene container was filtered through GF/C filters (except in the case of L227 where 100mL was filtered). The filters were immediately frozen until they could be analyzed at the FWI chemistry lab. Chlorophyll a was determined using the HPLC method (Stainton *et al.* 1977).

Calculations - DIC at each sampling time was determined from pCO_2 and the final DIC . See Appendix 3 for an outline of the calculations used. Linear regression analysis was conducted on the calculated DIC values. The slope from this line was then used as the carbon-uptake value for that light value and plotted on a photosynthesis-irradiance (P-I) curve. An example (Lake 240) of this series is presented in Appendix 7. If a particular value fell outside of the 95% confidence interval the point was dropped and the slope was recalculated. Statistical analysis was conducted using Systat 7.1 for Windows.

Photosynthesis-irradiance curves were generated using the "psparms" program of Fee (1990). The program uses the

Simplex algorithm (Caceci and Cacheris, 1984) to find the best fit for the equation:

$$P = \begin{cases} 0 & \text{if } I < I_k/20 \\ BP_m^B & \text{if } I \geq 2/I_k \\ B\alpha I \left[1 - \frac{I'}{4I_k} \right] & \text{otherwise.} \end{cases}$$

This equation is a variation of the hyperbolic tangent equation described by Jassby and Platt (1976). "P" is the photosynthetic rate, "I" is the photon flux of photosynthetically available radiation (PAR), "I_k" = P_m^B/α^B, "I'" = $I - I_k/20$, "B" is the chlorophyll concentration, P_m^B is the maximal rate of photosynthesis standardized to chlorophyll and α^B is the initial slope of the curve - standardized to chlorophyll. An initial estimate of P_m^B is calculated from the maximal photosynthetic rate divided by the chlorophyll a concentration and the initial estimate of α^B is obtained from linear regression of photosynthetic rates for PAR values less than 200μmol$\cdot$m$^{-2}\cdot$s^{-1} divided by the chlorophyll a concentration.

<u>^{14}C-Uptake Measurements During Chemostat Incubations</u>

^{14}C-uptake analysis was conducted in the same bottles as pCO_2 measurements on the second set of chemostat incubations. Two mL of aqueous $NaH^{14}CO_3$ (ca. 40μCu$\cdot$mL^{-1}) was added to the remaining 750mL of culture (once the sample for chemistry was removed). The chemostat was bubbled and

allowed to mix for one minute. Three 5mL samples were taken to determine initial specific activity. These were placed in glass scintillation vials containing 150μl of Carbo-Sorb (2-methoxyethylamine). Nine mL of scintillation fluor (Beckman Ready-Solv MP) was added to the vials.

The culture was then allocated to the five incubation bottles, bubbled, and then stoppered when all of the bottles had been filled, as described above. At the end of the incubation, once the samples had been acidified and the final pCO_2 measurement had been taken, the bottles were opened and 5mL from each bottle (three light and two dark) was added to a glass scintillation vial. One mL of 0.5N HCl was added to the scintillation vials. The samples were bubbled for twenty minutes in order to strip free CO_2 (Schindler *et al.* 1972) using a variation of the vacuum chamber described by Wessels and Birnbaum (1979). Nine mL of scintillation fluor was added to each vial. Specific activity of ^{14}C in the samples was determined using a scintillation counter (Beckman, LS 7500) as outlined by Shearer *et al.* (1985). From the initial activity of ^{14}C the uptake rate of carbon was determined from the following ratio:

$$\frac{\text{C uptake}}{\text{C available}} = \frac{^{14}\text{C uptake x 1.06}}{^{14}\text{C available}}$$

where 1.06 is a correction factor used to account for RUBISCO's (ribulose bisphosphate carboxylase/oxygenase)

preferential uptake of ^{12}C. Available carbon is determined from initial DIC, ^{14}C from the culture sampled at the beginning of the experiment, and ^{14}C-uptake is the measured activity of the sample after incubation. Thus C-uptake (or DIC-uptake) is the only unknown variable and is solved for by using the following equation:

$$\text{DIC-uptake} = \frac{(12.01)(1.06)(\text{initial DIC})(DPM_L - DPM_D)}{(DPM_I)(\text{incubation time})}$$

where: 12.01 = number of g/mole of carbon
DPM_L = ^{14}C-uptake in the light
DPM_D = ^{14}C-uptake in the dark
DPM_I = initial ^{14}C available.

Results

Chemostat Chemistry

Dilution rates for each chemostat did not always meet their target (Table 1). Differences in silicon hoses and variations in the restriction tube from the media reservoirs accounts for some of this variation. Targeted rates were not, however, specifically required for this study. The general dilution range of slow-growth chemostats was met.

Dissolved phosphorous and nitrogen concentrations in the media reservoirs feeding the chemostats, and the chemostat filtrate (filtered through GF/C) are given in Tables 2 and 3. Alkalinity changes calculated from the consumption of PO_4^{3-}, NO_3^-, and NH_4^+ were all positive (Tables 2 and 3) and summarized in Table 5. Measured alkalinity changes determined from chemical titrations (Table 4) were positive and negative in different chemostats indicating both net production and consumption during algal growth. Alkalinity changes in the cultures from all processes except nutrient uptake are included in the last column of Table 5. All of these values are negative indicating that the cultures had a net consumption of alkalinity when nutrient uptake is not considered. The largest changes in alkalinity were found to occur in phosphorous-limited chemostats, although contamination eliminated replicates and weakened this conclusion.

No specific test (such as nitrogen-debt, phosphorous-

debt or alkaline-phosphatase; Healey and Hendzel, 1980) was conducted on the algae to test which nutrient was present in limiting concentration but the target concentrations, coupled with the depletion of the limiting nutrient, and nutrients present in the culture filtrate provided a basis for concluding that the targeted nutrients were in limiting concentrations. The particulate ratios (Table 6) provide further evidence that the targeted limiting nutrients were indeed achieved. Although caution has always been attached to concluding the identity of a limiting nutrient on the basis of particulate nutrient ratios, the large variation in N:P molar ratios between P-limited (from 205:1 to 75:1) and N-limited (from 4:1 to 7:1) chemostats, compared to the Redfield ratio of 16:1, seems to indicate which nutrient was limiting. Healey and Hendzel (1980) also indexed particulate ratios with nutrient deficiency measures (nitrogen-debt, phosphorous-debt, etc.) on their nutrient limiting index. The N/P ratio from P-limited chemostats indicates severe P-limitation and for N-limited chemostats the ratios suggest severe N-limitation. Chemostats designed to be both N and P-limiting are more difficult to interpret. It has been argued that only one nutrient can be limiting at a particular time in the life-cycle of algal cells (excluding light limitation), however, both N and P were added at a limiting ratio to each other (40μM N and 2μM P). The low N:C ratios (30:1 to 60:1) suggest severe N-

limitation, although the N:P ratios do not clearly indicate that either N or P was limiting. Thus, it seems that the chemostats did obtain the respective target nutrient limitation targets (Table 6).

DIC was measured on the chemostat filtrate. Samples are not supposed to be filtered prior to analysis (Stainton *et al.* 1977), although the aerating effect of filtering was similar, in these experiments, to the bubbling of CO_2 that occurred in the chemostats. The values obtained from the chemical analysis, for the most part, were similar to those calculated in the bottles (Figure 3).

DOC measurements were high in the media reservoirs and in the culture filtrate (Table 7). The concentrations were the same order of magnitude as the particulate fraction (Table 6). DOC concentrations in the culture filtrate were different from in the reservoir, some having higher concentrations while others had lower concentrations. DOC decreased in P-limited chemostats, whereas in N-limited and NP-limited chemostats DOC was produced in all but two cases. The original source of DOC in the media reservoir was a combination of EDTA (ca. 700 μg/L carbon), vitamins (ca. 45μ/L carbon), and a large unexplained fraction. Implications of these values will be noted in the discussion.

Incubations of Chemostat Samples in Serum-Stopper Bottles

Figure 4 is a typical figure showing calculated DIC

changes during the incubation (figures for each chemostat are in Appendix 6). DIC decreased linearly with time in the light and increased with time in the dark. Linearity was evaluated by using least-squares regression. The slope of the least-squares regression line represents the uptake-rate of carbon. The rate of uptake remains constant for the duration of the experiment (Appendix 6). In general, the slope values are statistically significant (Table 8) and the r^2 values indicate high correlation (Appendix 5). The first sample (time zero) was not included in the regression analysis since it was taken immediately upon sealing the bottle. The liquid and gas phases in the bottle often were not at equilibrium due to elevated CO_2 concentrations from respiration by the researcher during sample manipulation in a closed room. These variations, therefore, usually saw the first data point having a higher DIC value (Appendix 6). Values of measured net photosynthesis and respiration are provided in Table 9. The R/GPP ratios indicated high respiration rates. Respiration accounted for roughly 50% of GPP in many of the chemostats and ratios greater than 1 were indicative of contaminated cultures.

Expected net photosynthetic rates, determined from the turnover rate of the particulate organic carbon (POC - theoretically equivalent to the effluent rate for suspended carbon) are plotted against measured NPP and GPP as determined from changes in pCO_2 measured in the bottle

incubations (Figures 5 and 6). Expected photosynthetic rates were determined using the equation:

$$\text{Particulate NPP} = \frac{(\text{POC})(\text{dilution rate per day})}{(24)(12.01)}.$$

Contaminated cultures 2P(ii) and 3P(ii) and culture 3N(i), which was considered to be an outlier, were excluded from all analyses. The point for 3N(i) is included in figure 2 for reference (solid circle), however, it is removed from all other figures.

Theoretically the ratio of particulate NPP and measured NPP should equal 1. When plotted, the slope of the relationship should not be significantly different from 1. This analysis was conducted using principle component analysis (for an example see Sokal and Rohlf, 1995) on both sets of culture data. The analysis suggests a linear relationship with a slope of 1.23 (r^2=0.78) for NPP (Figure 5) and 1.59 (r^2=0.72) for GPP (Figure 6). The slope from particulate NPP versus measured NPP is not significantly different from one (using a 95% confidence interval on the slope - see Jolicoeur, 1968) but it is significant for particulate NPP versus measured GPP. Y-intercepts for particulate NPP vs. NPP and GPP were -3.57 and -2.56 respectively. There isn't a specific test for a small sample using PCA to determine if the intercept is significantly different from zero, however, the y-intercept of the upper 95% confidence interval can be used as an

approximation (Kenkel, pers. comm.). Using this criteria, the y-intercept of the upper confidence-limit slope for particulate NPP versus measured NPP (-0.86) is significantly different from zero whereas it is not significantly different for particulate NPP versus measured GPP (1.89).

One of the assumptions in the calculations to determine DIC from pCO_2 is that alkalinity does not change significantly during the course of the incubation. There are two ways in which algal growth can effect alkalinity, either through production or consumption (note consumption equals negative production) of alkalinity. The uptake of negatively charged ions (NO_3^- and PO_4^{3-}) produces alkalinity, whereas the uptake of positively charged ions consumes it. The effect of both production and consumption were considered separately in the calculation of DIC.

Alkalinity changes (Table 5) were added into the equations for ΔDIC determination so that instead of assuming alkalinity remained constant for the duration of the incubation it changed at the same rate as that measured in the culture. Alkalinity change calculated from nutrient uptake (column 2, Table 5) and alkalinity production (column 3) were considered the two extreme cases for alkalinity change. The titratable alkalinity change (column 1) was considered to be the net change in alkalinity (true net change) for these cultures. The PCA slopes for these calculation adjustments are 1.08 (r^2=0.78), 1.37 (r^2=0.76)

and 1.21 (r^2=0.77) respectively and are summarized in Figure 7. Net alkalinity change adjusted NPP is shown with 95% confidence intervals on the slope in Figure 8. Using the same criteria for significance of slope and y-intercept as above, none of the alkalinity adjusted slopes are significantly different from one and they are all significantly different from zero.

Since each of these comparisons has the same Y_2 axis (x-axis, i.e. expected photosynthetic uptake rates based on particulate carbon turnover) it was possible to conduct a significance test of slopes using linear regression (which only accounts for variation of the y-variable) since the error attributed to the x-variable remains the same for each slope. Slope comparison was conducted as outlined by Sokal and Rohlf (1995). None of the slopes (unadjusted NPP and the three alkalinity adjusted values) are significantly different from any other.

There are only six culture comparisons of ^{14}C and pCO_2 since ^{14}C productivity was only conducted on the second set of chemostats (three of which were contaminated). In every case, except one chemostat 1NP(ii), ^{14}C underestimated net productivity as measured by pCO_2. The low number of samples affects the linear relationship, so that each line does not represent statistically correlated points. Figure 9 summarizes the PCA principle axis for ^{14}C, titratable-alkalinity corrected NPP and GPP. The respective slopes for

each measurement are 0.17 (r^2=0.11), 0.53 (r^2=0.40), and 0.62 (r^2=0.10).

Field Incubations using pCO_2

Photosynthesis-irradiance curves for the lakes studied are presented in Figures 10 through 22. Thirteen incubations were conducted, one on L227, L373, and L979; two on L240; and four on both L302S and L303. Curves were generated using the "psparms" program of Fee (1990). The program was adapted to accept negative values (net CO_2 production). Negative values are represented by an "X" whereas positive values are plotted as a "+". Circled points have not been included in the P-I curve calculations since they were evaluated to not follow the same photosynthesis-irradiance trend as the remainder of the points. One of the consequences of using "psparms" is that it displays productivity (carbon uptake) on the positive portion of the y-axis. Therefore field productivity measurements are discussed in terms of carbon uptake being positive and respiration being negative.

Each point on the P-I curve is a slope measurement determined from the change of DIC in the bottle at that given light intensity using least-squares regression analysis. An example of such a series is provided (Lake 240, Appendix 7). For most lakes, CO_2 limitation was not observed, even at the highest light intensities. Lake 302s (September 7, 1995), however, did show signs of carbon

limitation. In this case the linear portion of the slope was used to generate the instantaneous carbon-uptake rate. Significance (P) and r^2 values are summarized in Appendix 8 for every bottle of each lake sampled.

In general the regression analysis' of the slope measurements in the field study are highly correlated and significant ($P < 0.05$). Characteristic photosynthesis-irradiance (P-I) curves are evident for all lakes except 373 (Figure 21) and 240 on August 25 (Figure 11). Lake 240 on this date has several negative rates at low light intensities, but a distinct curve shape is never delineated by the points. Lake 373 is ultra-oligotrophic and had a chlorophyll value less than 1μg/L on August 2. P-I curves for the other days are more distinct and the curve generated by "psparms" fits the data with the same precision as it does with ^{14}C data.

None of the incubations were conducted in true duplicate fashion. However, on August 31 two samples (each collected separately) from Lake 303 (Figures 17 and 18) were incubated together. One sample was pressurized by adding 30mL of air to the head-space (10% by volume). The maximal photosynthetic rates were 2.23 (non-pressurized) and 2.29 (pressurized) mgC/mgChl/h. and both curves had similar initial slopes (α), 7.06 and 7.20 mgC/mgChl/μmol$\cdot$m^2 respectively.

As the photosynthetic rate approaches zero the

precision of the G.C. increases in importance until noise masks any measurable changes in DIC. Thus, points with a slope close to zero tend to have low correlation coefficients. This is observed in DIC uptake-slopes from bottles exposed to the lowest irradiances and some of the dark bottles.

Dark respiration values are highly variable (remember that positive values indicate uptake of carbon by algae). Respiration rates from four sampling dates were negative (CO_2 production). The percent of optimal photosynthesis were: Lake 227 (Figure 10) 8%, L302S-August 19 (Figure 13) 7.3 to 11% (the P-I curve doesn't plateau within the light data so the highest photosynthetic rate was used to determine approximately 11%) and L979 (Figure 22) 7%. One other date, L302S-September 2 (Figure 15), had a higher respiration rate of 27%. On the remainder of the dates sampled, each lake, on average, indicated net uptake of carbon in the dark. Often the dark "respiration" values were greater than the photosynthetic rates of samples incubated at the lowest irradiances.

One of the advantages of working at ELA was that productivity measurements (using ^{14}C) were routinely calculated on all lakes except L303. ^{14}C productivity was measured every two weeks and did not coincide with the dates pCO_2 measurements were taken. Therefore P_B^m was extrapolated (linearly) between dates and compared to pCO_2 measurements.

The relationship between pCO_2 and ^{14}C values (Figure 23) was not significant (r^2=0.53). Principle component analysis was conducted. The slope of the principle axis is 0.66 but the slope within the 95% confidence interval ranges from 0.05 to 2.0. Lake 227 (Figure 10) and both dates from L240 (Figures 11 and 12) have the lowest P_B^m with ratios (pCO_2:^{14}C) close to 1. Lake 302S-September 7 (Figure 16) had the highest P_B^m, 6.9:7.5 (pCO_2:^{14}C), also with a ratio close to 1. pCO_2 productivity measurements from L302S-September 2 (Figure 15) and L979 (Figure 22) were less than ^{14}C (2.1:4.7 and 4.2:6.3 respectively) whereas they were greater than ^{14}C on August 19 (Figure 13) and 24 (Figure 14) in L302S (3.6:1.7 and 4.1:2.1 respectively).

Discussion

Theoretical Considerations

The need for sensitivity in productivity measurements has led researchers to rely on an indirect method of measuring carbon fluxes in algal cells (^{14}C-carbon uptake). Since the ^{14}C method traces atoms, the pCO_2 method cannot be as sensitive. It is, however, sensitive enough to measure changes in DIC in oligotrophic systems at the Experimental Lakes Area.

Attempts at measuring direct changes in DIC have been limited to more productive waters or lakes with low DIC concentrations. They usually involve the uptake of DIC by macrophytes or in oligotrophic lakes to areas where algal biomass is concentrated or the volume to biomass ratio can be controlled such as by sampling epilithic algae (Turner et al. 1991). Sensitivity can be effectively increased by measuring changes in CO_2 since CO_2 is only one component of the DIC. For example, if both DIC and CO_2 can be measured with a precision of ±1% (using an IRGA and G.C, respectively) then in a pure water sample in a closed system at 20°C, pH 7.3, and a DIC concentration of 100μmol/L (CO_2 equals 10μmol/L) the DIC can be measured with a precision of ±1μmol/L while CO_2 can be measured with a precision of ±0.1μmol/L. This increased sensitivity is necessary when the non-pCO_2 DIC makes up a larger fraction of the DIC. Since it is the change in CO_2 that is actually measured, the

pCO_2 method effectively increases the sensitivity possible as opposed to measuring DIC changes directly. However, this difference in sensitivity changes with the ratio of CO_2/DIC (or pH). When the sample pH is high CO_2 is a small proportion of DIC and a significant amplification effect allows for increased precision. As the pH decreases to a point where $CO_2 \approx$ DIC the difference in sensitivities effectively becomes zero (Figure 24). Therefore when the pH is low, there is little to no amplification effect and either measurement can be used assuming similar detection limits and instrument error. At very low pCO_2 the method does not work.

One of the assumptions of the pCO_2 method may therefore seemingly, but incorrectly, be that algal cells can only use CO_2 as a substrate for photosynthesis. Such an assumption would go against the widely accepted view that algae can utilize HCO_3^-. Algal cells are now known to have carbonic anhydrase (CA) extracytoplasmically - within the periplasmic space or on the cell wall (Kimpel *et al.* 1983; Theilmann *et al.* 1990). CA catalyzes the hydration of CO_2: $CO_2 + H_2O \rightleftharpoons H_2CO_3$. Chemically this reaction proceeds at a slow rate (Kern, 1960). H_2CO_3 combines with OH^- to form HCO_3^- and H_2O (instantaneous). Thus, CA enhances a cell's ability to interconvert CO_2 and HCO_3^-. CA is thought to have an active role in the uptake and concentrating of inorganic carbon (C_i) (Raven, 1991). One way that CA is thought to work is

by converting HCO_3^- to CO_2 which can then be actively or passively taken up by the algal cell.

It is also now widely accepted that algae can transport HCO_3^- across their plasmalemma (Williams and Turpin, 1987; Sultemeyer, *et al.* 1989; Thielmann *et al.* 1990). In order to maintain a charge balance, cells either have to use a co-transport mechanism (symport carrier) by incorporation of a positive ion (H^+) or a counter-transport mechanism (antiport carrier) by elimination of a negative ion (OH^-). In either case, the incorporation of an H^+ or the extrusion of an OH^-, the uptake of HCO_3^- resembles the direct uptake of CO_2. H^+ uptake will leave a hydroxyl ion in the bulk media which combines with a CO_2 molecule to form HCO_3^-. The direct elimination of a hydroxyl ion will have the same result. Thus, the uptake of HCO_3^- by an algal cell is equivalent to the uptake of CO_2 or CO_2 derived from the uptake of catalytic dissociation of HCO_3^-.

At low pH's, when pCO_2 is a large proportion of the DIC, the region of linear-uptake occurs over the majority of DIC removal. When the pH is high, the linear relationship is shorter. Figures 25 (a to d) show the decrease in pCO_2 as total DIC removal in distilled water assuming bicarbonate alkalinity remains constant (Park, 1969). It is apparent that at a pH of 8.5 (distilled water - with added OH^-, initially at equilibrium with the atmosphere) there is only about a 3μmol/L region where the uptake remains linear.

However, this is where the pCO_2 method is advantageous since this corresponds to approximately a 12 μmol/L change in DIC.

Two physical variables, temperature and pressure, must be measured and controlled with extreme precision during incubations. Temperature affects the solubility constants and can have an effect on the precision of the results, in addition to changing the slope of the increase/decrease of CO_2 if allowed to drift in one direction. Pressure is important if the gas analyzer is an instrument similar to the MTI (see appendix 4).

Calculated concentrations of CO_2 are dependent upon Henry's solubility constant. Unregulated temperature during an incubation can provide a source of bias and increase the noise. There is approximately a 3% change in Henry's solubility constant for every degree change in temperature (Lange, 1979). Small changes in CO_2 can be amplified or masked if temperature is not tightly controlled since it is the slope between DIC values that is ultimately used. It was found that maintaining a constant temperature (±0.1°C) was the best policy. If temperature is allowed to change then potential lags in chemical equilibrium can occur adding noise to the data.

Despite its ability to measure small samples with extreme accuracy, determining CO_2 concentrations with the MTI does require the knowledge of the atmospheric pressure within the bottle. The initial pressure is easily

determined if bottles are equilibrated at ambient pressure and the temperature that will be used during the incubation. However, subsequent sampling removes a volume of air reducing the pressure. If this volume that is removed is not accurately known, it can effect the DIC uptake rate calculated. For example, at a pH of 6 and a DIC concentration of 50μmol/L the change in slope will be approximately 2μmol/L/h. for every millilitre that has been inaccurately determined (Figure 26). If (as I did) it is assumed that the MTI withdraws 0.25mL of air per sampling time but it actually removes 0.5mL, the difference in slope is a quarter of 2μmol/L/h. or 0.5μmol/L/h.

Much care was taken to maintain constant temperature throughout the incubations. The determination of air withdrawn was also measured several times. Manometric techniques were employed to measure the volume of air sucked per sampling time and changes in pressure were also measured in the head-space of the incubation bottles using a digital pressure meter (Neteck). The manometric technique and digital pressure meter both suggested that 0.25mL was withdrawn each sampling period. Therefore the error due to pressure changes in the samples measured during this study is presumed to be minimal.

pCO_2 Chemostat Incubations

Particulate carbon in the chemostats was used as the test to determine if the pCO_2 method accurately measures

productivity. The turnover rate of particulate carbon theoretically equals the dilution rate in the chemostat. Therefore the pCO_2 incubations must measure this predicted uptake rate with a ratio of 1:1. When this expected rate in chemostats of different growth rates (a combination of particulate carbon and turnover) are compared to pCO_2 the slope of the line should theoretically equal one and the intercept should equal zero. Figure 8 represents the crux of the culture experiments. The slope generated from PCA (eigenvector) for particulate NPP versus titratable alkalinity corrected measured DIC uptake is 1.21. The principle axis accounts for 94% of the variance (eigenvalue) with an r^2 of 0.78. This slope is slightly less than the uncorrected slope of 1.23.

Two extreme values of alkalinity change in the culture were from measurement of nutrient uptake and the difference between nutrient uptake and titratable alkalinity corrected measured DIC uptake. Corrected slopes for these were 1.08 and 1.37 respectively. None of the slopes were found to be significantly different from one, nor were they found to be significantly different from each-other. Uptake of nutrients (NO_3^-, NH_4^+ and PO_4^{3-}) affects alkalinity through the uptake/excretion of H^+ or OH^-. The finding that alkalinity corrected slopes are not significantly different from the uncorrected slope is in agreement with Stumm and Morgan (1981) who state that theoretical changes in

alkalinity from photosynthesis should be less than 15%.

Theoretically the intercept in Figure 8 should equal zero if only algal cells are considered and in practice it should not be significantly different from zero. It is significantly different from zero in these results. The intercept of -3.60 cannot be easily accounted for in the theoretical model where the slope equals one and the intercept equals zero. If there is an unknown relationship between actual growth rate and pCO_2 measurements, such that pCO_2 does not account for a certain proportion of growth (constant), then this relationship must be determined. Such a correction factor would be critical for assessment of productivity in most ecosystems, especially oligotrophic ones. This is unlikely, however, since field respiration rates were often positive (carbon uptake) which, if anything, would suggest a correction factor in the opposite direction.

Individual ratios for pCO_2:expected carbon-uptake vary between chemostats with phosphorous-limited cultures being, on average, close to one (mean = 1.08 ± 0.14), 1P(i)=1.23, 2P(i)=0.96, and 3P(i)=1.10. However, NP and N-limited cultures had ratios between 0.32 and 0.85 (mean = 0.60 ± 0.16). Although P-limited cultures were unsuccessfully replicated the discrepancy between P-limited and the NP and N-limited ratios is significant. The possibilities (not necessarily mutually exclusive) that can explain these

differences are 1) due to natural variability in pCO_2 measurements, 2) differences in the ability of pCO_2 to detect DIC changes in the different cultures (due to changes in alkalinity), 3) differences in the physiological status of C. *reinhardtii* under various nutrient regimes, 4) potential of chemical buffering effects from nutrient media (specifically EDTA), 5) effects of DOC, or 6) bacterial or fungal contamination.

The first possibility seems highly improbable unless there was an air leak into the bottle. Bottles were equilibrated to atmospheric pressure at the beginning of the experiment and samples were continuously being withdrawn creating a head-space with a lower pressure than the atmosphere. Therefore if a leak were to occur it is most probable that air would enter the head space. The discrepancy between P-limited and NP and N-limited is not explained by this. Again field incubation results can be used in support of this as they suggest an insignificant leakage of CO_2 into the head-space. Dark respiration values from the field study are often positive (meaning net uptake of carbon in the dark) and if there was a CO_2 leak respiration values would consistently be negative.

The second possibility was accounted for by adjusting the calculations for changes in alkalinity. Although this decreased the slope slightly, none of the alkalinity corrections were significantly different from each other.

Chlamydomonas reinhardtii is known to change its behaviour with different nutrient regimes. Most of the literature on its life cycle seems to pursue maximum growth rates under high light, high nutrient, and often high CO_2 (5%v/v) concentrations in a batch culture. It is, therefore, difficult to extrapolate much of C. *reinhardtii*'s behaviour to this study which employed low growth steady state cultures.

Nitrogen deficiency has been found to induce gametogenesis and subsequent zygospore production in C. *reinhardtii* and other species (Sager and Granick, 1953; Trainor, 1958). If zoospore formation occurred in chemostats to a great extent then they may not have been in steady state, and were in the process of slowly washing out. This population should have exclusively been composed of cells of the minus strain and C. *reinhardtii* is thought to be heterothallic, therefore no sexual reproduction should have occurred. Low dilution rates could have been responsible for maintaining cell numbers and optical density to meet the criteria used to define steady state while masking wash-out in the population. Under these conditions C. *reinhardtii* would be photosynthesising at a rate lower than that needed to replace static biomass. Such an effect would decrease the measured:expected ratio, increase the slope of the line defining the relationship between measured and expected photosynthetic rates and make the intercept

less negative.

EDTA could have an effect on the calculations since it increases the alkalinity of the culture media. EDTA is a weak acid with four dissociation constants, $pK_1 = 2.0$, $pK_2 = 2.67$, $pK_3 = 6.16$, and $pK_4 = 10.26$ (Schwarzenbach and Ackermann, 1947). The third dissociation constant is the only one of significance for these cultures. Since it acts as a buffer EDTA increases the alkalinity in the cultures and has the effect of increasing the measured pCO_2 NPP:expected NPP ratio. However, one of the problems of evaluating this potential explanation for a negative intercept is that EDTA has been found to degrade in light and during autoclaving. The major products of photodegradation are CO_2, formaldehyde, glycine, and larger derivatives of EDTA (see Lockhart and Blakeley, 1975). Lockhart and Blakeley found that EDTA solutions degraded by more than 50% at pH ca. 7. Since the media reservoirs were not in opaque containers and the residence time was often several weeks the proportion of EDTA remaining is unknown. EDTA breakdown has also been found to occur during autoclaving often causing precipitation (Dalton *et al.* 1983). Therefore the actual amount of EDTA present and its buffering capacity, in addition to potential buffering capacities of derivative molecules is unknown. As with the first option it seems unlikely that EDTA would have a selective buffering effect on only NP and N-limited

chemostats.

DOC measurements in these experiments were un-interpretable by the researcher. Expected values based on nutrient additions in preparation of the media were much lower than the values measured in the chemistry laboratory. It was assumed that algae would produce DOC (Azam *et al.* 1983; Bjornsen, 1988) and this could be accounted for in the carbon budget of the chemostat. The rate of DOC production in the chemostat should be added to the particulate carbon turnover since the pCO_2 method measures DOC produced during the incubation period. However, DOC values obtained in the media reservoirs were more than an order of magnitude higher than that which was added.

If cultures were contaminated (presumably using DOC as a carbon source) then there could be a corresponding increase in bacterial biomass which was unable to photosynthesize but that was respiring. This would explain why the ratios of measured pCO_2 rates:expected carbon-uptake rates, determined from particulate carbon, were less than one in some of the cultures. In P-limited cultures where nitrogen was present in sufficient concentrations C. *reinhardtii* could out-compete bacteria so that it constituted most of the biomass. Bacteria could out-compete C. *reinhardtii* in N-limited cultures so that bacteria constituted a significant portion of the particulate biomass.

The source of this unaccounted DOC is also difficult to explain. High DOC has been found in distilled water, however, when tested the Super-Q water used to make the media had DOC concentrations below its detection limit. Possible contamination by bacteria or fungus in the media reservoir is considered unlikely for two main reasons: 1) during daily algal counts no other species were observed and 2) within the media reservoirs the difference between added N:C and measured N:C (including the dissolved fractions) suggest any potential contaminant did not have nitrogen. However, bacterial or detrital output cannot be ruled out conclusively.

If it is assumed the cultures were not contaminated, then the most probable explanation for a negative intercept centres on culture conditions, either due to the unknown effects of DOC or changes in the physiological status of the C *reinhardtii*. Contamination by bacteria or fungi, however, provides the most comprehensive explanation because it can explain elevated DOC in both the media reservoirs and culture filtrate and the negative intercept in Figures 5 and 8. Biomass from bacteria or fungi would increase the expected NPP determined from the particulate biomass in the culture and decrease the measured NPP from pCO_2 incubations as a result of bacterial or fungal respiration. Although it was felt that cultures were not contaminated (except where noted), contamination provides the only possible explanation

for elevated DOC concentrations in the media reservoirs.

pCO_2 Field Incubations

P-I curves should have two distinct characteristics, a well-defined initial slope (α) and an asymptotic approached maximal rate (P_m). These two parameters are usually standardized in terms of chlorophyll, α^B and P_m^B to allow interspecific and intraspecific comparisons (Talling, 1984). α^B and P_m^B are useful descriptors since they reflect the biochemical and biophysical status of algae (Geider and Osborne, 1992). In addition both of these variables are important for estimating carbon budgets. Most of the P-I curves generated from the field data have both of these characteristics. Lake 240, August 24 is the only lake which shows no initial slope or maximal rate. This curve is difficult to explain since on September 6 when L240 was measured again the chlorophyll concentration was lower but a distinct P-I curve was generated.

Lake 303, August 31 was the only replicated sample. Two separate samples were taken at approximately the same time. Lake 303 is shallow (1.5m) and when the first sample was collected loose particles from the bottom were stirred up. Presumably this is why chlorophyll values are almost double for the non-pressurized sample. Past studies using ^{14}C (Lake 239, 1990) have shown that P_m^B values have a coefficient of variation of 17.6% (Schindler,E. pers.comm.).

The coefficient of variation for α^B (1.96%) and P_m^B (2.65%) are well within this variance.

One of the samples from L303, August 31, was pressurized to determine if air leakage into the bottles was significant. Leakage is most likely to occur during the insertion and removal of the sampling needle. No change in photosynthetic rates was found, although this study wasn't replicated.

Respiration rates of phytoplankton in oligotrophic systems are often unknown. One of the original reasons the pCO_2 method was devised was to elucidate these rates for natural plankton communities. As with rates of light-bottles incubated at low irradiances, the change in DIC was small, often below (absolute change) 4 $mgC/m^3/h.$, making them difficult to detect. Points used to generate these lines are often not highly correlated (r^2). This is expected to happen when DIC removal/consumption rates approach the natural variance in detection of CO_2 by the G.C. One way of increasing the sensitivity of this method would be to increase the length of incubation, especially for dark bottles or samples with low biomass.

Measurement of net carbon consumption in the dark was not expected. Dark uptake rates are often greater (in terms of carbon uptake) than those values calculated for bottles incubated at the lowest light irradiances (i.e. L240, August 25 and September 6; L302S, August 24, and September 2). The

difference could be explained in terms of increased respiration, i.e. photorespiration, in the light bottles (Beardall and Raven, 1990), however, this doesn't explain the unexpected measurement of net carbon consumption in the dark. Either this measurement is real or it is an artifact of sampling (i.e. baseline drift).

Dark fixation is routinely measured by ^{14}C methodology (Vollenweider, 1974) but is most often subtracted from light fixation since it is not considered to be photosynthetic (eg. Shearer et al. 1985). There is evidence for dark fixation of carbon (Kremer, 1979; Church *et al.* 1983), leading to the suggestion that subtraction of dark ^{14}C fixation can lead to the underestimate of primary production (Legendre *et al.* 1983). Since dark fixation accounts for both active (fixation) and inactive (diffusive) uptake Legendre *et al.* suggest stopping dark fixation by using DCMU so that only inactive uptake is corrected for. Conditions prior to incubation are known to affect dark fixation rates, in particular light conditions (Ignatiades *et al.* 1987) and nitrogen concentration (Syrett, 1962). Estimates of dark fixation (^{14}C) have ranged from 1% (Williams *et al.* 1993) to 63% (Herzig, 1993). The time that potential dark fixation could be sustained is largely unknown. It not only depends upon the physical conditions algae were exposed to prior to incubation but also to physiological processes. Legendre *et al.* (1983) and Ignatiades *et al.* (1987) found that the

highest rates of ^{14}C fixation occurred within the first thirty minutes of incubation, at which time they stabilized. Potential for net dark fixation is interesting and should be pursued. Since this study did not address this particular question there is not sufficient evidence to support or reject this possibility.

Baseline drift is the other potential explanation for positive respiration values. Changes in sensitivity of the detector during the course of the incubation or changes in physical parameters (i.e. temperature or head-space pressure) could account for this. Standard gases were used to calibrate the G.C. before and after each incubation. Differences between the calibration curves were always minimal (i.e. the y-intercept changed by less than 1% of measured head-space area and the percent difference in slope was less than 2.5%). Temperature was closely monitored (to 0.1°C) and pressure changes were predetermined. However, no examination of natural variability in pressure changes, as a result of head-space removal, was examined.

Alkalinity changes occurring during the incubation are assumed to be minimal. Crude estimates of alkalinity change were generated from ^{14}C productivity rates and suspended carbon, nitrogen, and phosphorous particulate data. P_m^B and eight hours of light saturating irradiance were used to determine potential alkalinity changes. The outer limits of nutrient generated alkalinity production were considered to

occur when NO_3^- or NH_4^+ were used as the nitrogen source. If the total nutrient requirements were acquired only during the brightest part of the day (eight hours) then for all lakes (L303 not included) sampled the change in alkalinity would have been less than 10% during that eight hours. Nitrogen uptake is known to occur in the dark, although light seems to stimulate higher rates of assimilation (Vincent, 1992). Since algal cells continuously move throughout the water column they will not be exposed to light irradiances at P_m^B and nutrient uptake occurs during the whole day. An upper-limit of 10% for alkalinity change during an incubation, therefore, seems to be an over-estimate.

One of the advantages of conducting an experiment over a light gradient is that each bottle acts as a pseudo-replicate. If we assume that each bottle represents the fixation of carbon at that given light intensity then, although no bottle is exactly replicated, each measurement in combination with all the other measurements (i.e. the rest of the bottles) telling a predictable story (i.e. a P-I curve) strengthens the hypothesis that we are measuring photosynthesis. Despite the unexplained "dark fixation" that was measured on many of the incubation dates, it seems that pCO_2 method was sensitive enough to detect phytoplankton photosynthesis in lakes at E.L.A. with chlorophyll concentrations greater than 1 μgChla/L.

Fee's computer program "psparms" is suitable for the modelling of P-I curves determined from ^{14}C-uptake. It was, however, found that in many situations the curve did not have a good fit for P-I curves determined from changes in pCO_2. The use of ^{14}C as a tracer has several problems,as outlined in the introduction. These centre around the treatment of ^{14}C once it has entered the cell. One parameter that is critical is light, as light intensity changes the treatment of ^{14}C within the cell changes. This leads to a P-I curve with a biased shape since the radio-isotope tracer acts differently as the light intensity changes, and will be different from the curve obtained by net carbon-uptake measurements. Not only does the cellular process involved in the fixation of ^{14}C have to be known at P_m^B but it must also be known at unsaturating light levels. Lack of this knowledge could confound what ^{14}C measures.

^{14}C versus pCO_2 productivity

Culture experiments: This experiment is a preliminary examination of what will inevitably be studied if the pCO_2 method is used to measure productivity in natural ecosystems. The results suggest that ^{14}C consistently underestimates carbon uptake as measured by changes in pCO_2 (Figure 9). This was expected since culture respiration rates were high, and the general opinion in the scientific community is that respiration is one of the key variables determining what ^{14}C measures (Richardson, 1984; Jesperson,

1994). Even if respiration rates cannot be measured, due to low sensitivity in some lakes, other parameters may help to elucidate how ^{14}C behaves in lake samples. More studies should be conducted in this area.

Field experiments: Field measurements using pCO_2 were not initially designed for comparison with ^{14}C. The need to extrapolate between dates to obtain ^{14}C productivity values weakens any possible conclusions. P_m^B was used as a comparison because at light saturating levels pCO_2 uptake values are the most significant. Figure 23 indicates that ^{14}C overestimates NPP, measures NPP, and underestimates NPP. This confirms the culture experiments and postulations in the literature (William and Goldman, 1981; Richardson *et al.* 1984 and others) that ^{14}C-measurements do not necessarily lie between net and gross.

Conclusion

Methodologies that first utilized changes in pCO_2 to estimate productivities were usually restricted to measuring *in situ* changes of pCO_2 in surface waters (Teal and Kanwisher, 1966). However, the sensitivity of the ^{14}C method gained favour in the scientific community and has become the most common method for estimating productivity in oligotrophic ecosystems. Inability to interpret results from ^{14}C has led researchers to question what it is measuring. The pCO_2 method seems to be a promising method of estimating NPP and respiration under certain conditions.

Culture experiments demonstrated that the pCO_2 method accurately determined algal growth rates (Figure 8), and field measurements at ELA proved the method is sensitive enough to measure changes in low-alkalinity oligotrophic lakes. DIC-uptake slopes were linear for both the culture and field study and there was minimal change in alkalinity during the incubations.

Although not emphasized in this study, comparisons with ^{14}C are somewhat confounding. ^{14}C underestimated pCO_2 in the culture experiments and both over and underestimated pCO_2 measurements in the field. Additionally, daily growth cannot be determined from ^{14}C unless respiration rates are estimated. Since no assumptions about carbon flow through cells are needed the pCO_2 method (or other interpretable methods) should replace ^{14}C in studies addressing energy

flow through food webs. This would also eliminate toxic fluors and expensive scintillation counters that are currently required for ^{14}C measurements. Also introduction of ^{14}C above natural levels is undesirable for studies using ^{14}C for radio-active carbon dating. pCO_2 can also be used as a tool to elucidate the meaning of ^{14}C measurements. More rigorous comparison studies should be conducted to determine if ^{14}C measurements can be corrected.

The major assumption of the pCO_2 method is that alkalinity changes during incubations are insignificant. Theoretically photosynthesis should not affect alkalinity by more than 15% (Stumm and Morgan, 1981). Culture work and field data both support this assumption.

Two aspects of the method that proved disappointing in this study were the inability to measure low respiration rates and the intensive labour required to conduct an incubation. If this method was employed on a regular basis it could be automated by using auto-injection loops connected to each bottle or by reducing the number of sampling times. There is an advantage to sampling each bottle several times because the rate can be measured with more confidence (as opposed to end point determinations). By having a time-course experiment the linearity can be checked and would provide additional confidence that the incubation was not limited at some point (CO_2 limited, for example).

One aspect of the pCO_2 method which requires more work is the determination of dark respiration. Each bottle was treated equally with respect to sampling regime for this study. Although this might seem scientific, it is unnatural because light intensities vary for each bottle that is incubated. Obviously algae exposed to saturating light will have a different effect on the chemistry of the water than those in a dark bottle. Respiration rates are usually lower (10% to 20% of P_m^B) so the samples should theoretically be able to incubate for longer periods of time. For some of the lakes this could have meant sampling dark bottles every two hours for ten hours instead of every hour for five hours. Being able to resolve this problem will unlock a critical component of aquatic ecosystems not currently accessible to researchers.

Field studies were conducted in low-alkalinity lakes at ELA which are the most forgiving systems for this method. This method needs to be tested in more alkaline systems, where it would be particularly useful since measuring direct changes in DIC becomes insensitive. In more alkaline lakes sensitivity becomes increasingly critical where a 1 μmol change in pCO_2 could correlate to a 3-4 μmol change in DIC. Therefore to accurately determine productivity the production rate must be higher, incubations longer, or the reproducibility of the G.C. must be increased.

Ultimately, I hope that the pCO_2 method will provide

researchers with a means of determining productivity from oligotrophic to eutrophic ecosystems that can be interpreted in terms of the physiologically interpretable components NPP and R. This will allow researchers to increase their understanding of the biological interactions within lakes and hopefully translate into sound conservation decisions regarding one of humans' greatest resources, water.

Literature Cited

Ahlgren, G. 1991. C14-uptake and growth rate of phytoplankton in continuous cultures. Verh.Internat. Verein.Limnol. **24**:1263-1267.

Ahlgren, G. 1988. Comparison of algal C14-uptake and growth rate in situ and in vitro. Verh.Internat. Verein.Limnol. **23**:1898-1907.

Atkins, W. 1923. The phosphate content of fresh and salt waters in its relationship to the growth of the algal plankton. J.Mar.Biol.Ass. U.K. **13**:119-150.

Atkins, W. 1922. The hydrogen ion concentration of sea water in its biological relations. J.Mar.Biol.Ass. U.K. **12**:717-771.

Azam, F., Fenchel, T., Field, J., Gray, J., Meyer-Reil, L., and Thingstad, P. 1983. The ecological role of water-column microbes in the sea. Mar.Ecol.Prog.Ser. **10**:257-263.

Bannister, T. 1974. Production equations in terms of chlorophyll concentration, quantum yield, and upper limit to production. Limnol.Oceanogr. **19**:1-12.

Beardall, J., and Raven. J. 1990. Pathways and mechanisms of respiration in microalgae. Mar.Microb. Food Webs **4**:7-30.

Bender, M., Grande, K., Johnson, K., Marra, J., Williams, P., Sieburth, J., Pilson, M., Landon, C., Hitchcock, G., Orchardo, J., Hunt, C., Donaghay, P., Hienemann, K. 1987. A comparison of four methods for determining planktonic community production. Limnol.Oceanogr. **32**:1085-1097.

Bjornsen, P. 1988. Phytoplankton exudation of organic matter: Why do healthy cells do it? Limnol.Oceanogr. **31**:151-154.

Brunskill, G., and Schindler, D. 1971. Geography and bathymetry of selected lake basins, Experimental Lakes Area, northwestern Ontario. J.Fish.Res. Board Can. **28**:139-155.

Caceci, M. and Cacheris, W. 1984. Fitting curves to data. Byte **9**:340-362.

Church, M., Cohen, R., Gallegos, C., and Kelly, M. 1983. Evidence for carbon uptake and storage in the dark with subsequent photosynthetic fixation by cultures of mixed Chlorophyceae. Arch.Hydrobiol. **98**:509-522.

Cleugh, T. and Hauser, B. 1971. Results of the initial survey of the Experimental Lakes Area, Northwestern Ontario. J.Fish.Res. Board Can. **28**:129-137.

Dalton, C., Iqbol, K. and Turner, D. 1983. Iron phosphate precipitation in Murashige and Skoog media. Physiol.Plant. **57**:472-476.

Dring, M., and Jewson, D. 1982. What does ^{14}C uptake by phytoplankton really measure: A theoretical modelling approach. Proc.R.Soc.Lond. B **214**:351-368.

Falkowski, P., Dubinsky, Z. and Wyman, K. 1985. Growth-irradiance relationships in phytoplankton. Limnol.Oceanogr. **30**:311-321.

Fee, E. 1990. Computer programs for calculating *in situ* phytoplankton photosynthesis. Can.Tech.Rep.Fish.Aquat.Sci. 1740: v + 27 p.

Fee, E., Hecky, R., Stainton, M., Sandberg, P., Hendzel., L., Guildford, S., Kling, H., McCullough, G., Anema, C., and Salki, A. 1989. Lake variability and climate research in Northwestern Ontario: Study Design and 1985-1986 data from the Red Lake District. Can.Tech.Rep.Fish.Aquat.Sci. 1662: 39p.

Gaarder, T., and Gran, H. 1927. Investigations of the production of plankton in the Oslo Fjord. Rapp. et Proc.-Verb Cons.Int.Explor.Mer. **42**:1-48.

Geider, R., and Osborne, B. 1992. *Algal Photosynthesis.* Chapmann and Hall, New York. 256p.

Goericke, R., and Welschmeyer, N. 1993. The chlorophyll-labelling method: Measuring specific rates of chlorophyll *a* synthesis in cultures and in the open ocean. Limnol.Oceanogr. **38**:80-95.

Goericke, R., and Welschmeyer, N. 1992. Pigment turnover in the marine diatom *Thalassiosira weissflogii*. I The $^{14}CO_2$-labelling kinetics of chlorophyll *a*. J.Phycol. **28**:498-507.

Goldman, J., McCarthy, J. and Peavy, D. 1979. Growth rate influence on chemical composition of phytoplankton in oceanic waters. Nature **279**:210-215.

Grande, K., Marra, J., Langdon, C., Hienemann, K., and Bender, M. 1989. Rates of respiration in the light measured in marine phytoplankton using an ^{18}O isotope-labelling technique. J.Exp.Mar.Biol.Ecol. **129**:95-120

Grande, K., Kroopnick, P., Burns, D., and Bender, M. 1982. ^{18}O as a tracer for measuring gross primary productivities in bottle experiments. Eos. **63**:107.

Grumbach, K., Lichtenthaler, H. and Erismann, K. 1978. Incorporation of $^{14}CO_2$ in photosynthetic pigments of *Chlorella pyrenoidosa*. Planta **140**:37-43.

Guillard, R. 1973. In: *Handbook of Phycological Methods: Culture Methods and Growth Measurements*. Ed. Stein, J.R. Cambridge University Press. pp289-311.

Guillard, R., and Lorenzen, C. 1972. Yellow-green algae with chlorophyllide. J.Phycol. **8**:10-14.

Harned, H., and Davis, R. 1943. The ionization constant of carbonic acid in water and the solubility of carbon dioxide in water and aqueous salt solutions from 0 to 50°. Amer.Chem.Soc.J. **65**:2030-2037.

Harned, H., and Scholes, S. 1941. The ionization constant of HCO_3^- from 0 to 50°. Amer.Chem.Soc.J. **63**:1706-1709.

Harris, G., and Piccinin, B. 1983. Phosphorus limitation and carbon metabolism in a unicellular alga: interaction between growth rate and the measurement of net and gross photosynthesis. J.Phycol. **19**:185-192.

Healey, F. 1985. Interacting effects of light and nutrient limitation on the growth rate of *Synechococcus linearis*. J.Phycol. **21**:134-146.

Healey, F., and Hendzel, L. 1980. Physiological indicators of nutrient deficiency in lake phytoplankton. Can.J.Fish.Res. Board Can. **37**:442-453.

Herzig, R. 1993. Dark carbon fixation in different algae species. J.Phycol. **29** suppl:12.

Hoflslagare, O. Samuelsson, G., Hallgren, JE. Pejryd, C. and Sjoberg, S. 1985. A comparison between three methods of measuring photosynthetic uptake of inorganic carbon in algae. Photosynthet. **19**:578-585.

Ignatiades, L., Karydis, M., and Pagou, K. 1987. Patterns of dark $^{14}CO_2$ incorporation by natural marine phytoplankton communities. Microb.Ecol. **13**:249-259.

Jassby, A., and Platt, T. 1976. Mathematical formulation of the relationship between photosynthesis and light for phytoplankton. Limnol.Oceanogr. **21**:540-547.

Jespersen, AM. 1994. Comparison of $^{14}CO_2$ and $^{12}CO_2$ uptake and release rates in laboratory cultures of phytoplankton. Oikos **69**:460-468.

Jespersen, AM., Nielsen, J., Riemann, B., and Sondergaard, M. 1992. Carbon-specific phytoplankton growth rates: a comparison of methods. J.Plank.Res. **14**:637-648.

Jolicoeur, P. 1968. Interval estimation of the slope of the major axis of a bivariate normal distribution in the case of a small sample. Biometrics. **24**:679-682.

Kana, T. 1990. Light-dependent oxygen cycling measured by an oxygen-18 isotope dilution technique. Mar.Ecol.Prog.Ser. **64**:293-300.

Keller, A. 1989. Modelling the effects of temperature, light, and nutrients on primary productivity: An empirical and mechanistic approach compared. Limnol.Oceanogr. **34**:82-95.

Kelly, C., Furutani, A., Rudd, J., and Hesslein, R. 1991. Measurement of net photosynthesis and respiration using changes in dissolved CO_2. Unpublished.

Kern, D. 1960. The hydration of carbon dioxide. J.Chem.Educ. **37**:14-37.

Kimpel, D., Togasaki, R. and Miyachi, S. 1983. Carbonic anhydrase in *Chlamydomonas reinhardtii* I. Localization. Plant Cell Physiol. **24**:255-259.

Kremer, B. 1979. Light independent carbon fixation by marine macroalgae. J.Phycol. **15**:244-247.

Lange, N. 1979. *Lange's Handbook of Chemistry*. 12th Edition. J. Dean, Ed., McGraw-Hill Book Co.

Lara, C., Romero, J. and Guerrero, M. 1987. Regulated nitrate transport in cyanobacterium *Anacystis nidulans*. J.Bacteriol. **169**:4376-4378.

Le Cren, E., and Lowe-McConnell, R. (ed.) 1980. *The functioning of freshwater ecosystems*. International Biological Programme **22**. Cambridge University Press. Cambridge.

Legendre, L., Demers, S., Yentsch, C. and Yentsch, C. 1983 The ^{14}C method: Patterns of dark CO_2 fixation and DCMU correction to replace the dark bottle. Limnol.Oceanogr. **28**996-1003.

Lockhart, H.Jr., and Blakeley, R. 1975. Aerobic photodegradation of Fe(III)-(Ethylenedinitrilo) tetraacetate (Ferric EDTA). Environ.Scien.Technol. **9**:1035-1038.

Mehler, A., and Brown, A. 1952. Studies on reactions of illuminated chloroplasts. III. Simultaneous photoproduction and consumption of oxygen studied with oxygen isotopes. Arch.Biochem.Biophys. **38**:365-370.

Odum, E. 1983. *Fundamentals of Ecology*. Second Edition. Plenum.

Park, P. 1969. Oceanic CO_2 system: an evaluation of ten methods of investigation. Limnol.Oceanogr. **14**:179-186.

Peterson, B. 1980. Aquatic primary productivity and the ^{14}C-CO_2 method: A history of the productivity problem. Ann.Rev.Ecol.Syst. **11**:359-385.

Platt, T., 1984. Primary productivity in the central North Pacific: comparison of oxygen and carbon fluxes. Deep-Sea Res. **31**:1311-1319.

Platt, T., Lewis, M., and Geider, R. 1984. Thermodynamics of the pelagic ecosystem: elementary closure conditions for biological production in the open ocean. In: *Flows of energy and materials in marine ecosystems*. Plenum. p.49-84.

Ramlal, P., Hesslein, R., Hecky, R., Fee, E., Rudd, J., and Guildford, S. 1994. The organic carbon budget of a shallow Arctic tundra lake on the Tuktoyaktuk Peninsula, N.W.T. Canada. Biogeochem. **24**:145-172.

Raven, J. 1991. Physiology of inorganic C acquisition and implications for resource use efficiency by marine phytoplankton: relation to increased CO_2 and temperature. Plant Cell Environm. **14**:779-794.

Redalje, D. 1983. Phytoplankton carbon biomass and specific growth rates determined with the labelled chlorophyll *a* technique. Mar.Ecol.Prog.Ser. **11**:217-225.

Redalje, D., and Laws, E. 1981. A new method for estimating phytoplankton growth rates and carbon biomass. Mar.Biol. **62**:73-79.

Richardson, K., Samuelsson, G., and Hallgren, JE. 1984. The relationship between photosynthesis measured by ^{14}C incorporation and by uptake of inorganic carbon in unicellular algae. J. Exp. Mar. Biol. Ecol. **81**:241-250.

Ryther, J., and Yentsch, C. 1957. The estimation of phytoplankton production in the ocean from chlorophyll and light data. Limnol.Oceanogr. **2**:281-286.

Ryther, J. 1956. The measurement of primary production. Limnol.Oceanogr. **1**:72-84.

Sager, R., and Granick S. 1953. Nutritional studies with *Chlamydomonas reinhardti*. Ann. N.Y. Acad.Sci. **56**:831-838.

Schindler, D., and Fee, E. 1973. Diurnal variation of dissolved inorganic carbon and its use in estimating primary production and CO_2 invasion in Lake 227. J.Fish.Res. Board Can. **30**:1501-1510.

Schindler, D., Schmidt, R., and Reid, R. 1972. Acidification and bubbling as an alternative to filtration in determining phytoplankton production by the 14C method. J.Fish.Res. Board Can. **29**:1627-1631.

Schwarzenbach, G., and Ackermann, H. 1947. Komplexone V. Die Athylendiamin-tetraessigsaure. Helv.Chim.Act. **30**:1798-1804.

Shearer, J., DeBruyn, E., DeClercq, D., Schindler, D., and Fee, E. 1985. Manual of phytoplankton primary production methodology. Can.Tech.Rep.Fish.Aquat.Sci. 1341: iv + 58p.

Shulenberger, E., and Reid, J. 1981. The pacific shallow oxygen maximum, deep chlorophyll maximum and primary productivity, reconsidered. Deep-Sea Res. **28**:901-919.

Smith, R., and Platt, T. 1984. Carbon exchange and ^{14}C tracer methods in nitrogen-limited *Thalassiosira pseudonana*. Mar.Ecol.Prog.Ser. **16**:75-87.

Sokal, R., and Rohlf, F. 1995. *Biometry*. 3rd ed. W.H.Freeman and Company. 887p.

Stainton, M., Capel, M., and Armstrong, F. 1977. The chemical analysis of fresh water, 2nd ed. Can.Fish.Mar.Serv.Spec.Publ. 25:180.

Steemann-Nielson, E. 1963. Productivity: definition and measurement. In: M.N. Hill [ed.], *The Sea*, v.2. Wiley. p.129-164.

Steemann-Nielson, E., and Hansen, V.Kr. 1959. Measurements with the carbon-14 technique of the respiration rates in natural populations of phytoplankton. Deep-Sea Res. **5**:222-233.

Steemann-Nielson, E. 1952. The use of radio-active carbon (C^{14}) for measuring organic production in the sea. J.Cons.Int.Expl.Mer. **18**:117-140.

Stumm, W., and Morgan, J. 1981. *Aquatic Chemistry*. Second Edition. John Wiley & Sons. 780p.

Sultemeyer, D., Miller, A., Espie, G., Fock, H., and Canvin, D. 1989. Active transport by the green alga *Chlamydomonas reinhardtii*. Plant Physiol. **89**:1213-1219.

Syrett, P. 1988. Uptake and utilization of nitrogen compounds. *Biochemistry of the algae and cyanobacteria*. Proc.Phytochemic.Soc.Europ. 28. Oxford Scientific Publications. 374p

Talling, J. 1984. Past and contemporary trends and attitudes in work on primary productivity. J.Plank.Res. **6**:203-217.

Teal, J., and Kanwisher, J. The use of pCO_2 for the calculation of biological production, with examples from waters off Massachusetts. J.Mar.Res. **24**:4-14.

Thielmann, J., Tolbert, N., Goyal, A., and Senger, H. 1990. Two systems for concentrating CO_2 and HCO_3^- during photosynthesis by *Scenedesmus*. Plant Physiol. **92**:622-629.

Trainor, F. 1958. Control of sexuality in *Chlamydomonas clamydogama*. Am.J.Bot. **45**:621-626.

Turner, M., Howell, E., Summerby, M., Hesslein, R., Findlay, D., and Jackson, M. 1991. Changes in epilithon and periphyton associated with experimental acidification of a lake to pH 5. Limnol.Oceanogr. **36**:1390-1405.

Turpin, D., Elrifi, I., Birch, D., Weger, H., and Holmes, J. 1988. Interactions between photosynthesis, respiration and nitrogen assimilation in microalgae. Can.J.Bot. **66**:2083-2097.

Vincent, W. 1992. The daily pattern of nitrogen uptake by phytoplankton in dynamic mixed layer environments. Hydrobiol. **238**:37-52.

Vollenweider, R. (ed.) 1974. *A Manual on Methods for Measuring Primary Production in Aquatic Environments.* International Biological Programme (IBP) Handbook No 12. 2nd Edition. Blackwell Scientific Publications, Oxford Great Britain. 225p.

Welschmeyer, N., and Lorenzen, C. 1984. Carbon-14 labelling of phytoplankton carbon and chlorophyll *a* carbon: Determination of specific growth rates. Limnol.Oceanogr. **29**:135-145.

Wessels, C., and Birnbaum, E. 1979. An improved apparatus for use with the ^{14}C acid-bubbling method of measuring primary production. Limonl.Oceanogr. **25**:360-364.

William. K., Irwin, B., and Dickie, P. 1993. Dark fixation of ^{14}C: Variations related to biomass and productivity of phytoplankton and bacteria. Limnol.Oceanogr. **38**:483-494.

William. K., and Goldman, J. 1981. Problems in estimating growth rates of marine phytoplankton from short-term ^{14}C assays. Microb.Ecol. **7**:113-121.

Williams, P., and Lefevre, D. 1996. Algal ^{14}C and total carbon metabolism. 1. Models to account for the physiological processes of respiration and recycling. J.Plank.Res. **18**:1941-1959.

Williams, P., and Robertson, J. 1991. Overall planktonic oxygen and carbon dioxide metabolism: The problem of reconciling observations and calculations photosynthetic quotients. J.Plank.Res. **13**:153-169. Suppl.

Williams, T., and Turpin, D. 1987. The role of external carbonic anhydrase in inorganic carbon acquisition by *Chlamydomonas reinhardtii* at alkaline pH. Plant Physiol. **83**:92-96.

Personal Communications

Kenkel, N. Professor, Department of Botany, University Manitoba, Winnipeg, Manitoba.

Schindler, E. Primary productivity curator for the Experimental Lakes Area, Department of Fisheries and Oceans, Freshwater Institute, Winnipeg, Manitoba.

Table 1: Chemostat dilution rates, chlorophyll concentrations and particulate (POC) production rates. Chemostat identifiers 1, 2, and 3 refer to dilution rates (approximately 0.1, 0.2, 0.3 per day; i and ii are duplicate cultures), NP = nitrogen and phosphorous limited, P = phosphorous limited, and N = nitrogen limited.

Chemostat	Dilution Rate (% dilution/24 hours)		Chlorophyll (µg chla/L)	ΔPOC (µmol/L/h.)
1NP(i)	7.9		4.8	2.4
1NP(ii)	14.2		5.7	5.3
2NP(i)	20.0		7.0	8.0
2NP(ii)	18.5		11.9	6.9
3NP(i)	27.5		20.7	10.5
3NP(ii)	31.8		10.9	7.3
1P(i)	9.1		93.6	9.3
1P(ii)	NA	C.C.*		
2P(i)	19.1		65.2	14.5
2P(ii)	22.7	C.C.*	1.6	12.8
3P(i)	30.0		61.4	13.7
3P(ii)	30.1	C.C.*	0.2	5.2
1N(i)	8.4		13.0	3.4
1N(ii)	9.9		3.0	4.0
2N(i)	17.4		9.4	5.4
2N(ii)	24.3		16.2	10.9
3N(i)	26.3		4.0	10.6
3N(ii)	29.3		5.7	6.2

* C.C.: contaminated culture

Table 2: Total dissolved phosphorous (TDP) in chemostat media reservoirs and culture filtrate (filtered through GF/C) at the time of incubation (standard deviation ± 13%). Alkalinity consumed assumes that TDP = PO_4^{3-}. Chemostat identifiers are outlined in Table 1.

Chemostat	TDP Media Reservoir (μg/L)	TDP Culture Filtrate (μg/L)	Calculated Alkalinity Produced (μEq/L/h.)
1NP(i)	67	4	0.020
1NP(ii)	58	10	0.027
2NP(i)	67	5	0.050
2NP(ii)	71	7	0.047
3NP(i)	74	6	0.075
3NP(ii)	68	10	0.074
1P(i)	52	13	0.014
2P(i)	65	15	0.039
2P(ii)	73	6	0.066
3P(i)	66	12	0.066
3P(ii)	68	10	0.070
1N(i)	455	102	0.119
1N(ii)	363	71	0.117
2N(i)	410	79	0.232
2N(ii)	361	41	0.313
3N(i)	444	95	0.370
3N(ii)	257	165	0.109

Table 3: Nitrate-N (NO_3^-) and ammonium-N (NH_4^+) in chemostat media reservoirs and culture filtrate at the time of incubation (standard deviation ± 2.0%). Alkalinity consumed determined from changes in NO_3^- and NH_4^+ and the dilution rate. Chemostat identifiers are outlined in Table 1.

Chemostat	Reservoir (μg/L)		Culture Filtrate (μg/L)		Calculated Alkalinity Produced (μEq/L/h.)
	NO_3^-	NH_4^+	NO_3^-	NH_4^+	
1NP(i)	600	5	1	15	0.14
1NP(ii)	450	5	3	10	0.19
2NP(i)	560	30	2	35	0.33
2NP(ii)	560	175	3	50	0.24
3NP(i)	580	35	52	45	0.44
3NP(ii)	570	205	2	25	0.37
1P(i)	6500	5	2200	20	1.17
2P(i)	6400	20	3580	20	1.60
2P(ii)	7500	5	3800	20	2.69
3P(i)	6900	40	4800	5	1.85
3P(ii)	7500	15	5500	15	1.78
1N(i)	530	15	1	5	0.13
1N(ii)	560	30	1	25	0.16
2N(i)	590	40	1	25	0.30
2N(ii)	600	30	2	45	0.44
3N(i)	585	40	2	40	0.09
3N(ii)	520	20	1	20	0.45

Table 4: Titratable alkalinity of the media reservoirs and culture filtrates at the time of chemostat incubation compared to alkalinity calculated in the incubation bottles. Chemostat identifiers are outlined in Table 1.

Chemostat	Alkalinity Media Reservoir (μEq/L)	Alkalinity Culture Filtrate (μEq/L)	Calculated Alkalinity From pCO_2 Bottles (μEq/L)
1NP(i)	194	NS*	196
1NP(ii)	189	176	165
2NP(i)	185	152	220
2NP(ii)	186	163	199
3NP(i)	174	179	219
3NP(ii)	155	189	205
1P(i)	238	474	543
2P(i)	229	347	392
3P(i)	253	267	308
1N(i)	148	173	170
1N(ii)	202	187	197
2N(i)	191	179	204
2N(ii)	204	202	239
3N(i)	200	175	194
3N(ii)	159	158	205

*NS: not sufficient sample available for analysis

Table 5: Production of alkalinity from titratable alkalinity measured in media reservoir and culture filtrate; alkalinity produced from nutrient uptake calculated from consumption of TDP (PO_4^{3-}) and TDN (NO_3^- and NH_4^+) as determined in Tables 2 and 3; and calculated alkalinity consumption (difference of Column 2 and 1) of the cultures. Chemostat identifiers are outlined in Table 1.

Chemostat	Titratable Alkalinity Produced (μEq/L/h.)	Alkalinity Produced From Nutrient Uptake (μEq/L/h.)	Calculated Alkalinity Produced From Other Changes (μEq/L/h.)
1NP(i)	NS*	0.16	**
1NP(ii)	-0.08	0.22	-0.30
2NP(i)	-0.27	0.39	-0.66
2NP(ii)	-0.18	0.28	-0.46
3NP(i)	0.06	0.52	-0.46
3NP(ii)	0.45	0.47	-0.02
1P(i)	0.90	1.18	-0.29
2P(i)	0.94	1.64	-0.70
3P(i)	0.18	1.91	-1.74
1N(i)	0.09	0.25	-0.16
1N(ii)	-0.06	0.28	-0.34
2N(i)	-0.09	0.53	-0.62
2N(ii)	-0.02	0.76	-0.78
3N(i)	-0.27	0.46	-0.73
3N(ii)	-0.01	0.56	-0.57

*NS: not sufficient sample available for analysis

Table 6: Suspended carbon (standard deviation ± 3.0%), nitrogen (standard deviation ± 4.3%), and phosphorous (standard deviation ± 6.0%) ratios for chemostat cultures. Redfield molar ratio, C:N:P= 106:16:1; N:C= 151:1 μmol/mmol. Chemostat identifiers are outlined in Table 1.

Chemostat	Suspended C/N/P (μg/L)	Molar Ratio C:N:P	Ratio N:C (μmol/mmol)
1NP(i)	8600/302/20	1109: 33:1	30:1
1NP(ii)	10660/485/66	416: 16:1	39:1
2NP(i)	11480/458/72	411: 14:1	34:1
2NP(ii)	10750/488/58	478: 19:1	39:1
3NP(i)	10990/522/60	472: 19:1	41:1
3NP(ii)	6586/460/46	369: 22:1	60:1
1P(i)	29300/3712/40	1889:205:1	109:1
2P(i)	21840/2607/48	1173:120:1	102:1
2P(ii) C.C.	16230/2432/43	973:125:1	128:1
3P(i)	13150/1255/37	916: 75:1	82:1
3P(ii) C.C.	5010/1002/38	340: 58:1	171:1
1N(i)	11760/465/214	142: 5:1	34:1
1N(ii)	11760/468/277	109: 4:1	34:1
2N(i)	8980/393/235	99: 4:1	38:1
2N(ii)	12960/544/295	113: 4:1	36:1
3N(i)	11650/500/183	164: 6:1	37:1
3N(ii)	6060/477/149	105: 7:1	63:1

Table 7: Dissolved organic carbon (DOC) in chemostat media reservoirs and culture filtrate (GF/C) at the time of incubation (standard deviation ± 1.7%) . Chemostat identifiers are outlined in Table 1.

Chemostat	Reservoir (μg/L)	Culture Filtrate (μg/L)	Difference* (μg/L)
1NP(i)	2522	6726	4204
1NP(ii)	3400	4620	1220
2NP(i)	5164	13451	8287
2NP(ii)	32427	34829	2402
3NP(i)	3003	10929	7926
3NP(ii)	6245	42035	35790
1P(i)	60050	32307	-27743
2P(i)	19456	18736	-720
2P(ii) C.C.	12250	17415	5165
3P(i)	47440	32427	-15013
3P(ii) C.C.	3723	18736	15013
1N(i)	2402	9848	7446
1N(ii)	88874	54045	-34829
2N(i)	8287	26782	18495
2N(ii)	17775	23420	5645
3N(i)	17415	8167	-9248
3N(ii)	11530	15613	4083

* Positive numbers denote excretion of DOC whereas negative values indicate DOC uptake.

Table 8: Slopes (ΔDIC) with standard errors of the regression coefficient for each bottle incubated in the chemostat study. Code: light bottles 1 to 3 (LB1, LB2, LB3) and dark bottles 1 and 2 (DB1, DB2). Symbols relate to each of the bottles respective markers in Appendix 6. Chemostat identifiers are outlined in Table 1. Units = μmol DIC/L/h.

Chemostat	LB1 □	LB2 ○	LB3 △	DB1 ■	DB2 ●
1NP(i)	-0.79±0.06	-0.82±0.04	-0.64±0.04	3.59±0.02	2.86±0.09
1NP(ii)	-1.91±0.15	-4.91±0.59	-1.38±0.13	NS	8.30±0.35
2NP(i)	-4.03±0.05	-4.41±0.15	-3.92±0.06	6.89±0.08	8.30±0.23
2NP(ii)	-4.50±0.18	-3.99±0.18	-4.17±0.17	4.86±0.35	3.67±0.19
3NP(i)	-7.13±0.26	-6.36±0.24	-6.32±0.14	7.29±0.24	6.71±0.19
3NP(ii)	-6.80±0.18	-5.84±0.08	-5.44±0.13	5.62±0.38	3.10±0.18
1P(i)	-9.52±0.78	-8.03±0.67	-16.71±0.73	8.60±0.57	9.79±0.68
2P(i)	-11.16±1.94	-17.15±2.45	-13.39±1.19	8.39±0.80	8.62±1.31
2P(ii)C.C.	16.32±0.71	13.54±0.43	14.06±0.52	15.80±0.33	15.37±1.37
3P(i)	-14.83±0.72	-16.13±1.23	-14.47±0.68	9.18±0.23	9.42±0.15
3P(ii)C.C.	9.83±0.32	7.26±2.34	15.57±0.36	16.36±0.16	7.36±1.24
1N(i)	-2.00±0.07	-2.51±0.22	-2.17±0.12	5.10±0.08	5.46±0.25
1N(ii)	-2.38±0.27	-2.32±0.10	-3.83±0.45	NS	2.61±0.20
2N(i)	-4.82±0.11	-4.85±0.08	-4.18±0.14	5.24±0.27	5.83±0.17
2N(ii)	-5.28±0.38	-5.01±0.24	-4.74±0.31	NS	3.86±0.34
3N(i)	-2.68±0.06	-2.92±0.06	-1.95±0.07	8.10±0.21	9.05±0.13
3N(ii)	-3.34±0.21	-2.38±0.32	-2.64±0.37	3.97±0.41	4.10±0.433

Table 9: Rate of change in carbon concentration during serum-bottle incubations of chemostat samples. Rates represent the averages of regression line slopes, two slopes for positive changes = respiration (R), and three slopes for negative changes = net photosynthesis (NPP), as determined from changes in DIC during the incubation. GPP = NPP - R. Chemostat identifiers are outlined in Table 1.

Chemostat	Respiration Rate (μmol/L/h.)	Uncorrected NPP (μmol/L/h.)	Titratable Corrected NPP (μmol/L/h.)	R/GPP
1NP(i)	3.21	- 0.75	***	0.81
1NP(ii)	8.30	- 2.73	- 2.81	0.75
2NP(i)	7.60	- 4.12	- 4.39	0.65
2NP(ii)	4.22	- 4.22	- 4.39	0.50
3NP(i)	7.00	- 6.69	- 6.63	0.51
3NP(ii)	4.36	- 6.03	- 5.58	0.42
1P(i)	9.19	-11.42	-10.53	0.45
2P(i)	8.51	-13.90	-13.17	0.38
3P(i)	9.30	-15.14	-14.96	0.38
1N(i)	5.23	- 2.23	- 2.14	0.70
1N(ii)	2.61	- 2.84	- 2.90	0.48
2N(i)	5.54	- 4.62	- 4.70	0.55
2N(ii)	3.86	- 5.01	- 5.03	0.44
3N(i)	8.52	- 2.52	- 2.79	0.77
3N(ii)	4.04	- 2.94	- 2.95	0.58

1) Chemostat Incubation Experimental Design

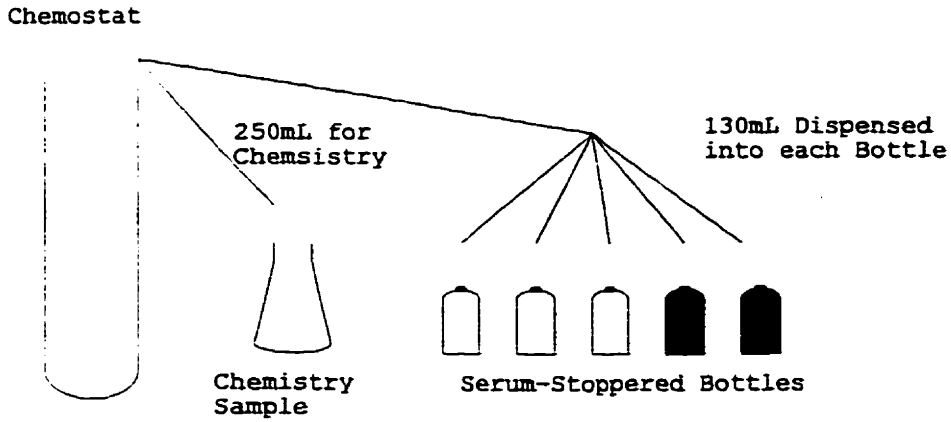

2) Field Incubation Setup

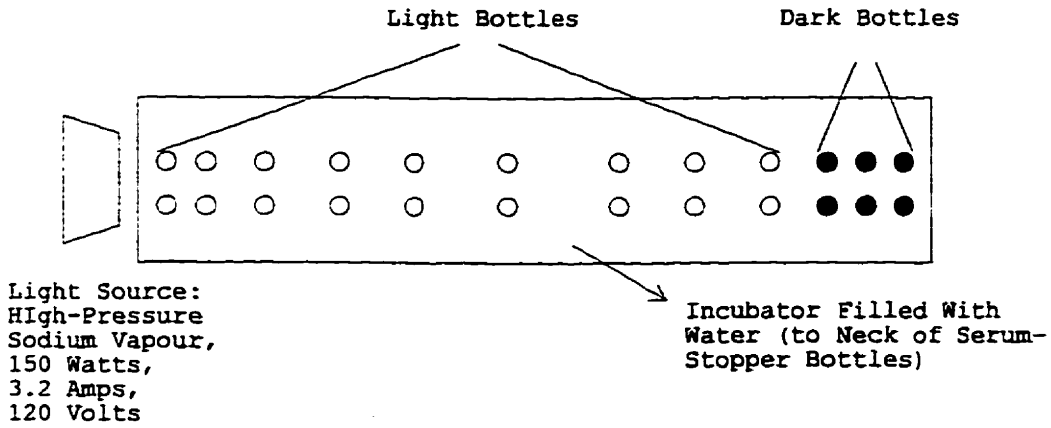

Figure 1: Experimental design for 1) culture study and 2) field study. 1) Three nutrient regimes were used, nitrogen-limited, phosphorous-limited, and nitrogen and phosphorous-limited. Each nutrient regime was grown at three different dilution rates (0.1, 0.2, and 0.3 per day) and duplicated. Duplicates were not averaged. Duplicate phosphorous-limited cultures were contaminated and the data was not used. 2) Incubator used for measuring photosynthesis-irradiance curves.

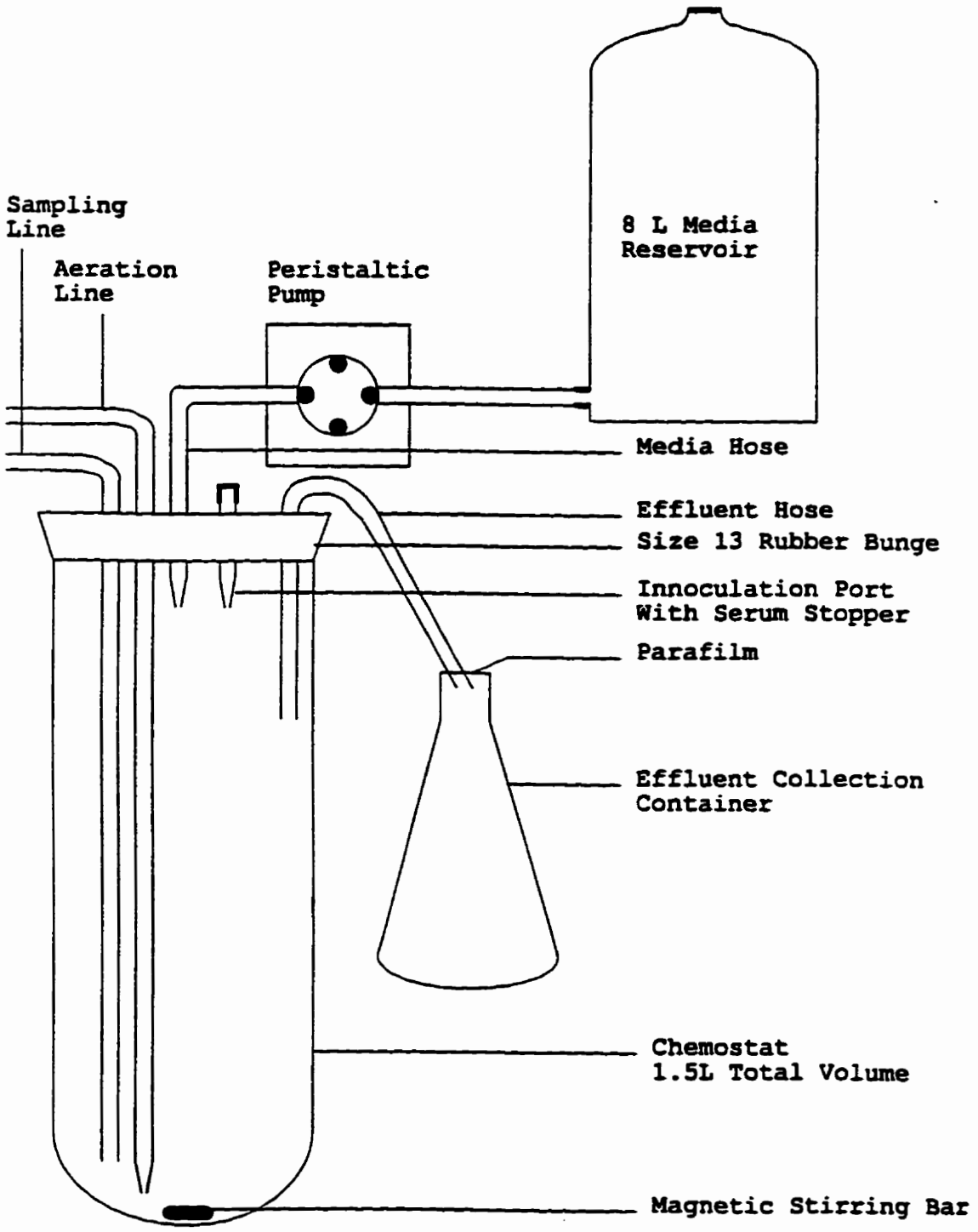

Figure 2: Schematic diagram of Chemostat.

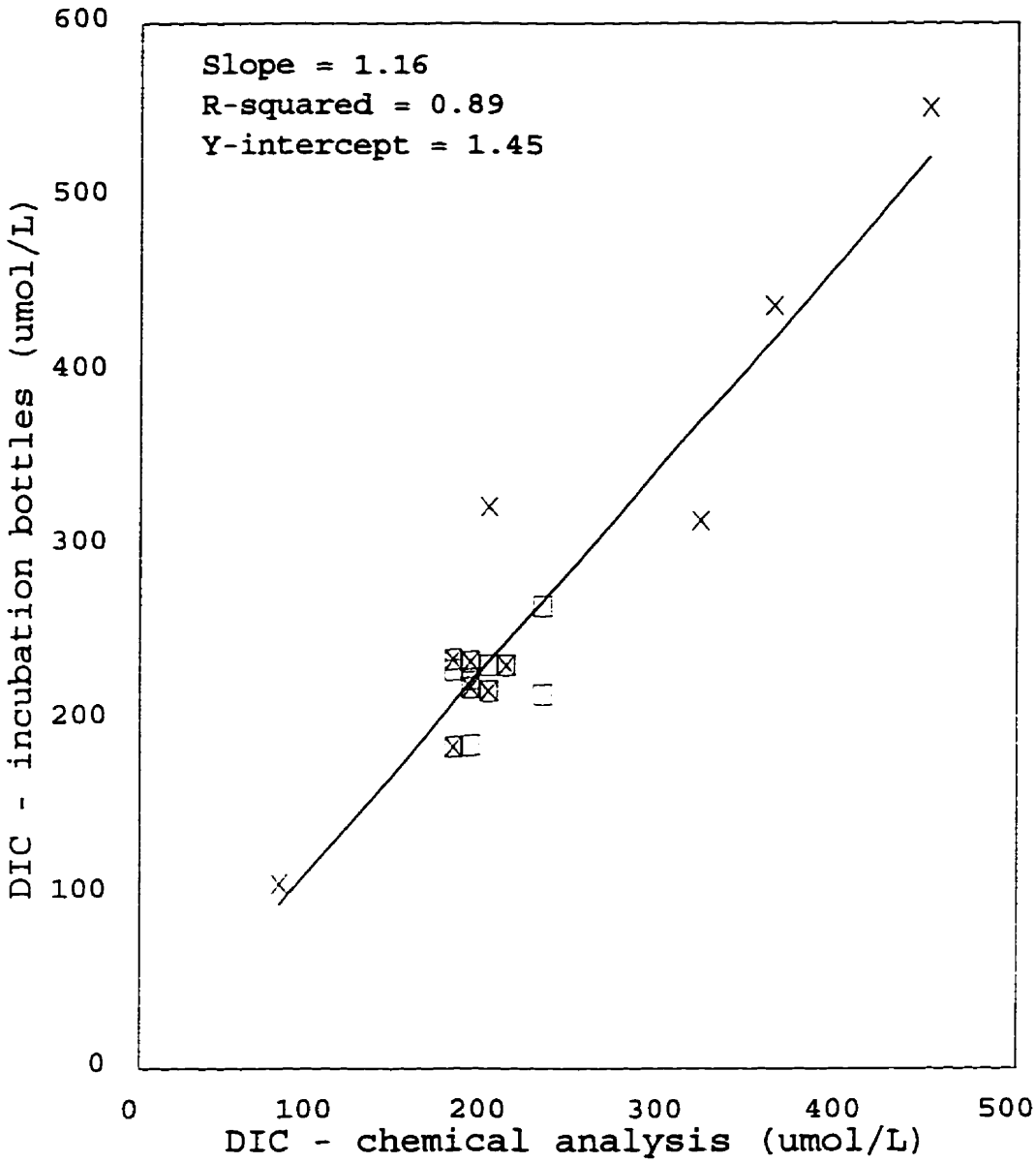

Figure 3: DIC determined by chemical analysis (standard deviation ± 1.8%) versus average DIC calculated in pCO_2 serum-stoppered bottles. ⊠ = NP-limited, **x** = P-limited, and □ = N-limited chemostats.

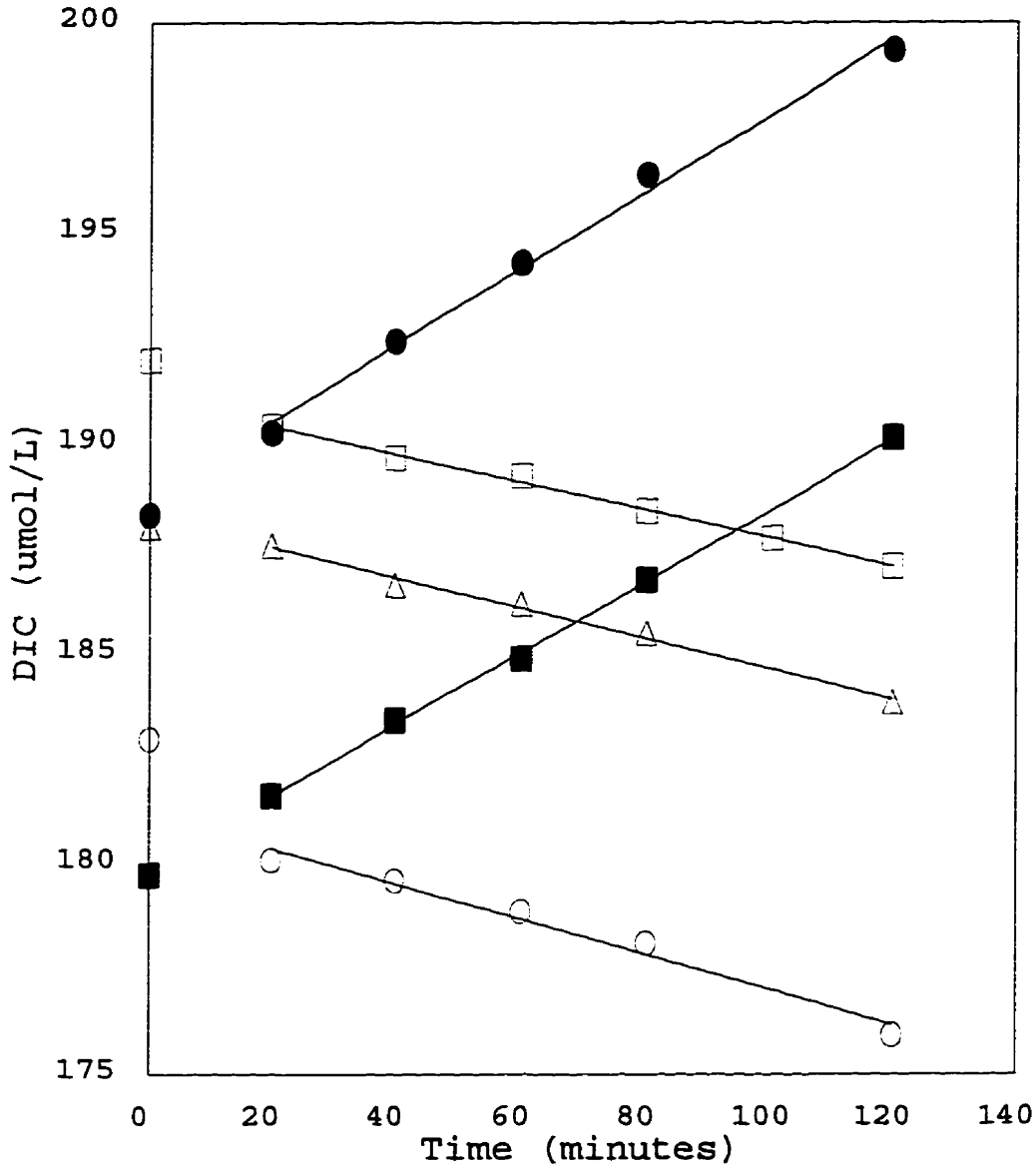

Figure 4: Typical DIC versus time plot for chemostat study, Chemostat 1N(i). See appendix 5 for plots of every chemostat. Light bottle = LB; Dark bottle = DB: LB1(□), LB2(○), LB3(△), DB1 (■), and DB2(●).

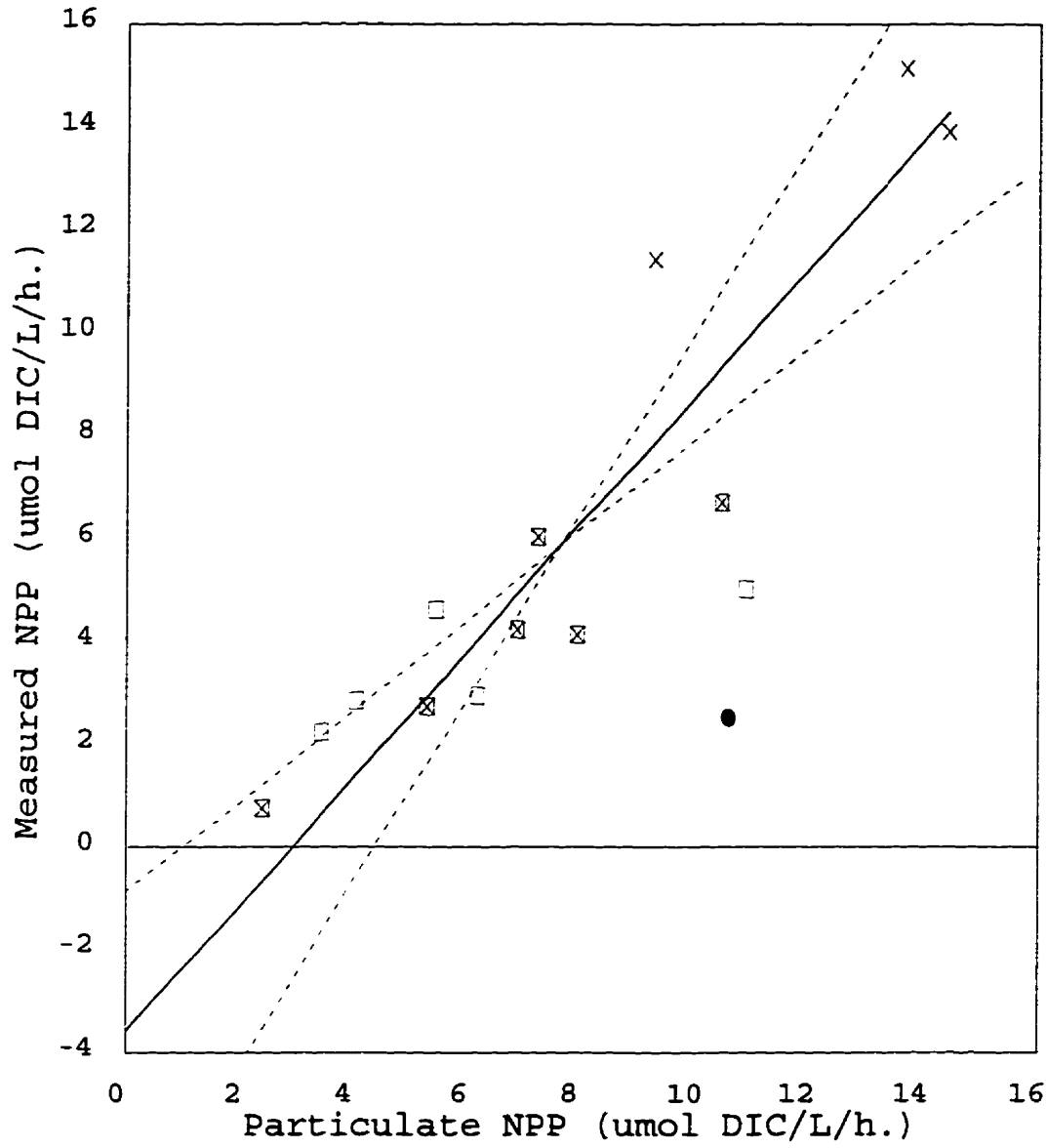

Figure 5: Expected NPP determined from measured particulate carbon versus measured uptake of DIC (NPP) in pCO_2 serum-stoppered bottles. Dashed lines represent the 95% confidence interval on the slope. ⊠ = NP-limited, X = P-limited, and □ = N-limited chemostats.

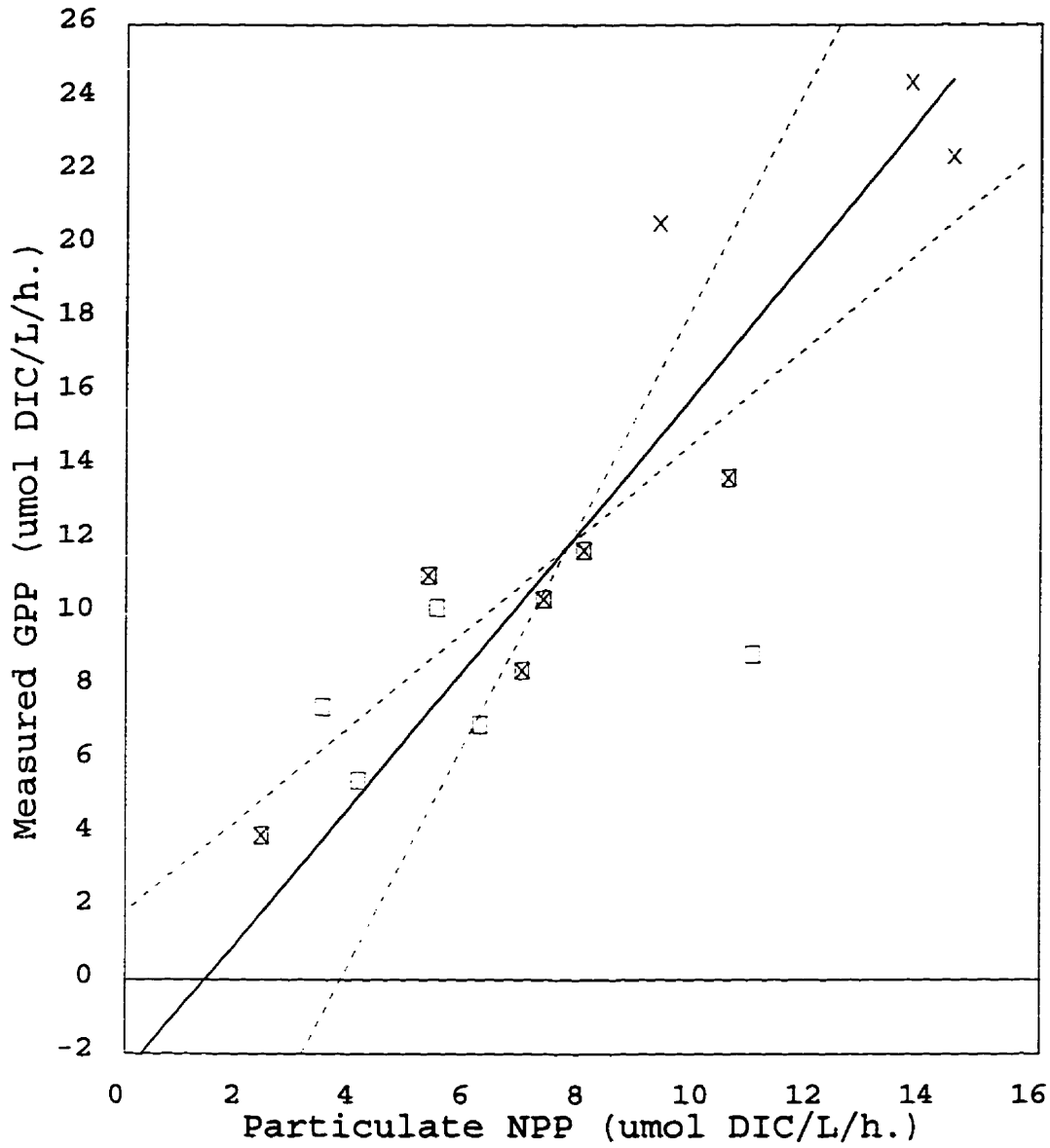

Figure 6: Expected NPP determined from measured particulate carbon versus measured uptake of DIC plus measured respiration (GPP) in pCO_2 serum-stoppered bottles. Dashed lines represent the 95% confidence intervals on the slope. ⊠ = NP-limited, x = P-limited, and □ = N-limited chemostats.

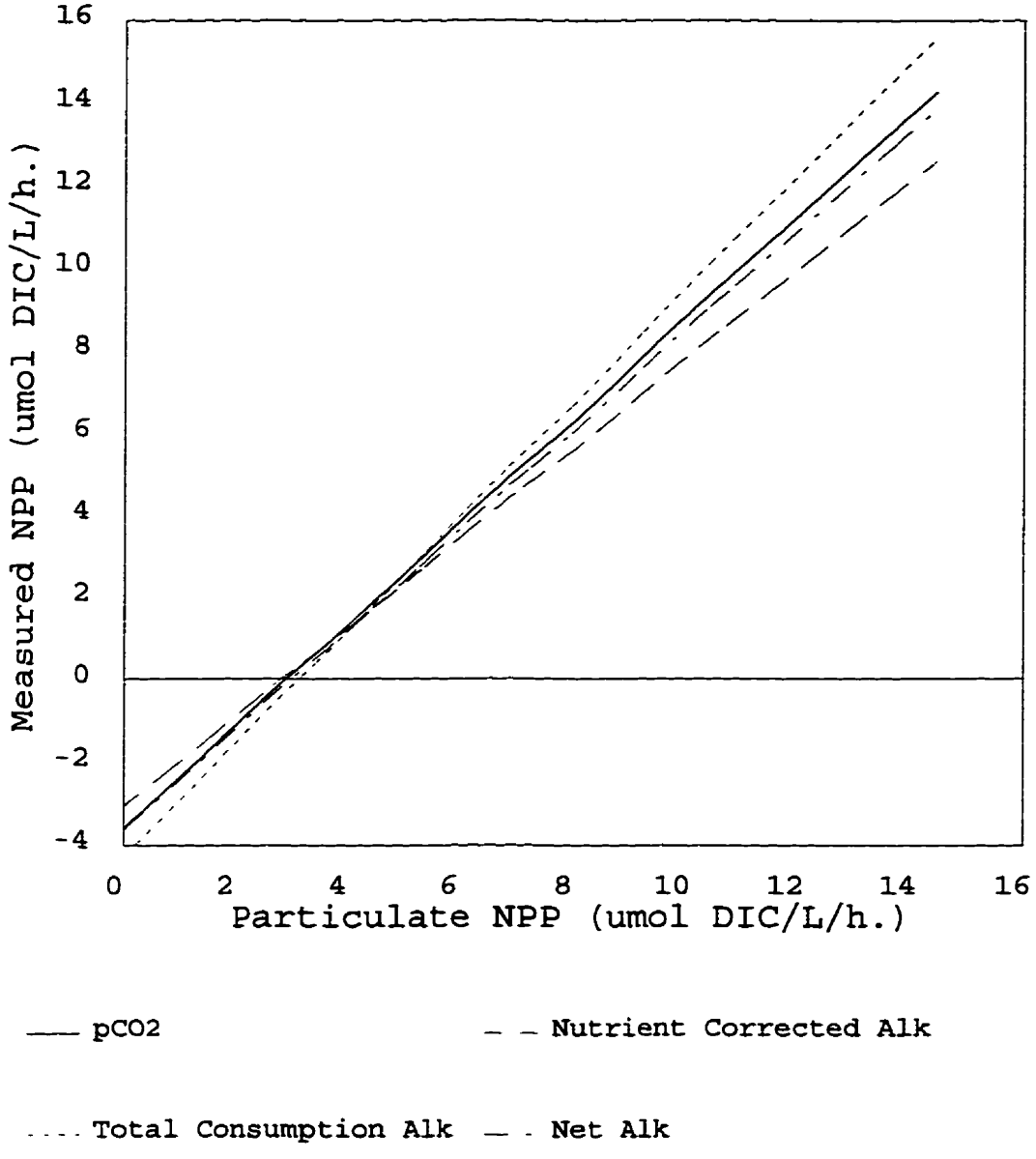

Figure 7: Expected NPP determined from measured particulate carbon versus net alkalinity corrected DIC uptake, nutrient corrected DIC uptake, and calculated alkalinity corrected DIC uptake.

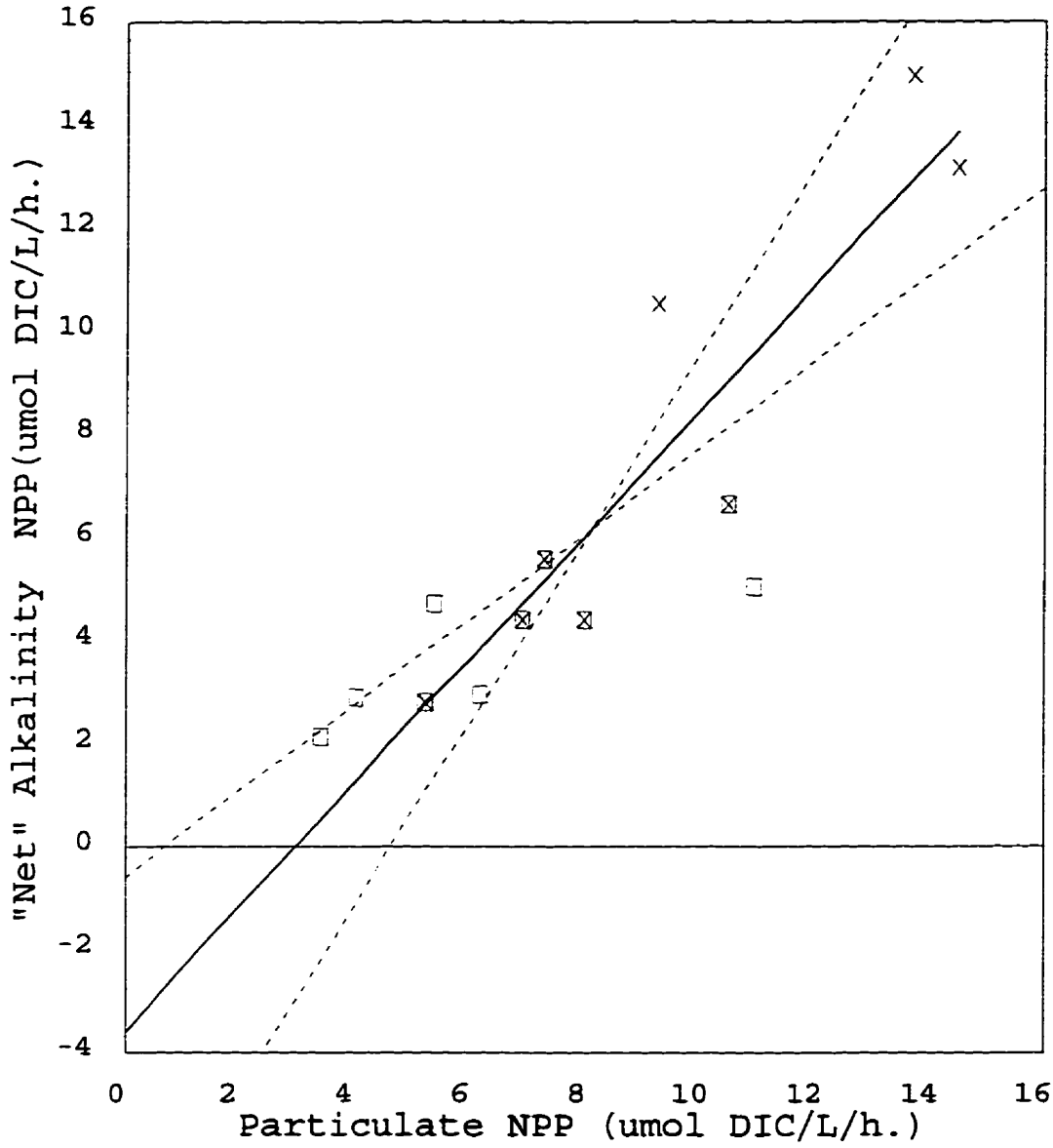

Figure 8: Expected NPP determined from measured particulate carbon versus net alkalinity corrected DIC uptake. Dashed lines represent the 95% confidence interval on the slope. ⊠ = NP-limited, X = P-limited, and □ = N-limited chemostats.

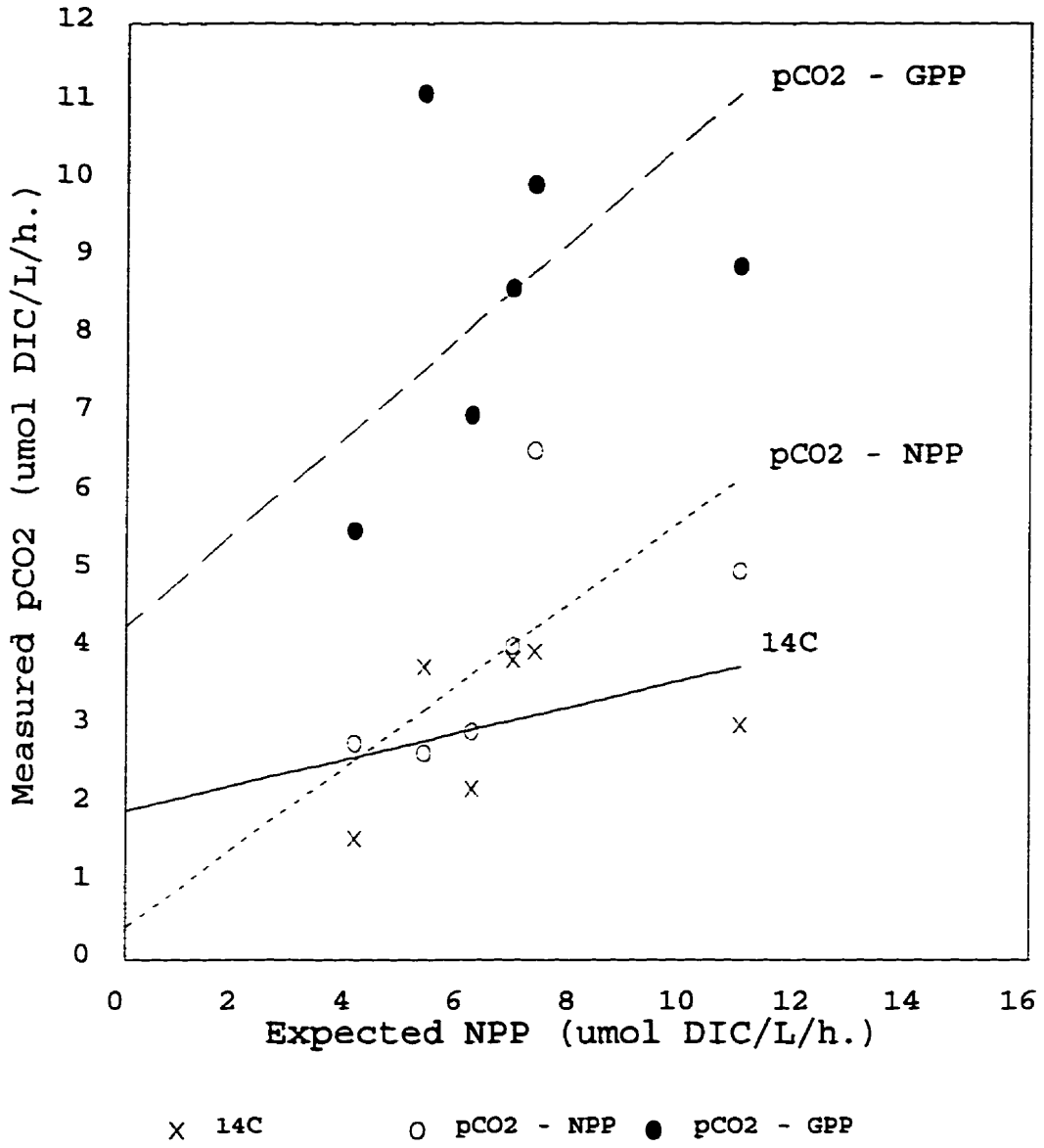

Figure 9: Expected NPP determined from measured particulate carbon versus pCO_2 and ^{14}C determined productivity for chemostats 1NP(ii), 2NP(ii), 3NP(iii), 1N(ii), 2N(ii), and 3N(ii).

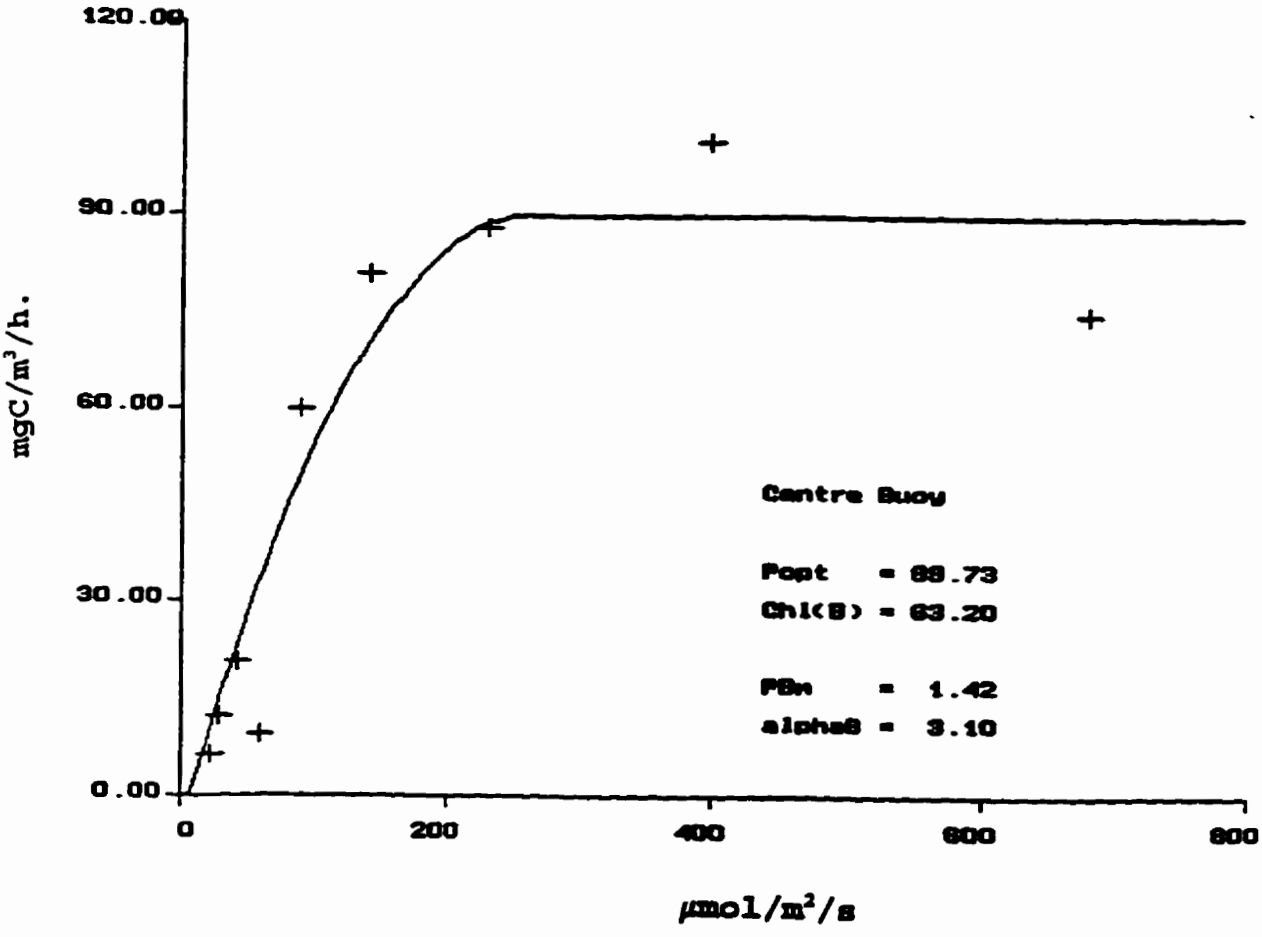

Figure 10: Photosynthesis-Irradiance curve for L227, August 23, 1995. Dark respiration ($mgC/m^3/h.$): -8.8, -5.5, -7.5. Descriptors: Popt = rate of photosynthesis at optimal irradiance, Chl(B) = chlorophyll concentration, PBm = Popt/B, and alphaB = slope of photosynthesis-irradiance curve at low irradiance values divided by B.

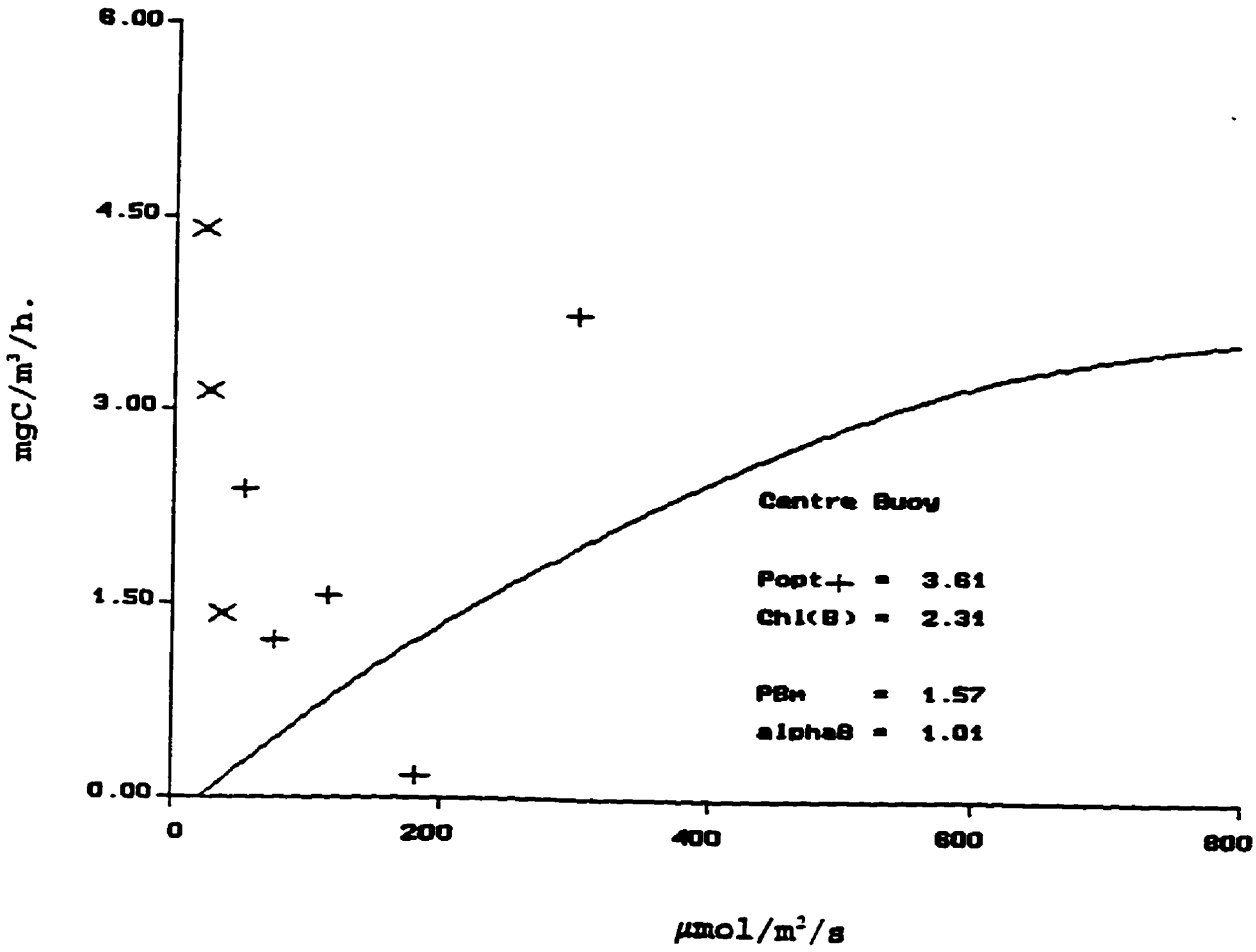

Figure 11: Photosynthetic-Irradiance curve for L240, August 25, 1995. Dark respiration ($mgC/m^3/h.$): -2.1, 1.8, 1.5.Descriptors: Popt = rate of photosynthesis at optimal irradiance, Chl(B) = chlorophyll concentration, PBm = Popt/B, and alphaB = slope of photosynthesis-irradiance curve at low irradiance values divided by B. "X's" represent net respiration.

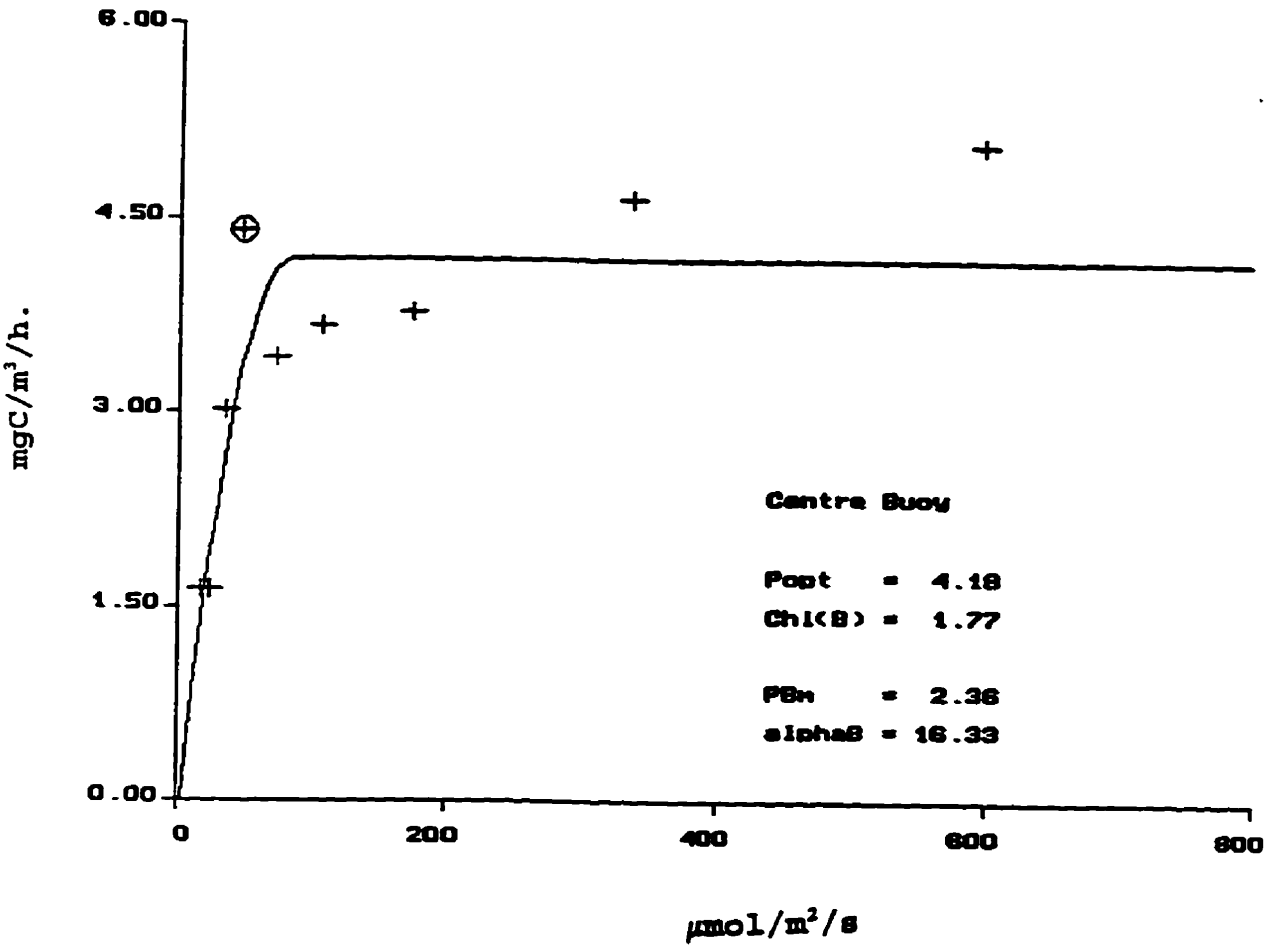

Figure 12: Photosynthetic-Irradiance curve for L240, September 6, 1995. Dark respiration (mgC/m³/h.): 4.1, 3.0, 3.8. Descriptors: Popt = rate of photosynthesis at optimal irradiance, Chl(B) = chlorophyll concentration, PBm = Popt/B, and alphaB = slope of photosynthesis-irradiance curve at low irradiance values divided by B. Circled point was not included in the data analysis.

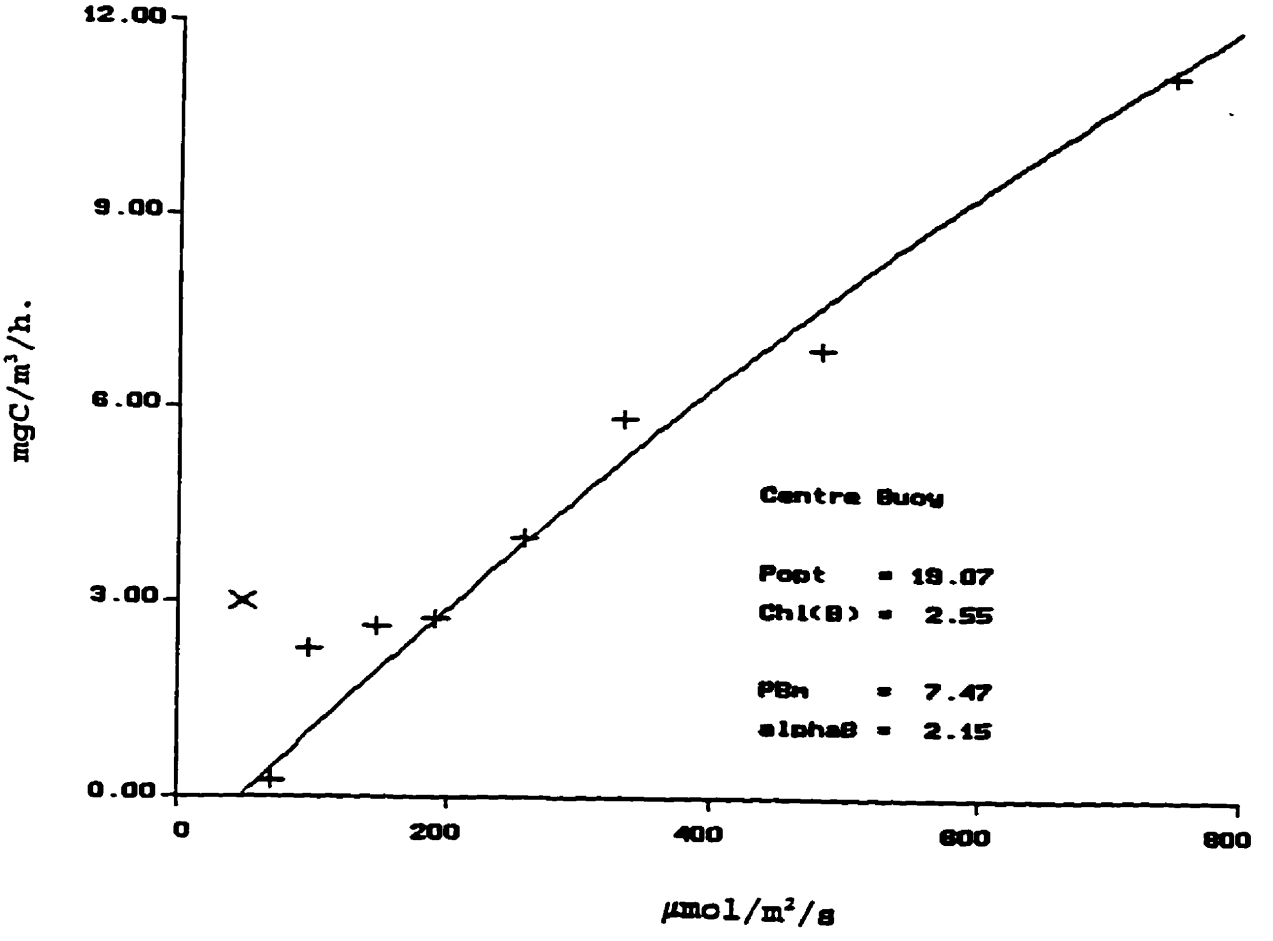

Figure 13: Photosynthetic-Irradiance curve for L302s, August 19, 1995. Dark respiration (mgC/m^3/h.): -0.4, -1.4, -2.4. Descriptors: Popt = rate of photosynthesis at optimal irradiance, Chl(B) = chlorophyll concentration, PBm = Popt/B, and alphaB = slope of photosynthesis-irradiance curve at low irradiance values divided by B. "X" represents net respiration.

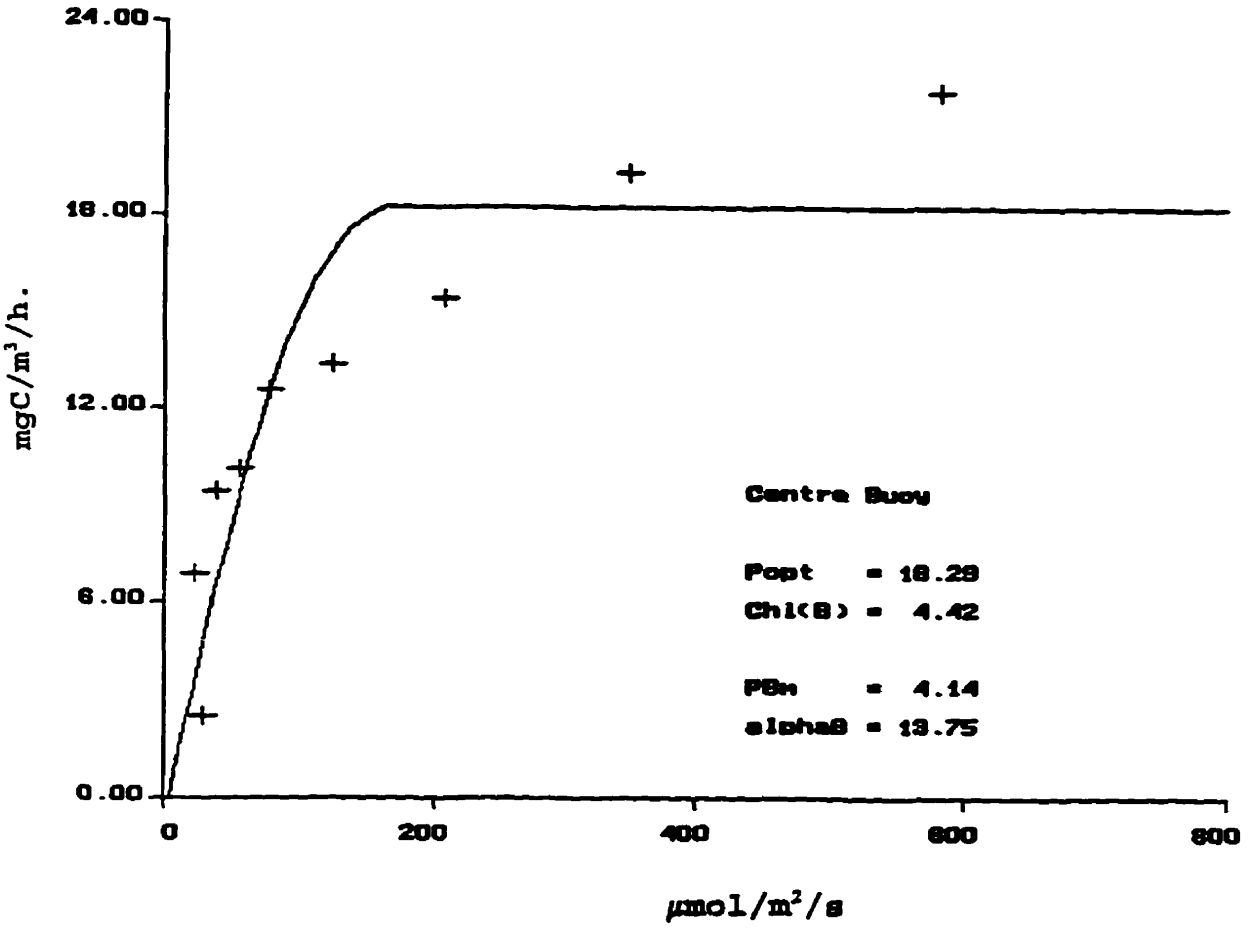

Figure 14: Photosynthetic-Irradiance curve for L302s, August 24, 1995. Dark respiration (mgC/m³/h.): 1.6, 5.5, 7.3. Descriptors: Popt = rate of photosynthesis at optimal irradiance, Chl(B) = chlorophyll concentration, PBm = Popt/B, and alphaB = slope of photosynthesis-irradiance curve at low irradiance values divided by B.

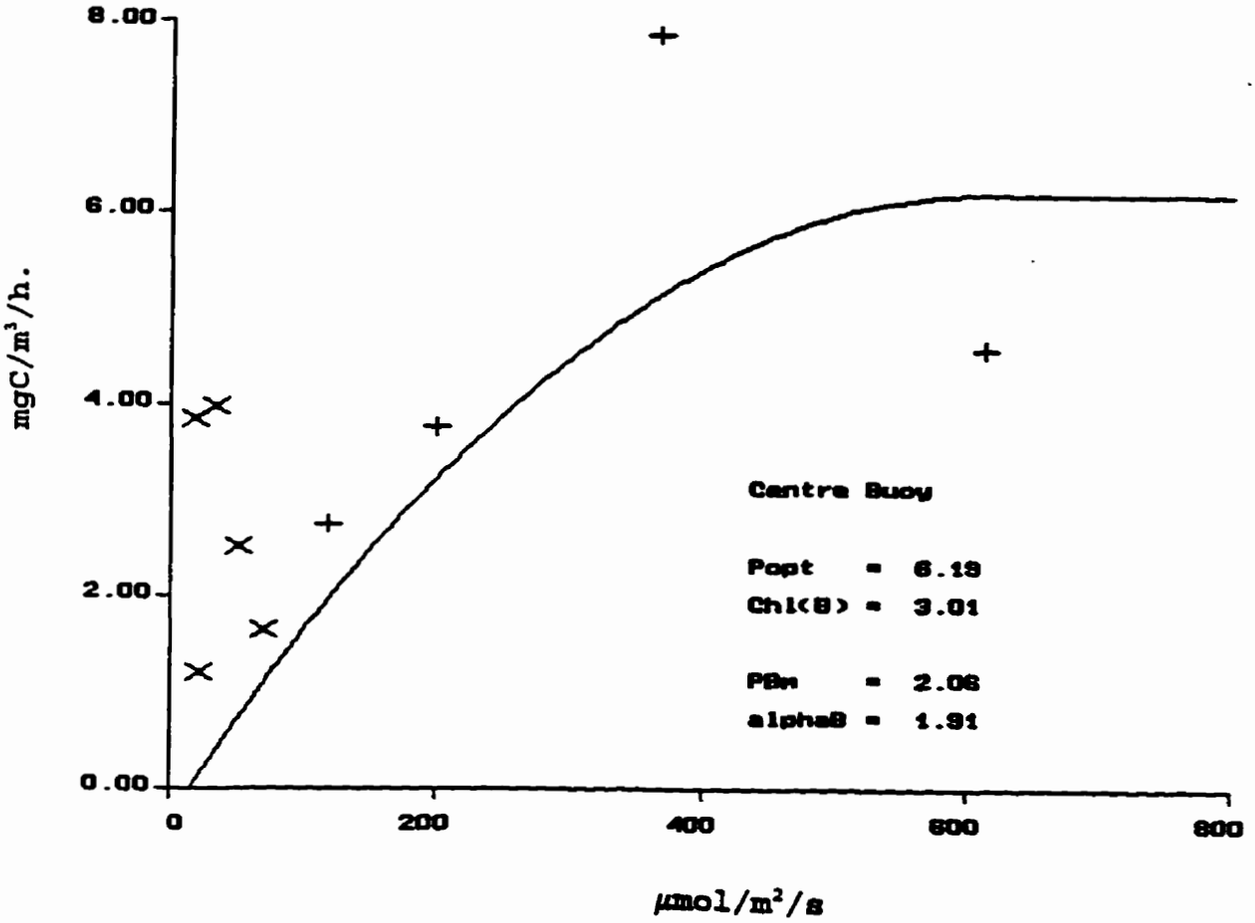

Figure 15: Photosynthetic-Irradiance curve for L302s, September 2, 1995. Dark respiration (mgC/m³/h.): -1.5, -3.7, 0.1. Descriptors: Popt = rate of photosynthesis at optimal irradiance, Chl(B) = chlorophyll concentration, PBm = Popt/B, and alphaB = slope of photosynthesis-irradiance curve at low irradiance values divided by B. "X's" represent net respiration.

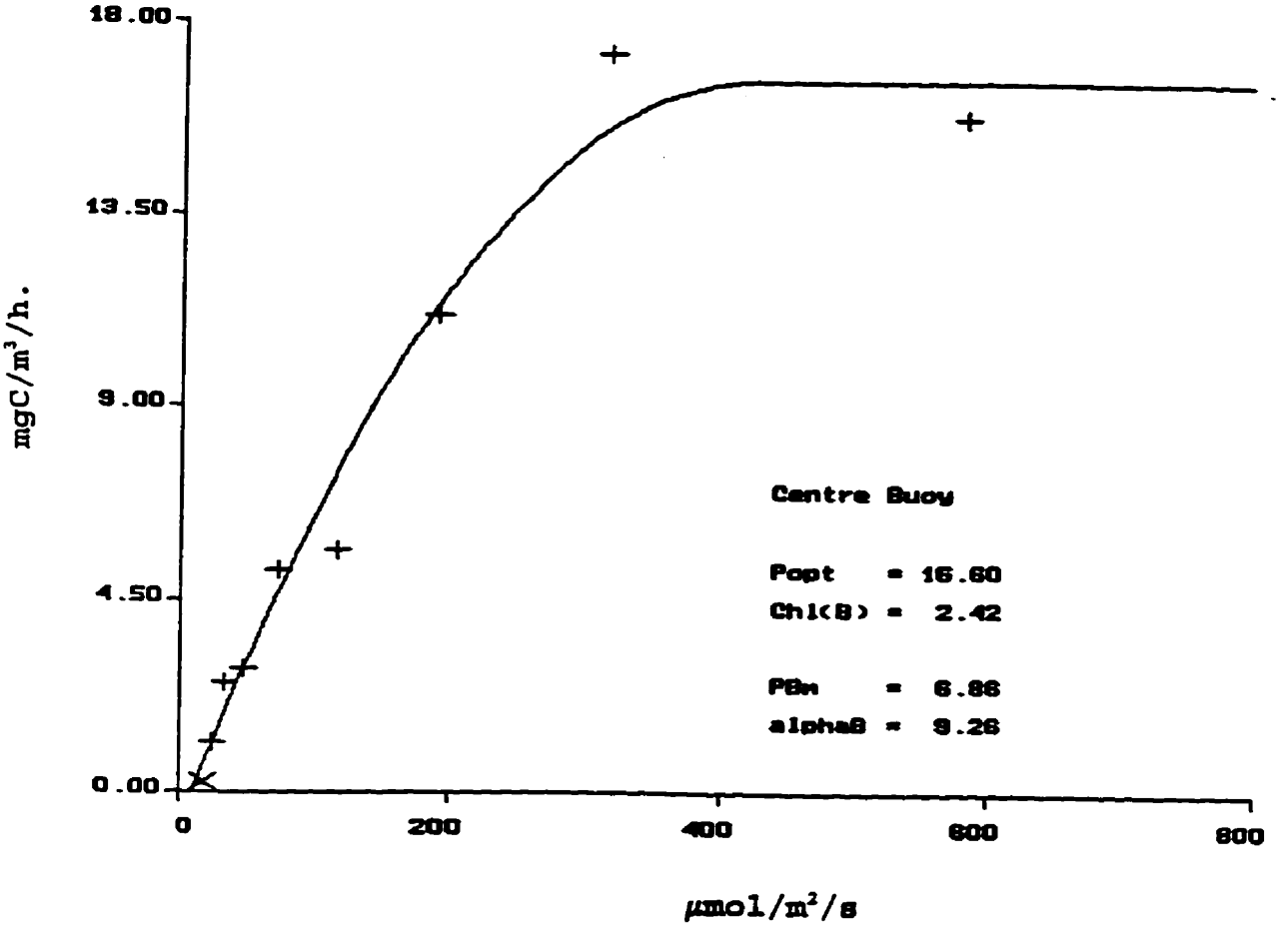

Figure 16: Photosynthetic-Irradiance curve for L302s, September 7, 1995. Dark respiration ($mgC/m^3/h.$): 0.6, 1.2, 0.7. Descriptors: Popt = rate of photosynthesis at optimal irradiance, Chl(B) = chlorophyll concentration, PBm = Popt/B, and alphaB = slope of photosynthesis-irradiance curve at low irradiance values divided by B. "X" represents net respiration.

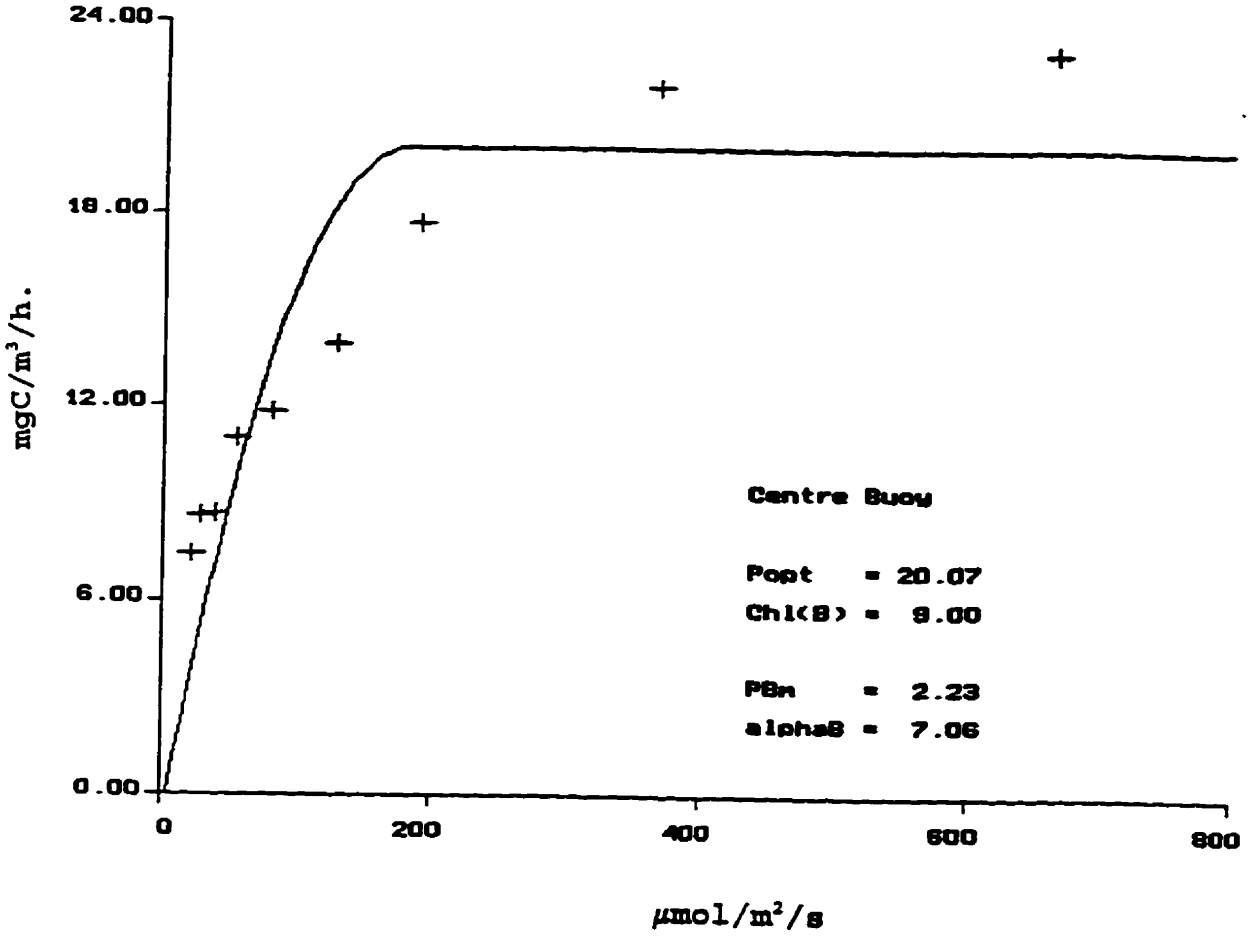

Figure 17: Photosynthetic-Irradiance curve for L303 non-pressurized, August 31, 1995. Dark respiration ($mgC/m^3/h.$): 4.2, 7.5, 3.8. Descriptors: Popt = rate of photosynthesis at optimal irradiance, Chl(B) = chlorophyll concentration, PBm = Popt/B, and alphaB = slope of photosynthesis-irradiance curve at low irradiance values divided by B.

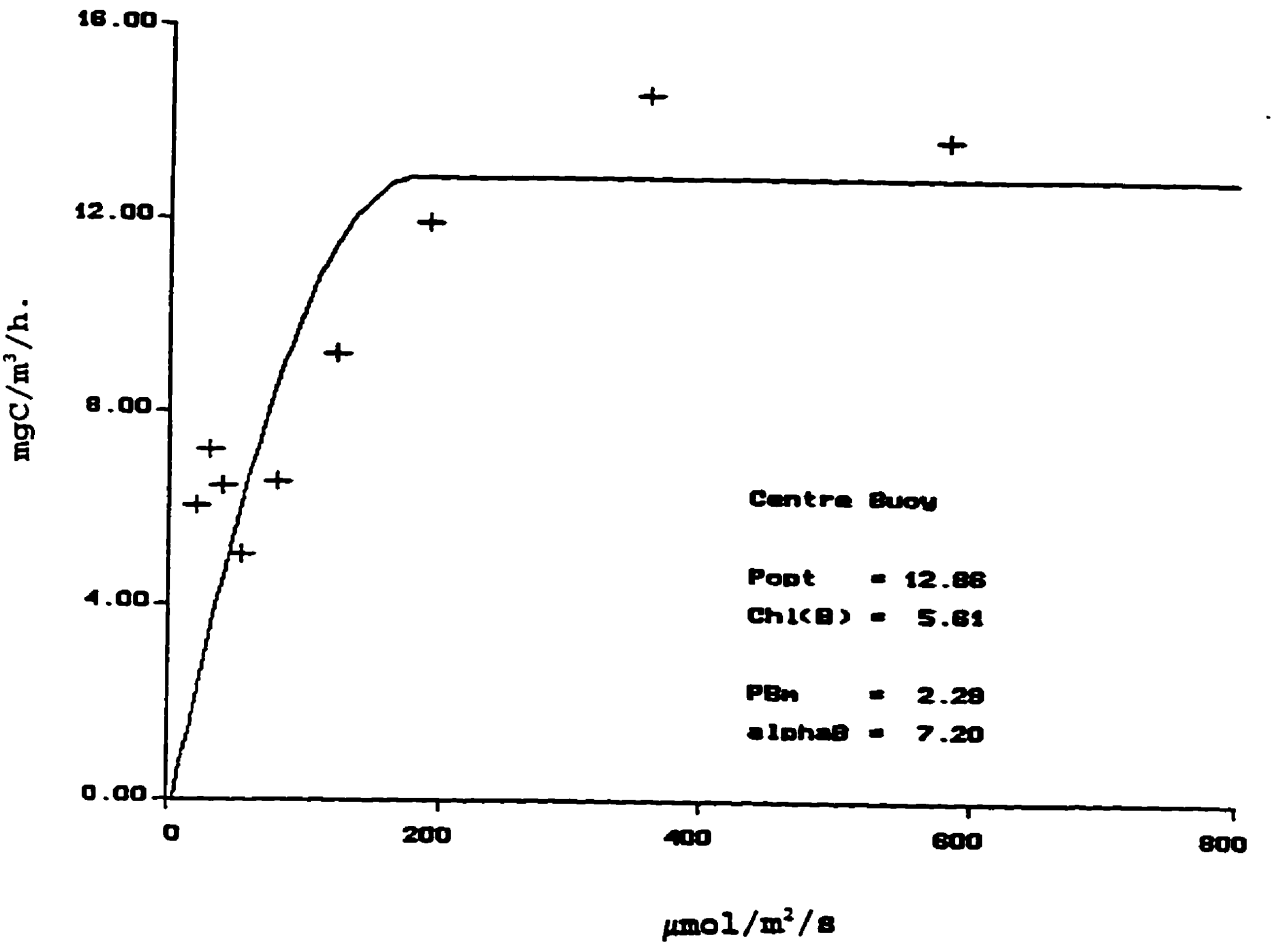

Figure 18: Photosynthetic-Irradiance curve for L303 pressurized, August 31, 1995. Dark respiration ($mgC/m^3/h.$): 4.6, 8.3, 4.1. Descriptors: Popt = rate of photosynthesis at optimal irradiance, Chl(B) = chlorophyll concentration, PBm = Popt/B, and alphaB = slope of photosynthesis-irradiance curve at low irradiance values divided by B.

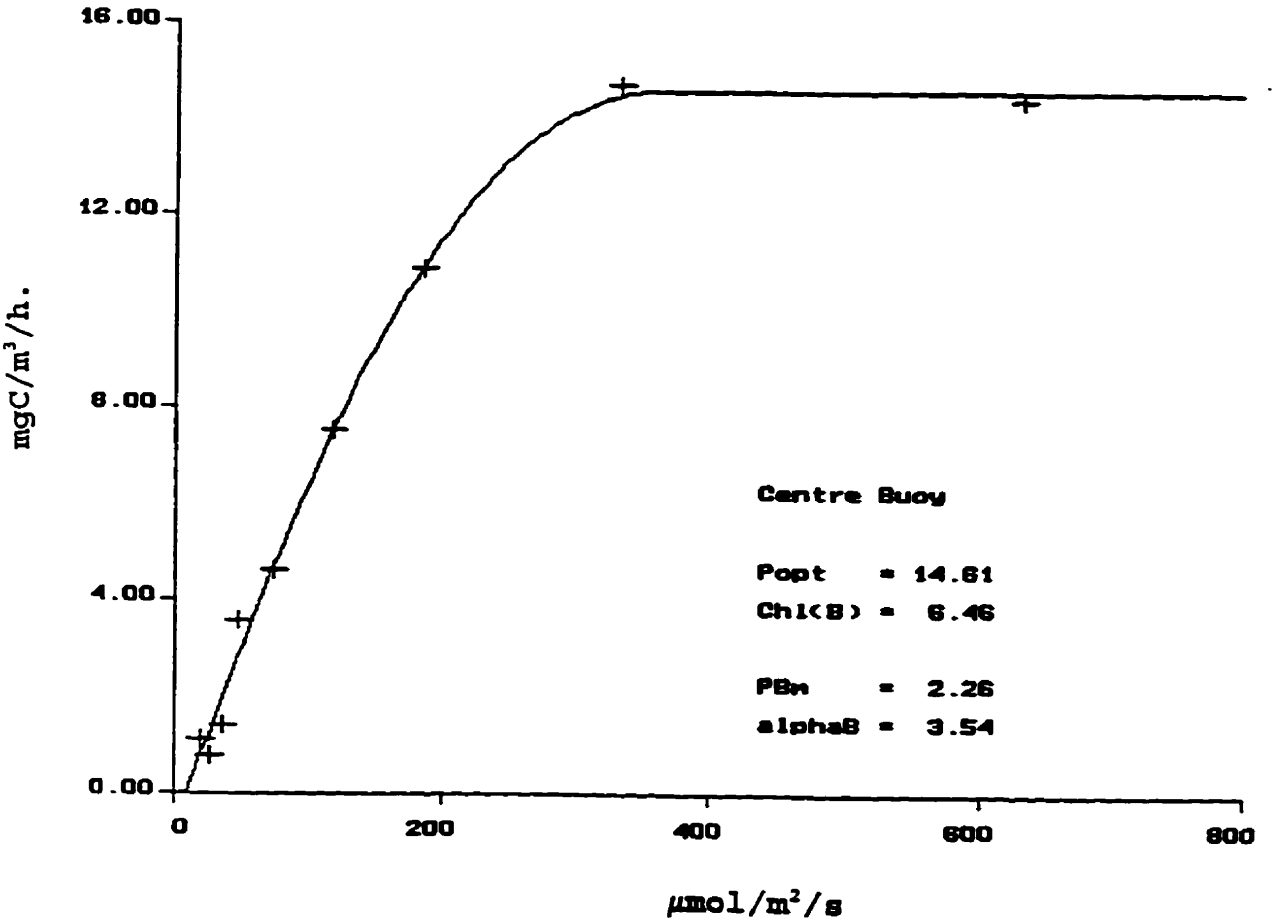

Figure 19: Photosynthetic-Irradiance curve for L303, September 7, 1995. Dark respiration ($mgC/m^3/h.$): 1.3, -0.1, 0.3. Descriptors: Popt = rate of photosynthesis at optimal irradiance, Chl(B) = chlorophyll concentration, PBm = Popt/B, and alphaB = slope of photosynthesis-irradiance curve at low irradiance values divided by B.

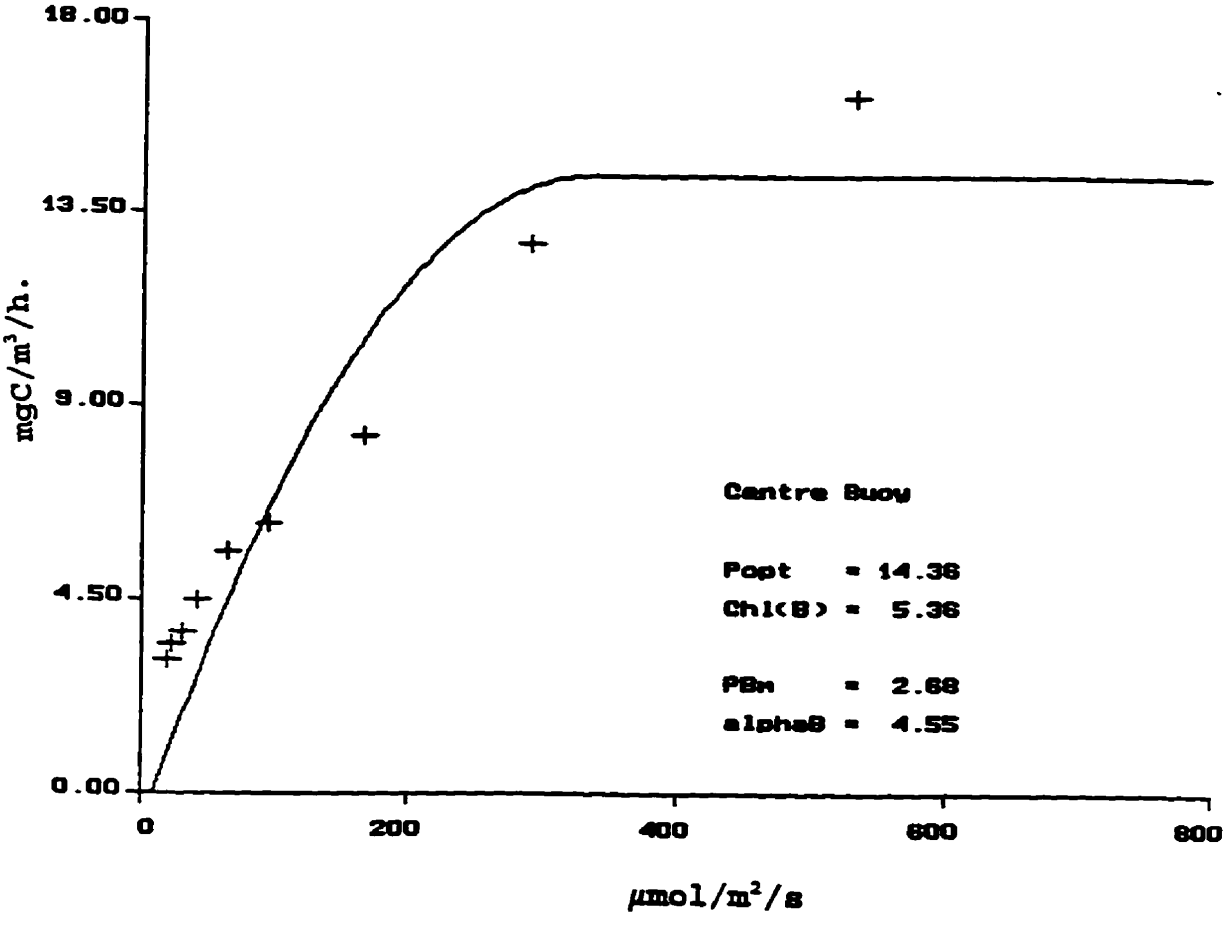

Figure 20: Photosynthetic-Irradiance curve for L303, September 11, 1995. Dark respiration ($mgC/m^3/h.$): 2.5, 1.7, 0.2. Descriptors: Popt = rate of photosynthesis at optimal irradiance, Chl(B) = chlorophyll concentration, PBm = Popt/B, and alphaB = slope of photosynthesis-irradiance curve at low irradiance values divided by B.

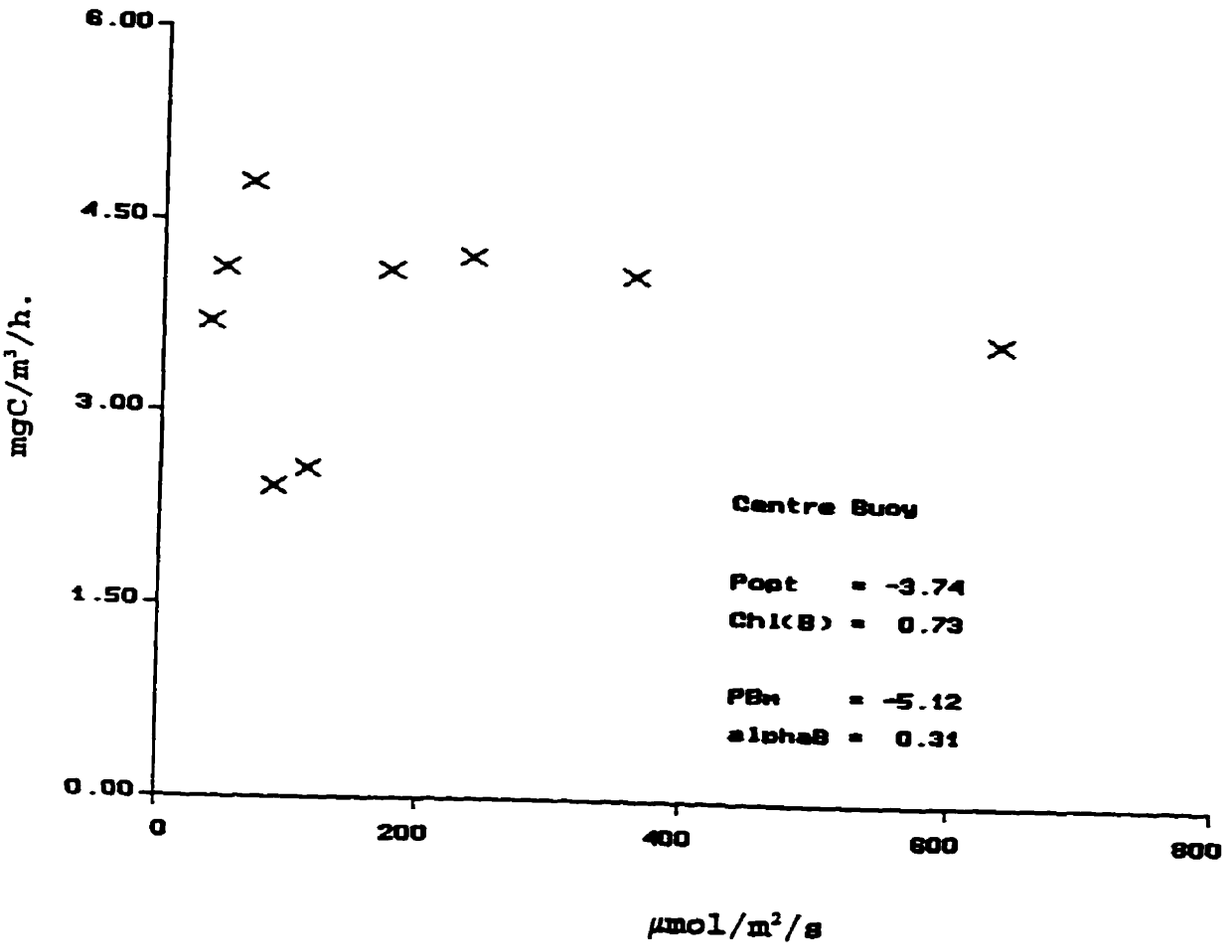

Figure 21: Photosynthetic-Irradiance curve for L373 August 2, 1995. Dark respiration (mgC/m^3/h.): -5.0, -4.4, -3.8. Descriptors: Popt = rate of photosynthesis at optimal irradiance, Chl(B) = chlorophyll concentration, PBm = Popt/B, and alphaB = slope of photosynthesis-irradiance curve at low irradiance values divided by B. "X's" represent net respiration.

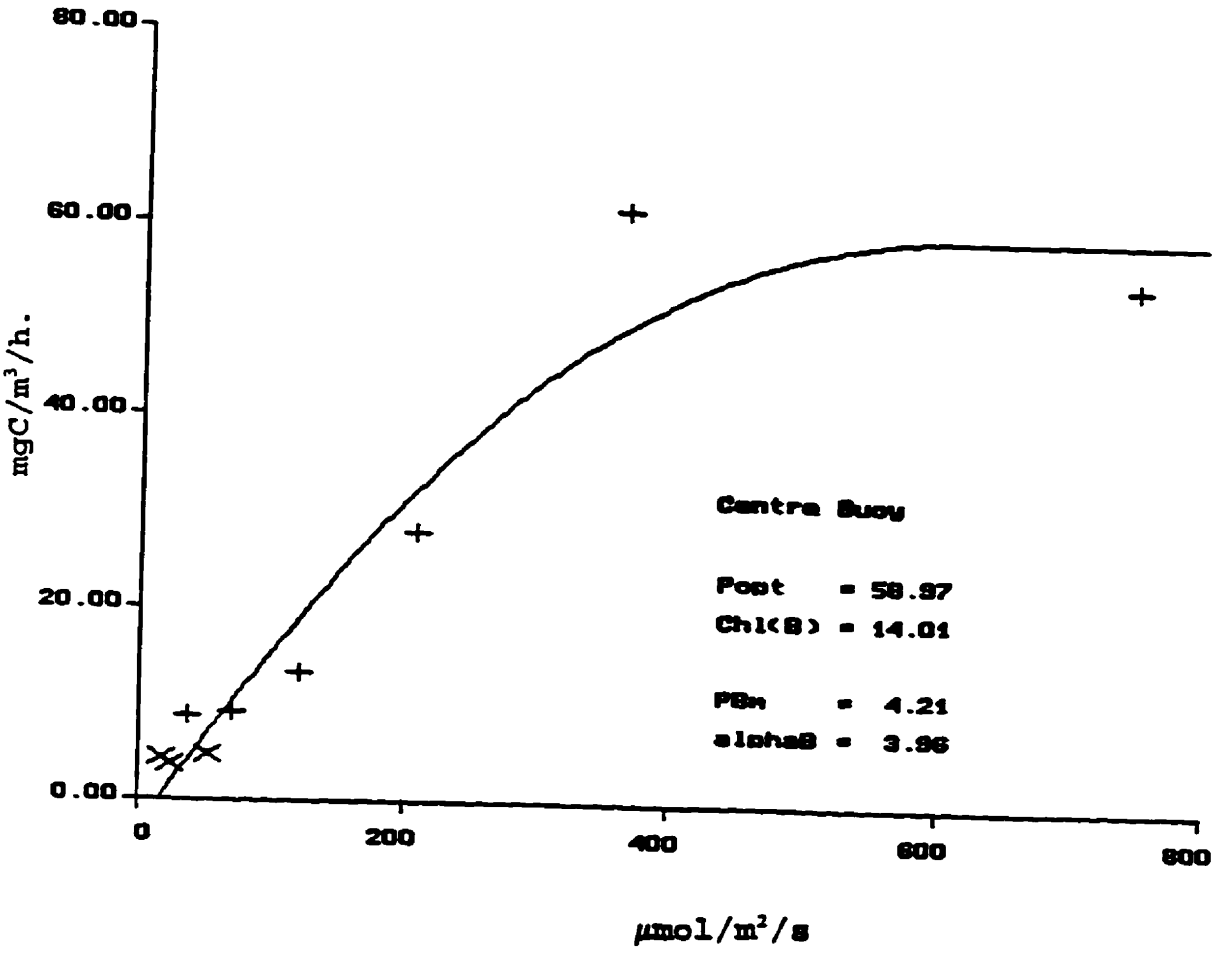

Figure 22: Photosynthetic-Irradiance curve for L979, September 2, 1995. Dark respiration ($mgC/m^3/h.$): -0.8, -2.0, -9.6. Descriptors: Popt = rate of photosynthesis at optimal irradiance, Chl(B) = chlorophyll concentration, PBm = Popt/B, and alphaB = slope of photosynthesis-irradiance curve at low irradiance values divided by B. "X's" represent net respiration.

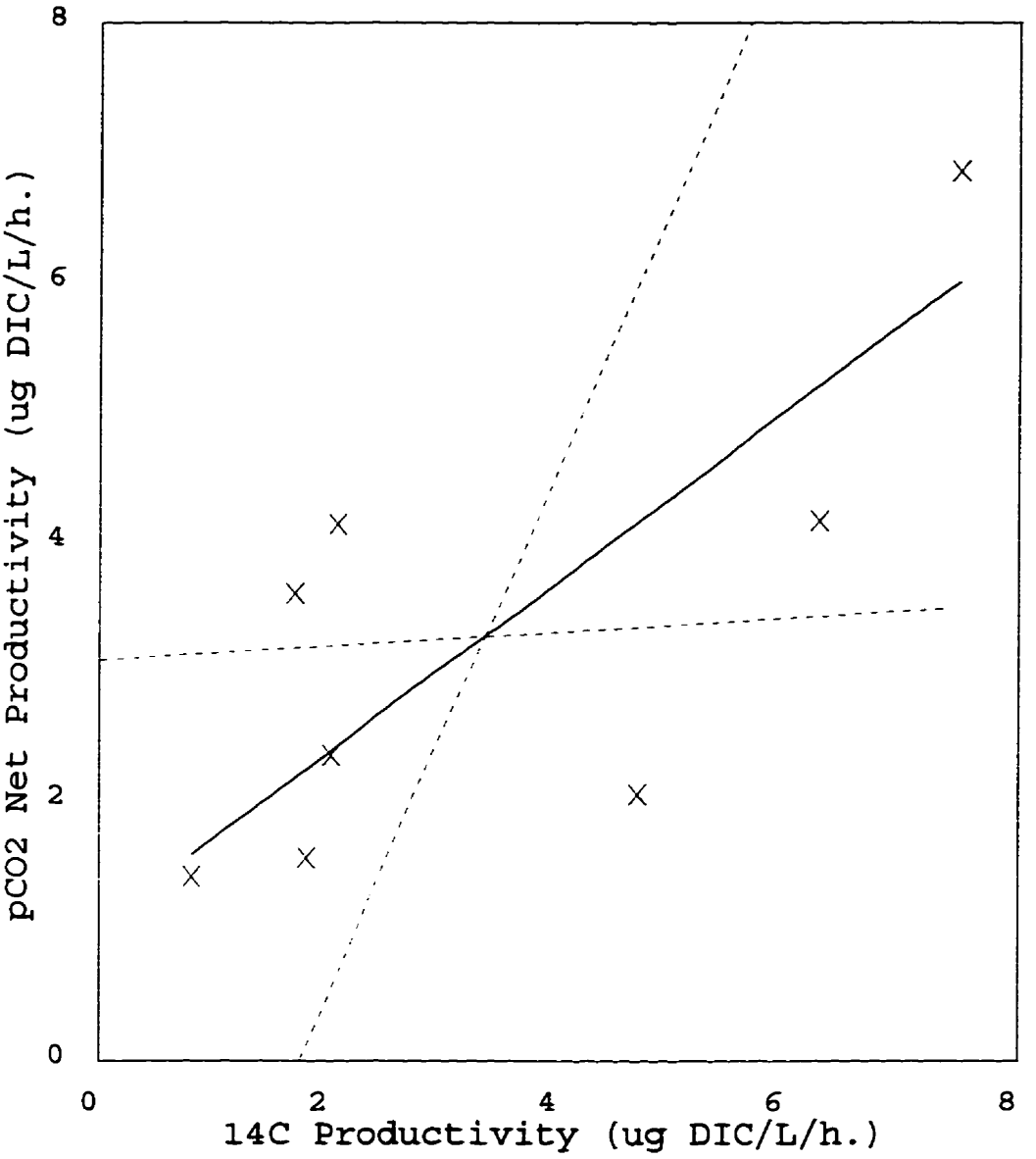

Figure 23: ^{14}C versus pCO_2 productivity for field measurements at the ELA.

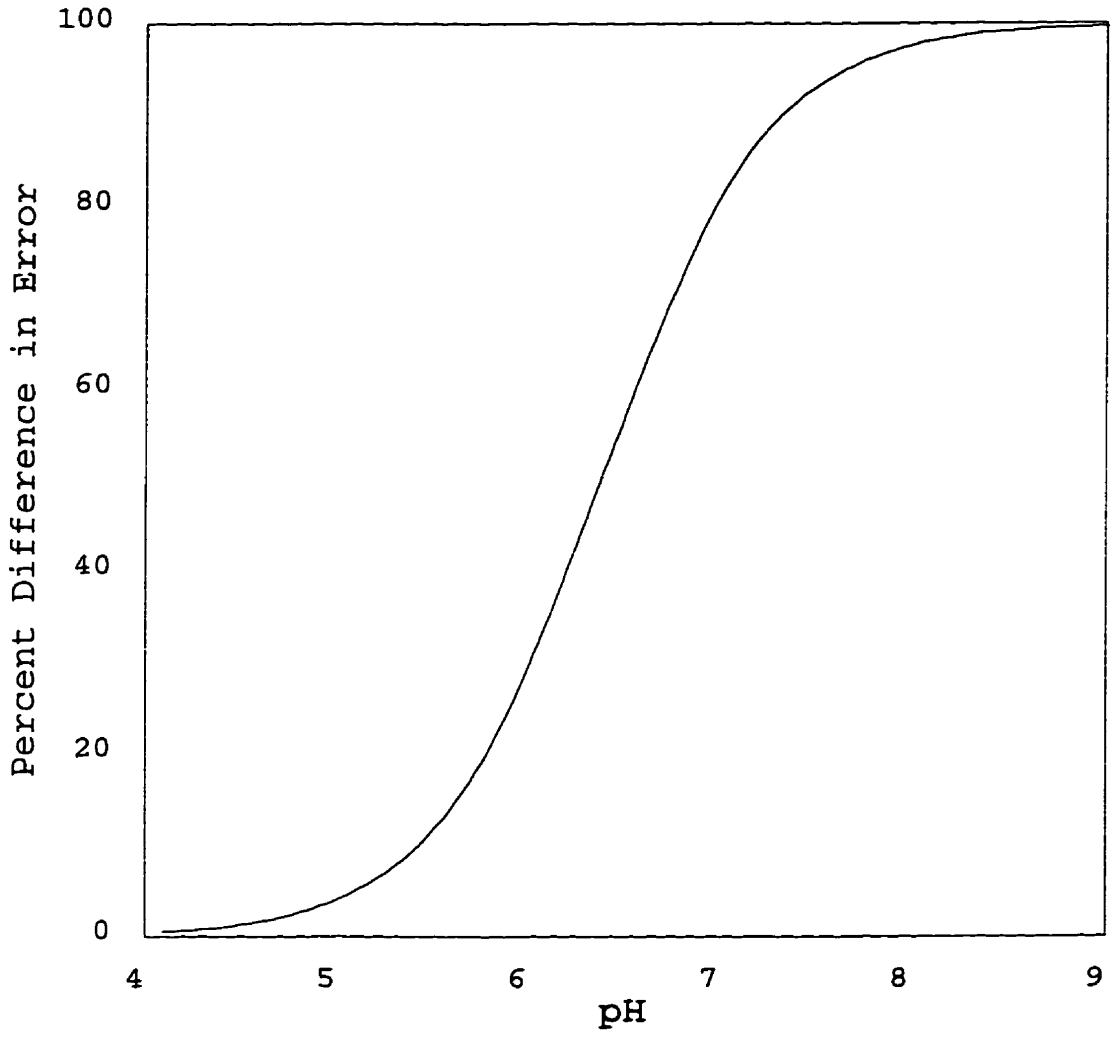

Figure 24: Percent difference in error between measuring CO_2 and DIC (assuming each measurement has the same error in CO_2 analysis) with change in pH (or the ratio of CO_2/DIC).

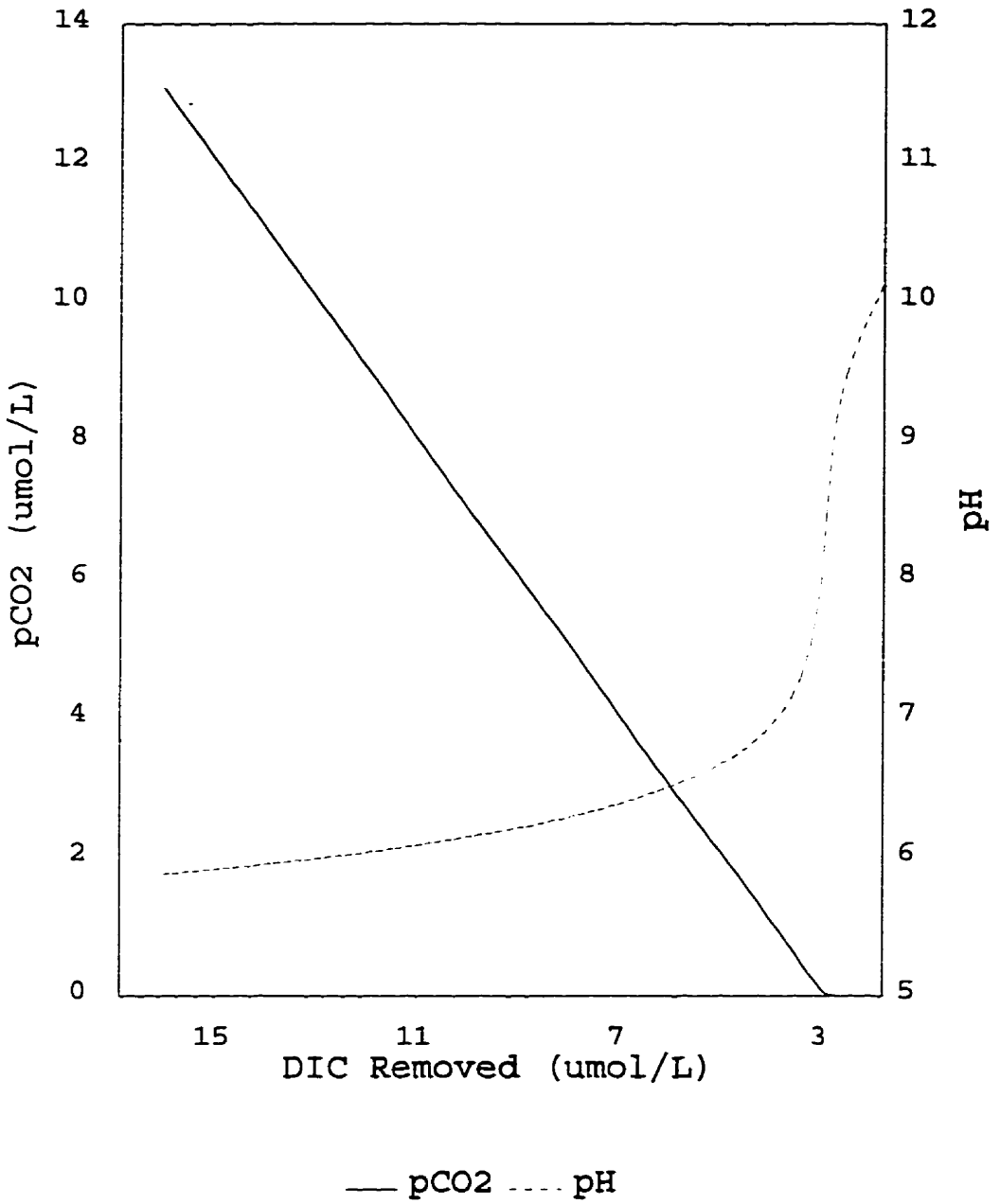

Figure 25a: pCO_2 decrease versus DIC removal assuming constant alkalinity for distilled water initially at a pH of 6. pH change with DIC removal is represented by the dashed line.

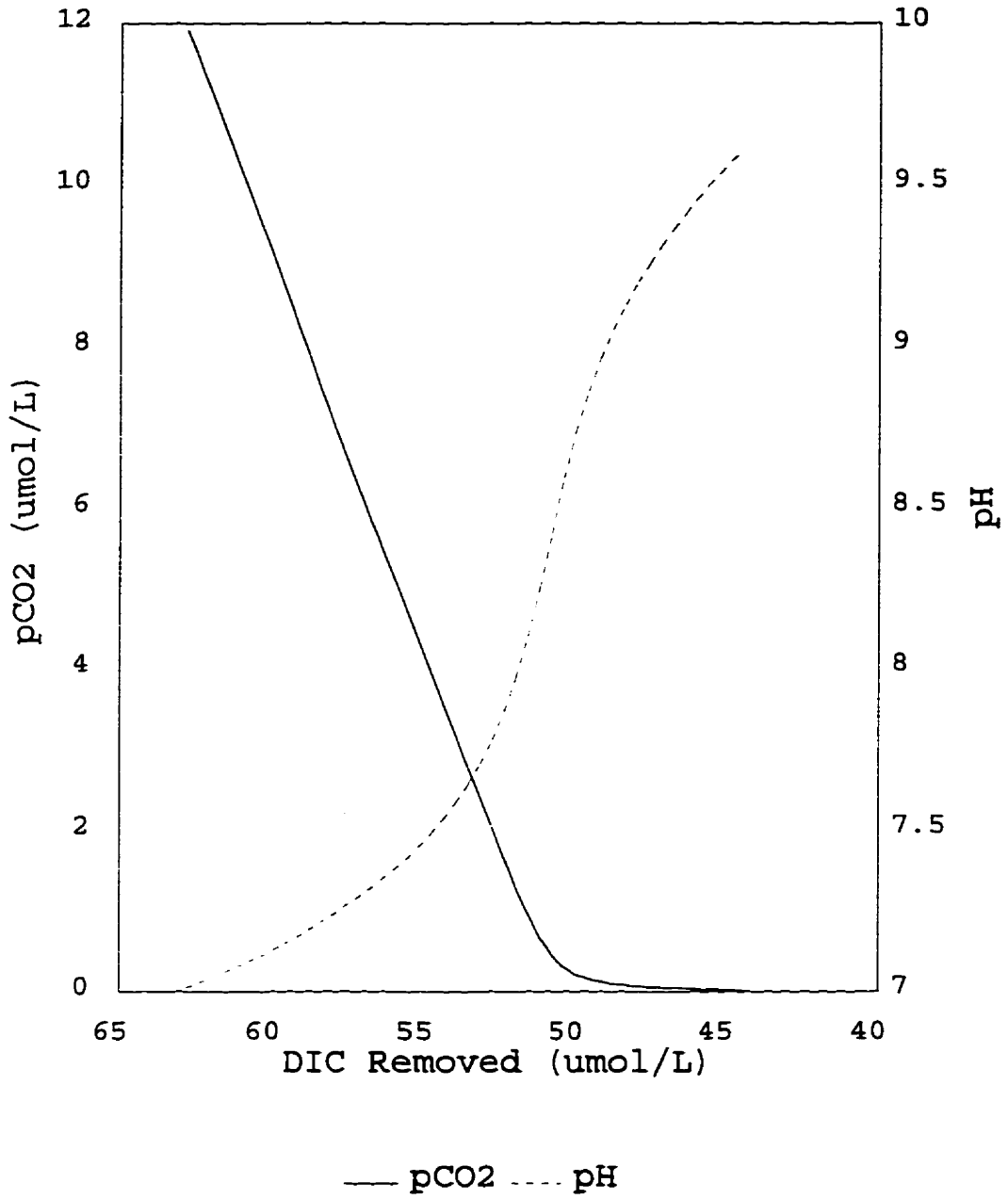

Figure 25b: pCO_2 decrease versus DIC removal assuming constant alkalinity for distilled water initially at a pH of 7. pH change with DIC removal is represented by the dashed line.

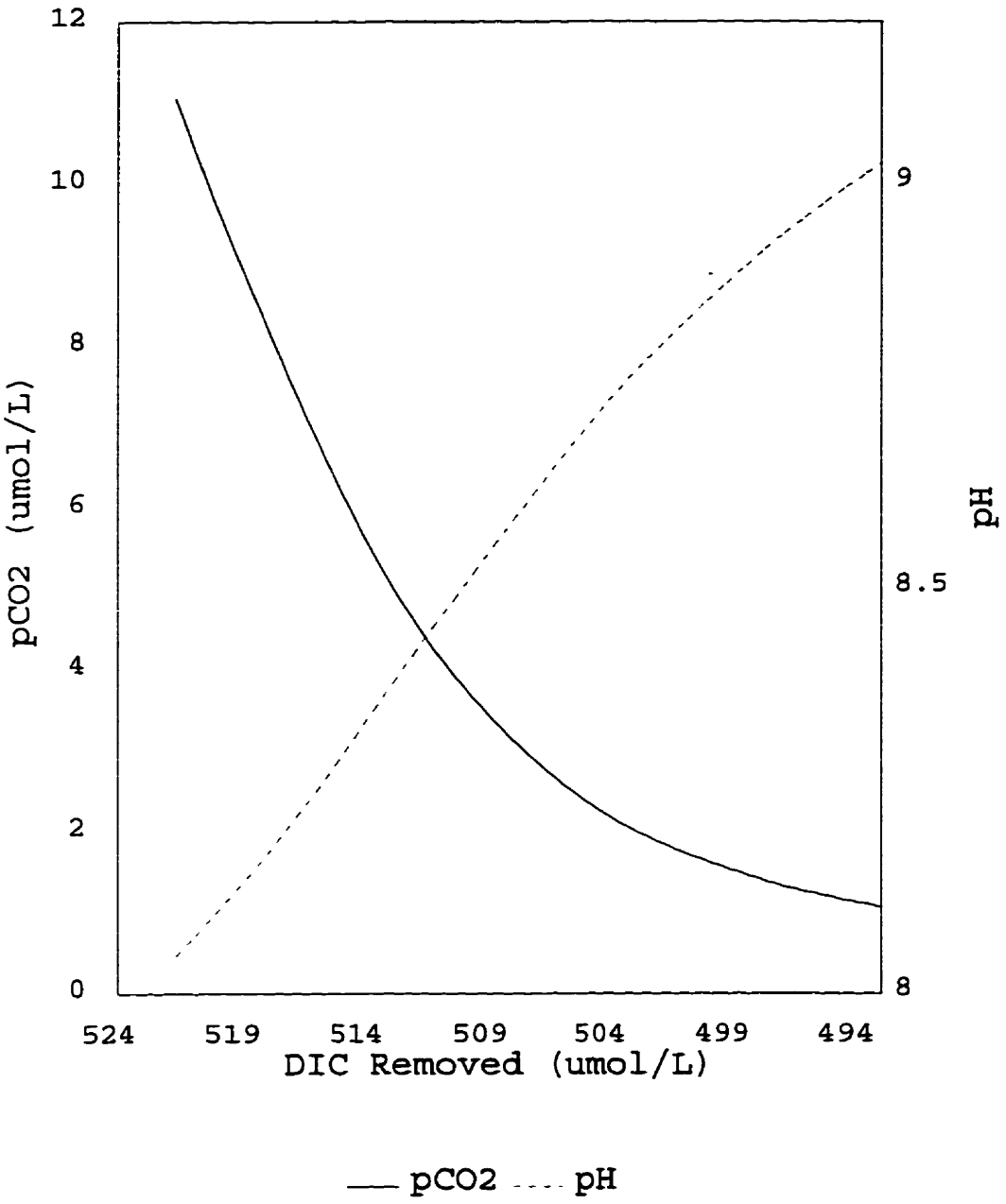

Figure 25c: pCO_2 decrease versus DIC removal assuming constant alkalinity for distilled water initially at a pH of 8. pH change with DIC removal is represented by the dashed line.

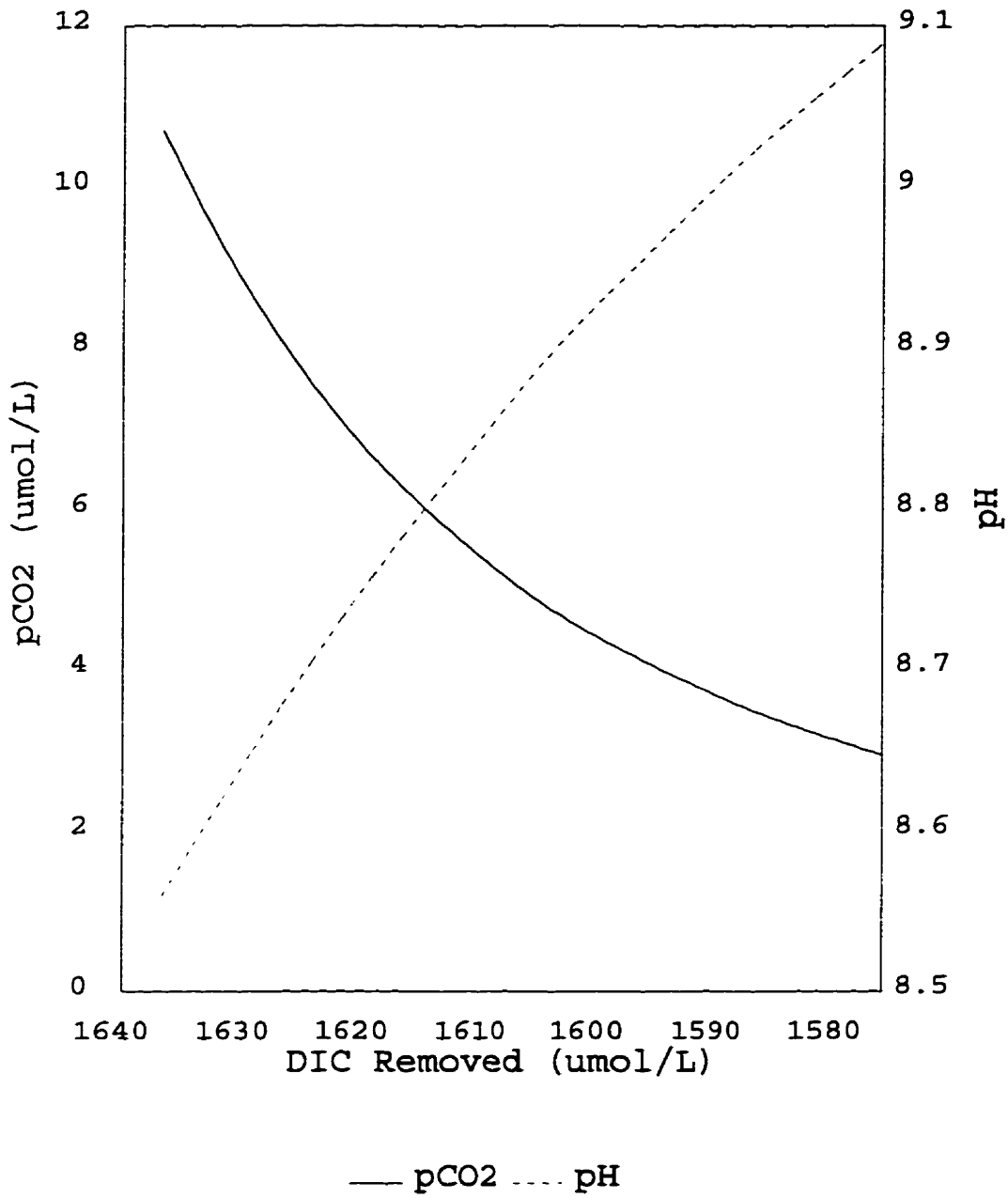

Figure 25d: pCO_2 decrease versus DIC removal assuming constant alkalinity for distilled water initially at a pH of 8.5. pH change with DIC removal is represented by the dashed line.

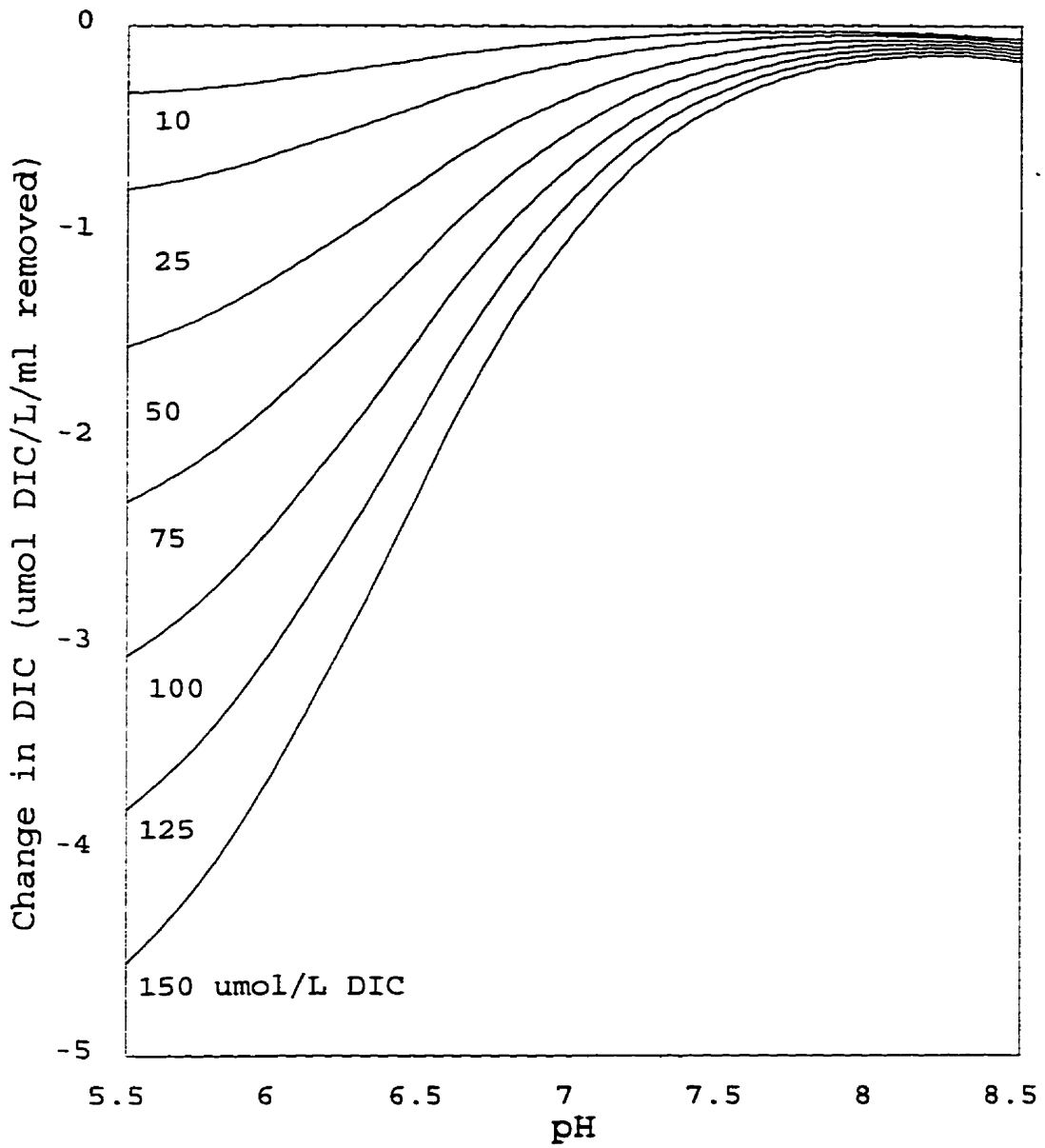

Figure 26: Effect on slope of DIC vs. volume removed as a function of pH at several DIC concentrations.

APPENDIX 1: Composition of WC' media.

	mg/litre	μM
$NaNO_3$	3.4	40
	42.5	500
K_2HPO_4*	0.27	2
	1.36	10
KCl	3.7	50
$MgSO_4 \bullet 7H_2O$	37.0	150
$CaCl \bullet 2H_2O$	36.8	250
$NaHCO_3$	16.8	200
$Na_2SiO_3 \bullet 9H_2O$	56.8	200

Trace metals*	mg/litre compound	weight/litre element	μM element
Na_2EDTA	2.18	-	ca. 5.85(EDTA)
$FeCl_3 \bullet 6H2O$	1.58	0.33 mg Fe	ca. 5.85
H_3BO_3	0.5	0.087 mg B	ca. 8.09
$MnCl_2 \bullet 4H_2O$	0.09	0.025 mg Mn	ca. 0.45
$ZnSO_4 \bullet 7H_2O$	0.011	2.50 μg Zn	ca. 0.038
$CoCl_2 \bullet 6H_2O$	0.005	1.24 μg Co	ca. 0.021
$CuSO_4 \bullet 5H_2O$	0.005	1.27 μg Cu	ca. 0.020
$Na_2MoO_4 \bullet 2H_2O$	0.003	1.19 μg Mo	ca. 0.012

Vitamins	
Thiamine (B_1)	0.1 mg/L
B_{12}	0.5 μg/L
Biotin	0.5 μg/L

* K_2HPO_4 and trace elements were autoclaved separately from each other and the rest of the media. Using aseptic techniques both were added to the media after at least one week from autoclaving.

Appendix 2: Theory of Gas Chromatographic Techniques.

Pressure-Lok® Syringe Technique

Standards: The G.C. measures the mass of CO_2 injected. The mass of CO_2 in the sample injected is dependent upon its pressure and volume. The parts-per-million (ppm) is known. Thus, in order to use standards for calculating the concentration of CO_2 in an unknown sample the standard injected must be corrected to either pressure and volume or the unknowns must be corrected to the conditions that the standards were measured under. It is simpler to inject the standards by first equilibrating them to atmospheric pressure, which is easily measured. If the volume of standards and samples is kept constant than no correction factor is needed for volume when calculating unknown concentrations. Therefore, the G.C. measures the mass of CO_2 in a fixed volume with a known partial pressure.

Unknown Samples: The unknown mass is calculated as an area from gas chromatography. From the area, volume of the unknown injected gas, and a standard curve of known CO_2 concentration, the concentration of CO_2 in the head-space can be determined. Samples of unknown concentration must be injected into the G.C. under the same pressure as they exist in the sample bottle (i.e. the Pressure-Lok® syringe must be closed before removing it from the sample and opened only

after the needle has penetrated the septum of the G.C.'s sampling port). The area from the unknown is corrected for the pressure (atmospheric) that the standards were measured at.

For example:

> A bottle of known concentration (1000ppm) has a pressure of 1520mmHg. Initially it is treated as a standard and injected at atmospheric pressure (760mmHg). If the same sample is treated as unknown and injected under pressure (1520mmHg) the calculated area integrated will be twice that obtained when it was injected as a standard, and thus twice the ppm (2000). This value is corrected for the pressure that the standard was measured at (760mmHg) by calculating the partial pressure of the CO_2 in the sample (pCO_2):
>
> pCO_2=(mL CO_2/mL gas)(pressure of standard/760mmHg)
>
> =(2000/1000000)(760mmHg/760mmHg)
>
> = 0.002

In a bottle which has a head-space/liquid partition the CO_2 in the liquid is determined using the calculated pCO_2 and Henry's solubility constant ($\propto$). The physical parameters required for this calculation are temperature and salt concentration (salt concentrations were considered to be zero for these experiments). In addition, head-space and liquid volumes are needed to calculate the concentration in μmol/L.

$$\propto = 10^{-(-a/T + d - cT)}$$

where: a = 2389.13 - 187.87(i)
d = 14.042 - (1.0126)(i)
c = 0.015303 - (0.00162283)(i)
T = absolute temperature (Kelvin)

$$[CO_2] = \propto (pCO_2)$$

M.T.I. "Vacuum-Pump" Technique

Standards: The MTI draws a sample through its sample loop, the sample valve closes, the vacuum pump turns off and a switch valve connects to the pressure regulator (carrier gas) which pressurizes the sample loop. The pressurized sample is then injected into the column. The amount of sample injected depends on the length of time the inject valve is open (user-defined, usually 40msec). The sample is not concentrated but is pressurized using the carrier gas. Therefore every sample will be at atmospheric pressure (briefly) before it is pressurized and subsequently injected. If the inject time remains constant then no correction for volume is needed. Thus, the mass of CO_2 measured from standards represents the volume (or ppm) of CO_2 at any pressure.

Unknown Samples: The area generated from gas chromatography represents the mass of the unknown sample at injection pressure. The pressure in the unknown sample must therefore be known in order to calculate the pCO_2 at the sample pressure.

Using the same example as above:

CO_2=(mL CO_2/mL gas)(pressure of standard/760mmHg)

=(1000/1000000)(1520mmHg/760mmHg)

= 0.002.

In a bottle that has several samples removed over time, a correction must be made for the change in head-space pressure. If the initial head-space pressure is known (i.e. it is equilibrated to atmospheric pressure before it is sealed) then the head-space pressure can be calculated by factoring the removal rate of gas for each sample:

$$P_t = P_0 - P_0(VR/H)$$

where: P_0 = pressure before sampling
P_t = pressure after sampling
VR = volume removed
H = head-space volume.

Appendix 3: Calculations used to determine DIC from pCO_2, and their derivations.

Calculations were performed using a spreadsheet in Quattro Pro 6.0 for Windows 3.1x. The pCO_2 at each sampling time and the DIC_a (after acidification) were measured using gas chromatography. From these values the DIC at each sampling time (DIC_t) was calculated assuming that the alkalinity did not change significantly relative to CO_2 during the incubation period (see Stumm and Morgan, 1981). The following is an outline of the calculations used to determine DIC_t.

Determination of Constants

Four constants are required for these calculations: Henry's Solubility Constant (K_h), the first and second dissociation constants of H_2CO_3 (K_1 and K_2), and the ion product of water (K_w). The effect of salts on the following equations are not considered since all of the incubations were conducted on samples from Canadian shield lakes which have low salt concentrations (assume M=0). All of the constants are temperature dependent (T=absolute temperature).

- K_h is defined by the equation (Harned and Davis, 1943):

$$-\log K_h = -(2385.73/T) + 14.0184 - 0.0152642*T$$

- K_1 is defined by the equation (Harned and Davis, 1943):

$$\log K_1 = -(3404.71/T) + 14.8435 - 0.032786*T$$

·K_2 is defined by the equation (Harned and Scholes, 1941):

$$\log K_2 = -(2902.39/T) + 6.4980 - 0.02377*T$$

·K_w is defined by the equation (Stumm and Morgan, 1981):

$$\log K_w = -(4470.99/T) + 6.0875 - 0.01706*T$$

Concentration of CO_2 in each bottle

The concentration of CO_2 (μmol/L) must first be determined for the head-space and liquid partitions within each bottle. For the liquid partition (μmol/L):

$$pCO_2 = (ppm\_CO_2)(mmHg\_atm.p./760mmHg)K_h \quad \textbf{(1)}$$

·where mmHg_atm.p. equals the atmospheric pressure in mmHg. For the head-space partition this equals (μmol/L):

$$pCO_2 = (ppm\_CO_2)(mmHg\_atm.p./760mmHg)(273K/K\_temp)(1/22.26) \quad \textbf{(2)}$$

In order to determine the actual amount of CO_2 in the liquid partition for each bottle multiply the concentration obtained from equation (1) by the mL_liquid volume/1000mL. Likewise, in order to determine the number of μmols of CO_2 in the head-space multiply the concentration obtained from equation (2) by the number of mL_gas volume/1000mL.

$CO_{2(aq)}$ equals the μmol in head-space + μmol in liquid (if concentration per L is desired multiply by 1000mL/mL_liquid volume). In essence this method "pushes" the CO_2 in the head-space back into the liquid partition. The volume of the liquid phase (not the volume of the whole bottle) is used in the determination of CO_2 concentration.

·For each bottle the values that are known are:

$CO_{2(aq)t}$ $CO_{2(aq)f}$ (f=final) DIC_f (equals $CO_{2(aq)a}$)

·The unknown species are:

H^+_t $HCO_3^-_t$ $CO_3^{2-}_t$ H^+_f $HCO_3^-_f$ $CO_3^{2-}_f$.

Determination of Hydrogen Ion (at final sampling time)

By definition: $DIC_f = CO_{2(aq)f} + HCO_3^-_f + CO_3^{2-}_f$ **(3)**

From Henderson-Hasselbalch equations we know:

$$K_1 = \frac{[H^+][HCO_3^-]}{[CO_2]} \quad \text{therefore} \quad [HCO_3^-] = \frac{K_1[CO_2]}{[H^+]} \qquad \textbf{(4)}$$

$$K_2 = \frac{[H^+][HCO_3^-]}{[HCO_3^-]} \quad \text{so that} \quad [CO_3^{2-}] = \frac{K_2[HCO_3^-]}{[H^+]}$$

·by further substitution for HCO_3^- (from equation 4):

$$[CO_3^{2-}] = \frac{K_1K_2[CO_2]}{[H^+]^2} \qquad \textbf{(5)}$$

·substitute for $HCO_3^-_f$ (equation 4) and $CO_3^{2-}_f$ (equation 5) into equation 3:

$$DIC_f = CO_{2(aq)f} + \frac{K_1[CO_{2(aq)f}]}{[H^+_f]} + \frac{K_1K_2[CO_{2(aq)f}]}{[H^+_f]^2}$$

·multiply all terms by: $\dfrac{[H^+_f]^2}{[CO_{2(aq)f}]}$

$$\frac{DIC_f[H^+_f]^2}{[CO_{2(aq)f}]} = \frac{[CO_{2(aq)f}][H^+_f]^2}{[CO_{2(aq)f}]} + \frac{K_1[H^+_f]^2[CO_{2(aq)f}]}{[H^+_f][CO_{2(aq)f}]} + \frac{K_1K_2[H^+_f]^2[CO_{2(aqf)}]}{[H^+_f]^2[CO_{2(aq)f}]}$$

·cancel and rearrange:

$$\frac{DIC_f[H^+_f]^2}{[CO_{2(aq)f}]} = [H^+_f]^2 + K_1[H^+_f] + K_1K_2$$

·so that:

$$0 = \left(1 - \frac{DIC_f}{[CO_{2(aq)f}]}\right)[H^+_f]^2 + K_1[H^+_f] + K_1K_2$$

Which is in the form of a quadratic equation ($0 = ax^2 + bx + c$) and can be solved using the quadratic formula:

$$x = \frac{-b \pm \sqrt{b^2 - 4ac}}{2a}$$

·then:

$$[H^+_f] = \frac{-K_1 \pm \sqrt{K_1^2 - 4K_1K_2\left(1 - \frac{DIC_f}{[CO_{2(aq)f}]}\right)}}{2\left(1 - \frac{DIC_f}{[CO_{2(aq)f}]}\right)}$$

Determination of Bicarbonate, Carbonate and Hydroxyl Ions

$$[HCO_3^-] = \frac{K_1[CO_2]}{[H^+]}$$

$$[CO_3^{2-}] = \frac{K_2[HCO_3^-]}{[H^+]}$$

and:

$$[OH^-] = \frac{K_w}{[H^+_f]} \qquad (6)$$

Determination of Alkalinity

Alk_f (final bicarbonate alkalinity) can now be solved:

$$Alk_f = HCO_3^-{}_f + 2(CO_3^{2-}{}_f) + OH^- - H^+$$

Determination of Bicarbonate (at time "t")

Assuming that $Alk_f = Alk_t$ then we can solve for $HCO_3^-{}_t$:

$$Alk_t = HCO_3^-{}_t + 2(CO_3^{2-}{}_t) + OH^- - H^+$$

·substitute for $CO_3^{2-}{}_t$ (equation 5) and OH^- (equation 6):

$$Alk_t = HCO_3^-{}_t + \frac{2K_1K_2[CO_{2(aq)t}]}{[H^+_t]^2} + \frac{K_w}{[H^+_t]} - H^+_t \quad (7)$$

From equation 4 we know that: $[H^+] = \frac{K_1[CO_2]}{[HCO_3^-]}$ (8)

·substitute for H^+_t (equation 8) into equation 7, so that the only unknown is $HCO_3^-{}_t$:

$$Alk_t = HCO_3^-{}_t + \frac{2K_1K_2[CO_{2(aq)t}][HCO_3^-{}_t]^2}{(K_1[CO_{2(aq)t}])^2} + \frac{K_w[HCO_3^-{}_t]}{(K_1[CO_{2(aq)t}])} - \frac{K_1[CO_{2(aq)t}]}{[HCO_3^-{}_t]}$$

·cancel like terms:

$$Alk_t = HCO_3^-{}_t + \frac{2K_2[HCO_3^-{}_t]^2}{K_1[CO_{2(aq)t}]} + \frac{K_w[HCO_3^-{}_t]}{(K_1[CO_{2(aq)t}])} - \frac{K_1[CO_{2(aq)t}]}{[HCO_3^-{}_t]}$$

·multiply both sides by $HCO_3^-{}_t$:

$$Alk_t[HCO_3^-{}_t] = [HCO_3^-{}_t]^2 + \frac{2K_2[HCO_3^-{}_t]^3}{K_1[CO_{2(aq)t}]} + \frac{K_w[HCO_3^-{}_t]^2}{(K_1[CO_{2(aq)t}])} - K_1[CO_{2(aq)t}]$$

·rearrange according to power:

$$0 = \frac{2K_2[HCO_3^-{}_t]^3}{K_1[CO_{2(aq)t}]} + \left(\frac{K_w}{K_1[CO_{2(aq)t}]} + 1\right)[HCO_3^-{}_t]^2 - Alk_t[HCO_3^-{}_t] - K_1[CO_{2(aq)t}]$$

Which is in the form of a cubic equation:

$$0 = ny^3 + p'y^2 + q'y + r'$$

where:

$y = [HCO_3^-{}_t]$; $n = \frac{2K_2}{k_1[CO_{2(aq)t}]}$; $p' = p(n)$; $q' = q(n)$; $r' = r(n)$

and: $p = (K_w/K_1[CO_{2(aq)t}] + 1)/n$

$q = -Alk_t/n$

$r = -K_1[CO_{2(aq)t}]/n$

·multiply all terms by 1/n so that the equation takes the form:

$$0 = y^3 + (p'/n)y^2 + (q'/n)y + r'/n$$
$$0 = y^3 + py^2 + qy + r \quad \textbf{(8)}$$

In equation 8 if y is replaced by: "x - p/2" it can be reduced to equation 10:

$$y = x - \frac{p}{2} \quad \textbf{(9)}$$

$$0 = x^3 + ax + b \quad \textbf{(10)}$$

where: $a = 1/3(3p - q^3)$
$b = 1/27(2p^3 - 9pq + 27r)$

Note: this solution for a cubic equation is based on that which is outlined in the CRC Mathematical Tables

Note: the trigonometric solution is used for solving this equation (this avoids the use of imaginary numbers which arise in the algebraic solution)

In the equation $x^3 + ax + b = 0$

Let $x = m\cos\theta$ **(11)**

·so that:

$$0 = m\cos^3\theta + am\cos\theta + b \quad \textbf{(12)}$$

From trigonometric identities we know that:

$$\cos(3\theta) = 4\cos^3\theta - 3\cos\theta$$
so that: $0 = 4\cos^3\theta - 3\cos\theta - \cos(3\theta)$ **(13)**

Since both equations 12 and 13 equal zero:

$$m\cos^3\theta + am\cos\theta + b = 4\cos^3\theta - 3\cos\theta - \cos(3\theta) \quad \textbf{(14)}$$

From equation 14, where both sides have the form "$ax^3 + bx + c$" and x is the same on both sides, we know that the following are true:

$$\frac{4}{m^3} = \frac{-3}{am} \tag{15}$$

and

$$\frac{-3}{am} = \frac{-\cos(3\theta)}{b} \tag{16}$$

Note: we can put "m" in the denominator since m cannot equal zero. This is part of the assumption when the cubic equation is reduced to the form "$x^3 + ax + b = 0$" since a*b cannot equal zero.

From equation 15: $$m = 2\sqrt{(-a/3)} \tag{17}$$

From equation 16: $$\cos(3\theta) = \frac{3b}{am} \tag{18}$$

Remember that: $x = m\cos\theta$ (equation 11)
·so that: $m = x/\cos\theta$
·therefore by substitution into equation 17:

$$x_1 = 2\sqrt{(-a/3)}\cos\theta_1$$

$$x_2 = 2\sqrt{(-a/3)}\cos\theta_2$$

$$x_3 = 2\sqrt{(-a/3)}\cos\theta_3$$

where θ_1, θ_2, and θ_3 are the solution to: $\cos(3\theta) = \frac{3b}{am}$

Note: if θ_1 is the smallest then: $\theta_2 = \theta_1 + \frac{2\pi}{3}$

$$\theta_3 = \theta_1 + \frac{4\pi}{3}$$

•Solve for "m" (equation 17) using "a" as defined in equation 11

•Solve for "θ" (equation 18) using "b" as defined in equation 11

•Solve for "x" (equation 11)

•Solve for "y" (equation 9)

$HCO_3^-{}_t = y$

Determination of DIC (at time "t")

$$DIC_t = CO_{2(aq)t} + HCO_3^-{}_t + CO_3^{2-}{}_t$$

·substitute for $CO_3^{2-}{}_t$ (equation 5):

$$DIC_t = CO_{2(aq)t} + HCO_3^-{}_t + \frac{K_1K_2[CO_{2(aq)t}]}{[H^+_f]^2} \qquad (19)$$

·substitute for $[H^+_f]$ (equation 8) into equation 19:

·therefore $$DIC_t = CO_{2(aq)t} + HCO_3^-{}_t + \frac{K_1K_2[CO_{2(aq)t}][HCO_3^-{}_t]^2}{K_1^2[CO_{2(aq)t}]^2}$$

$$DIC_t = CO_{2(aq)t} + HCO_3^-{}_t + \frac{K_2[HCO_3^-{}_t]^2}{K_1[CO_{2(aq)t}]}$$

Appendix 4: Location of field study area.

Experimental Lakes Area, Northwestern Ontario

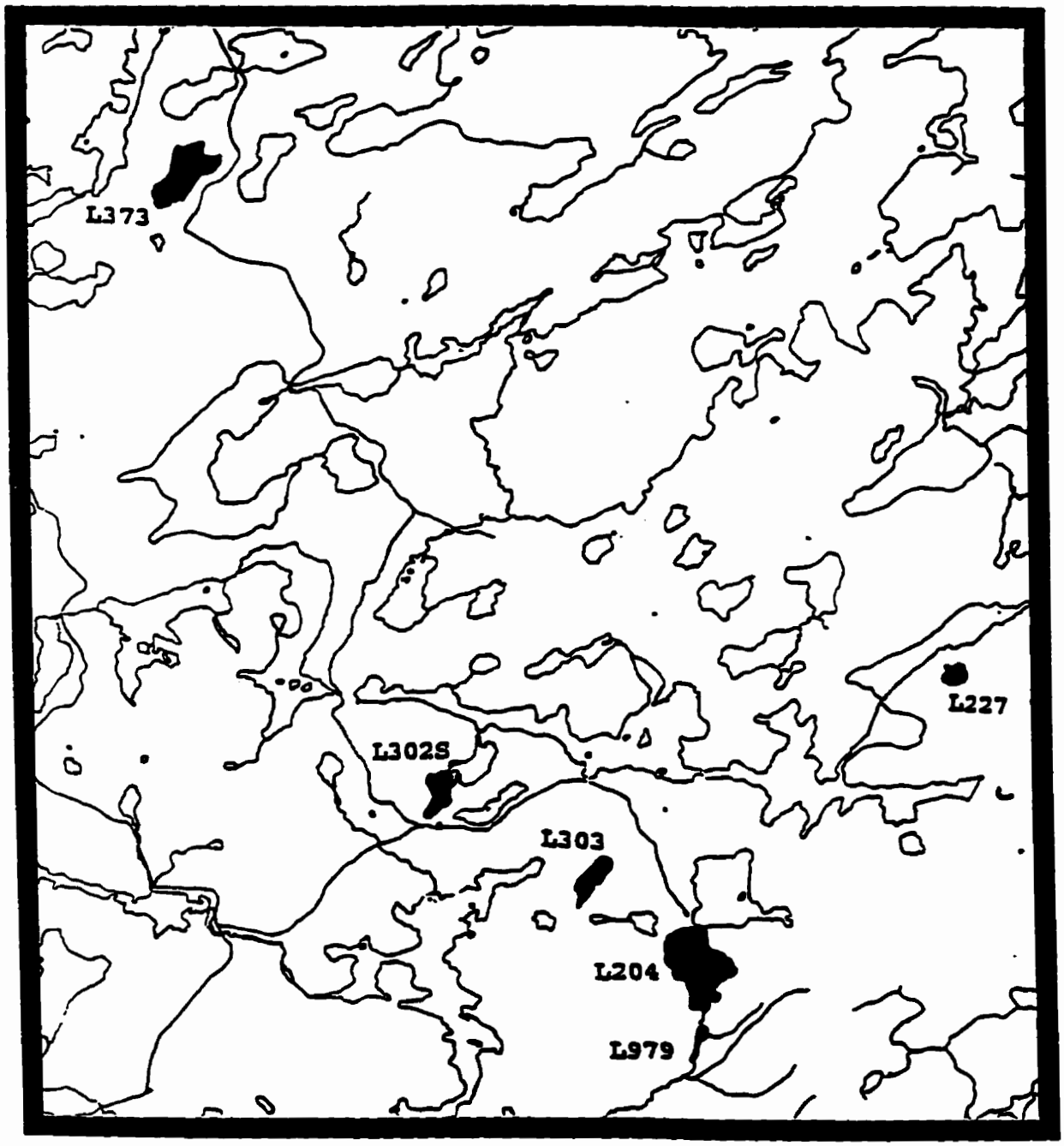

Appendix 5: R-squared values from slope calculations determined from the change in DIC concentrations during chemostat incubations. Code: light bottles 1 to 3 (LB1, LB2, LB3) and dark bottles 1 and 2 (DB1, DB2). The symbols relate to each of the bottle's respective markers in Appendix 6. Chemostat identifiers are outlined in Table 1.

Chemostat	LB1 □	LB2 ○	LB3 △	DB1 ■	DB2 ●
1NP(i)	0.980	0.989	0.986	0.999	0.996
1NP(ii)	0.976	0.944	0.965	NS	0.992
2NP(i)	0.999	0.995	0.999	0.999	0.997
2NP(ii)	0.993	0.992	0.993	0.979	0.990
3NP(i)	0.995	0.995	0.998	0.996	0.997
3NP(ii)	0.997	0.999	0.998	0.981	0.987
1P(i)	0.974	0.973	0.993	0.983	0.982
2P(i)	0.891	0.924	0.977	0.973	0.935
2P(ii) C.C.	0.992	0.998	0.995	0.998	0.977
3P(i)	0.988	0.971	0.989	0.997	0.999
3P(ii) C.C.	0.996	0.705	0.998	0.999	0.922
1N(i)	0.995	0.977	0.992	0.999	0.994
1N(ii)	0.952	0.992	0.957	NS	0.982
2N(i)	0.998	0.999	0.995	0.990	0.997
2N(ii)	0.980	0.990	0.983	NS	0.969
3N(i)	0.998	0.998	0.995	0.997	0.999
3N(ii)	0.983	0.962	0.944	0.959	0.957

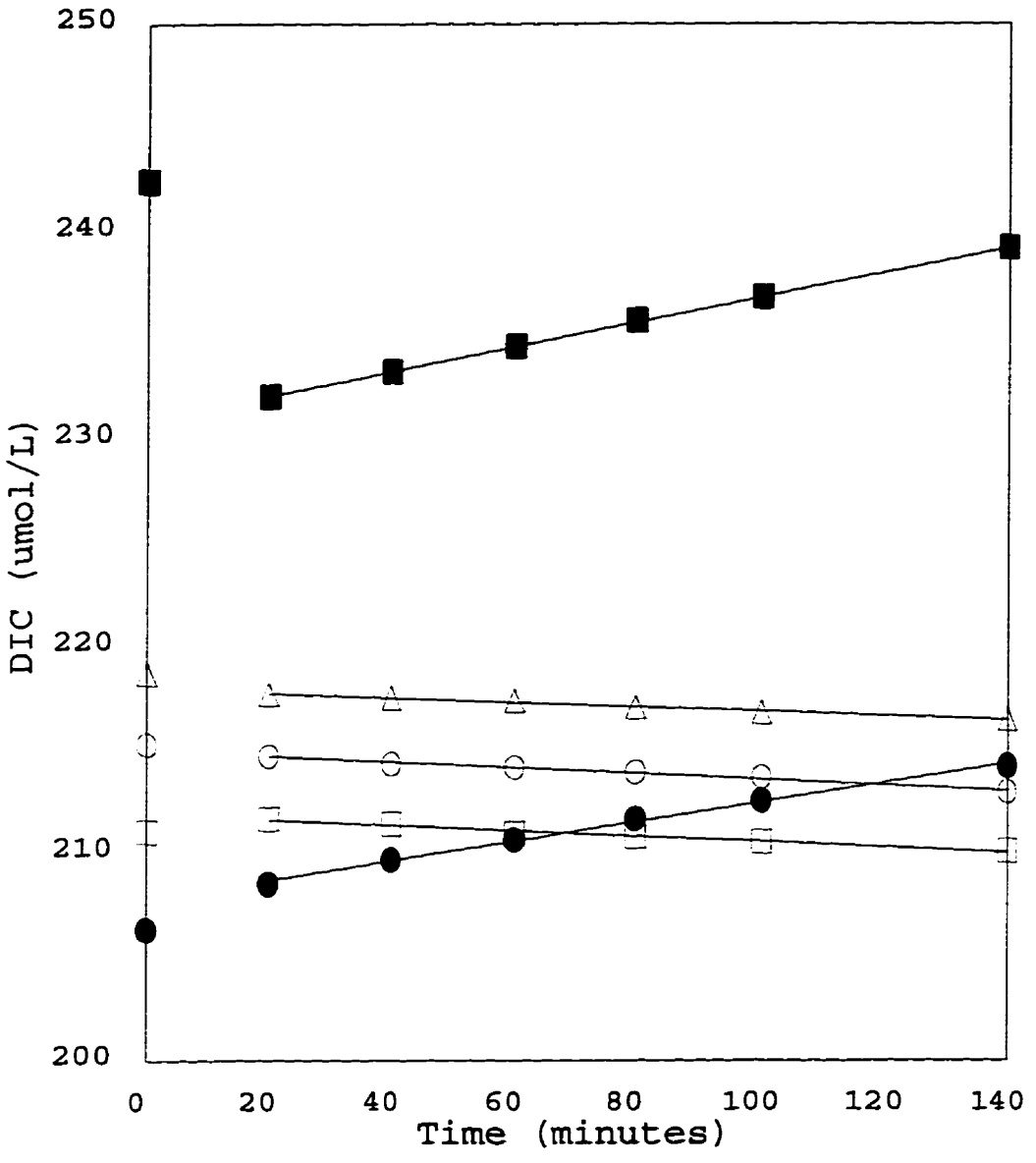

Appendix 6(a): Summary of incubation for chemostat 1NP(i). Light bottle = LB; Dark bottle = DB: LB1(□), LB2(○), LB3(△), DB1 (■), and DB2(●).

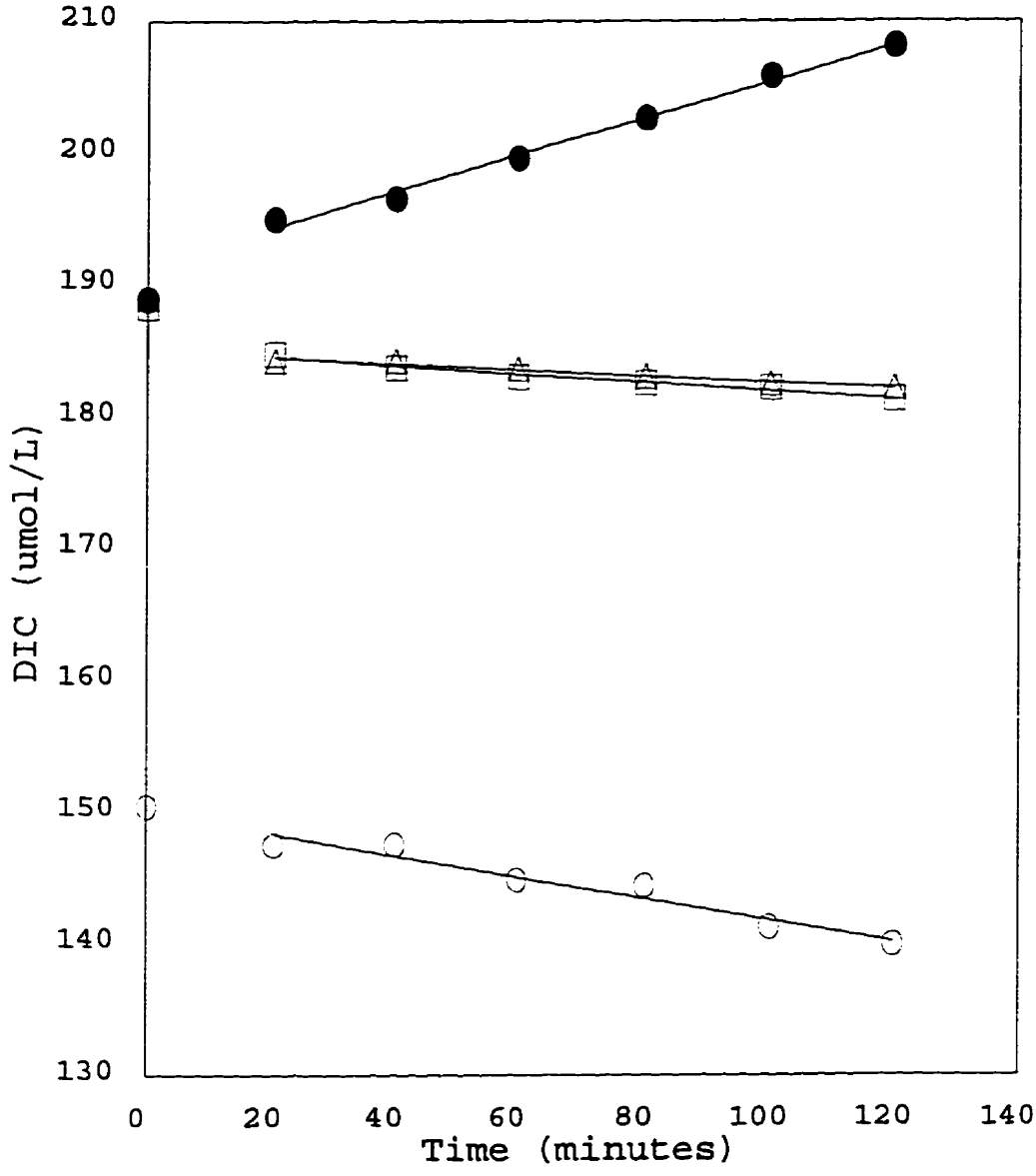

Appendix 6(b): Summary of incubation for chemostat 1NP(ii). Light bottle = LB; Dark bottle = DB: LB1(□), LB2(○), LB3(△), and DB2(●).

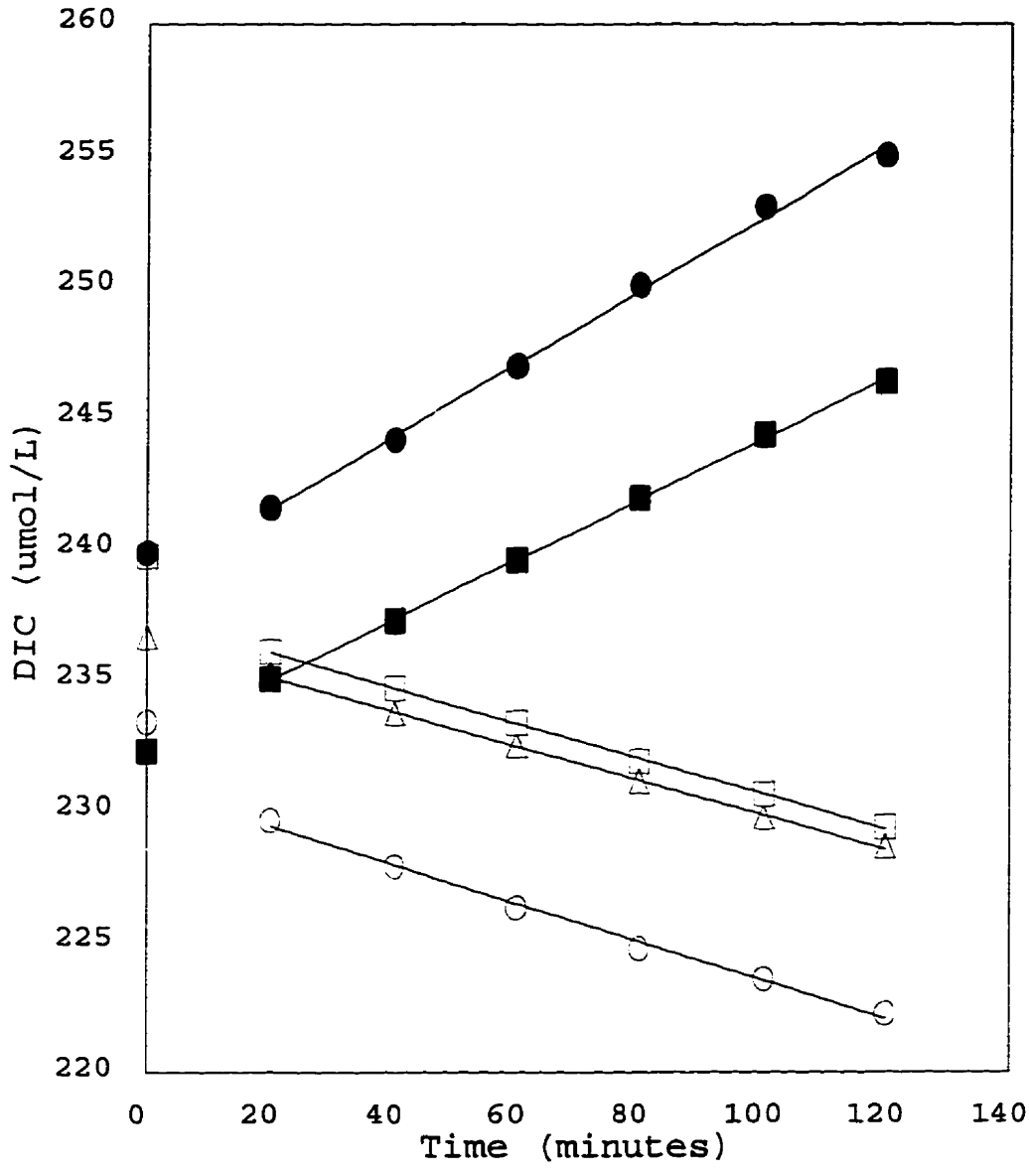

Appendix 6(c): Summary of incubation for chemostat 2NP(i). Light bottle = LB; Dark bottle = DB: LB1(□), LB2(○), LB3(Δ), DB1 (■), and DB2(●).

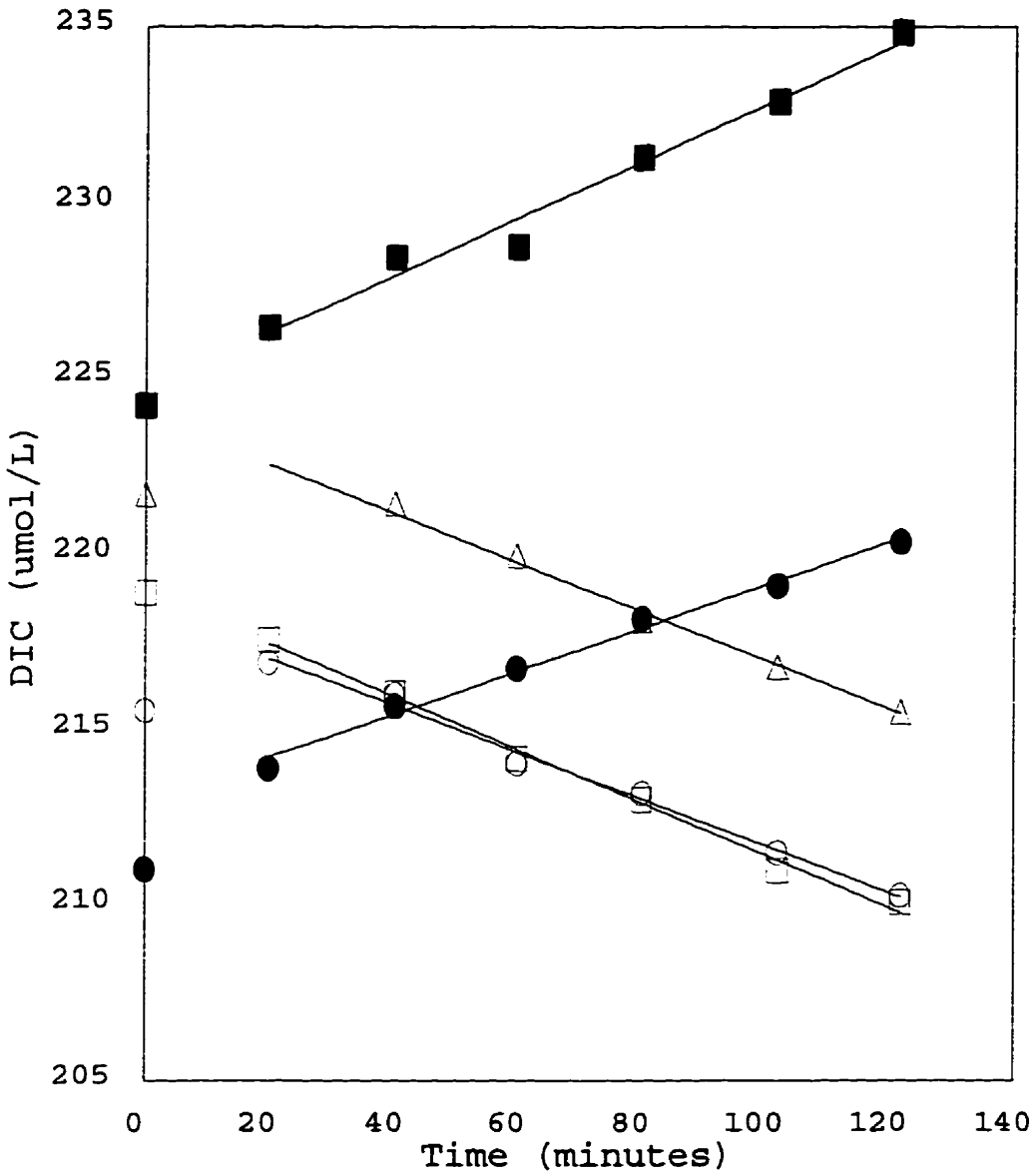

Appendix 6(d): Summary of incubation for chemostat 2NP(ii). Light bottle = LB; Dark bottle = DB: LB1(□), LB2(○), LB3(△), DB1 (■), and DB2(●).

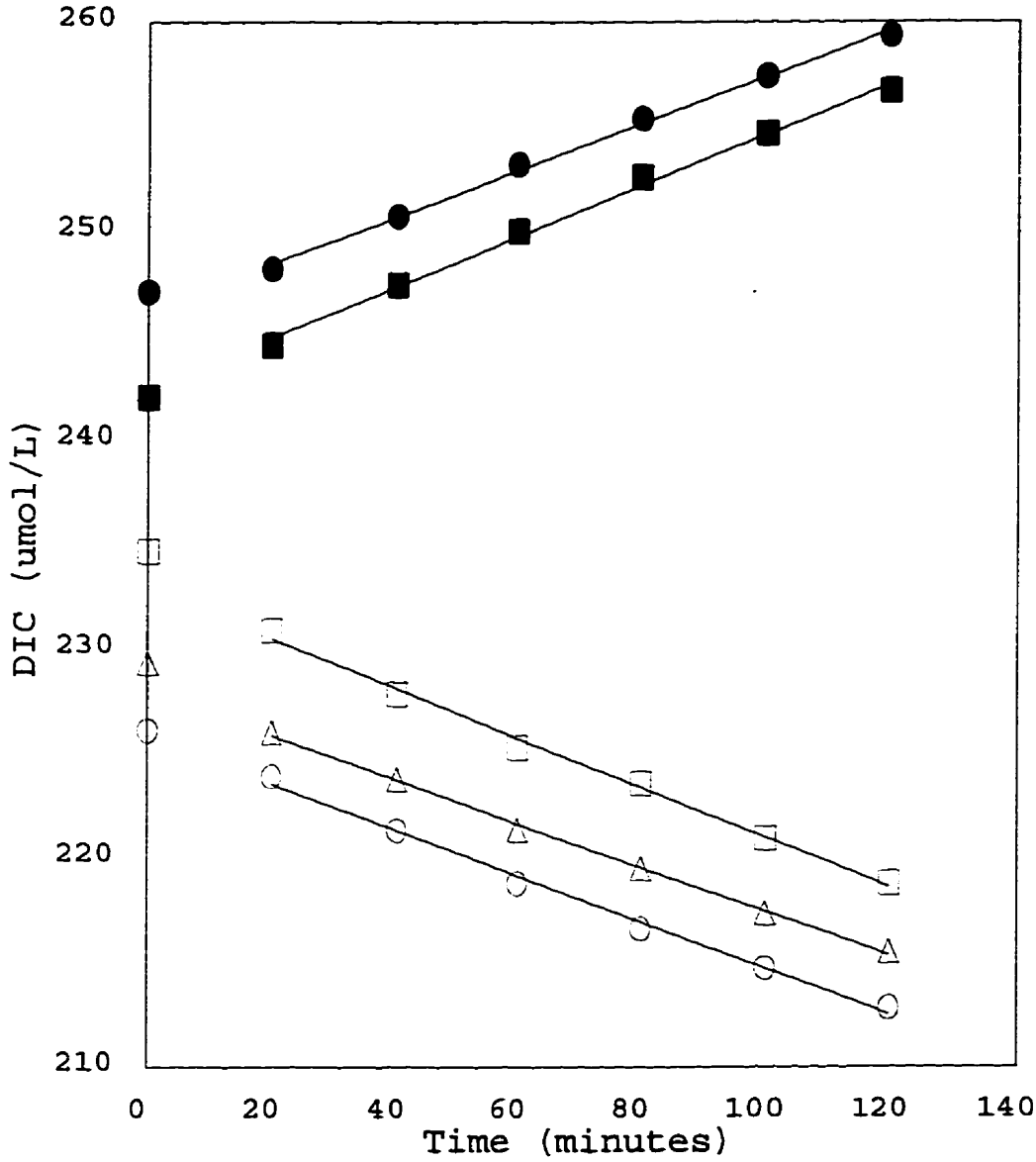

Appendix 6(e): Summary of incubation for chemostat 3NP(i). Light bottle = LB; Dark bottle = DB: LB1(□), LB2(○), LB3(△), DB1 (■), and DB2(●).

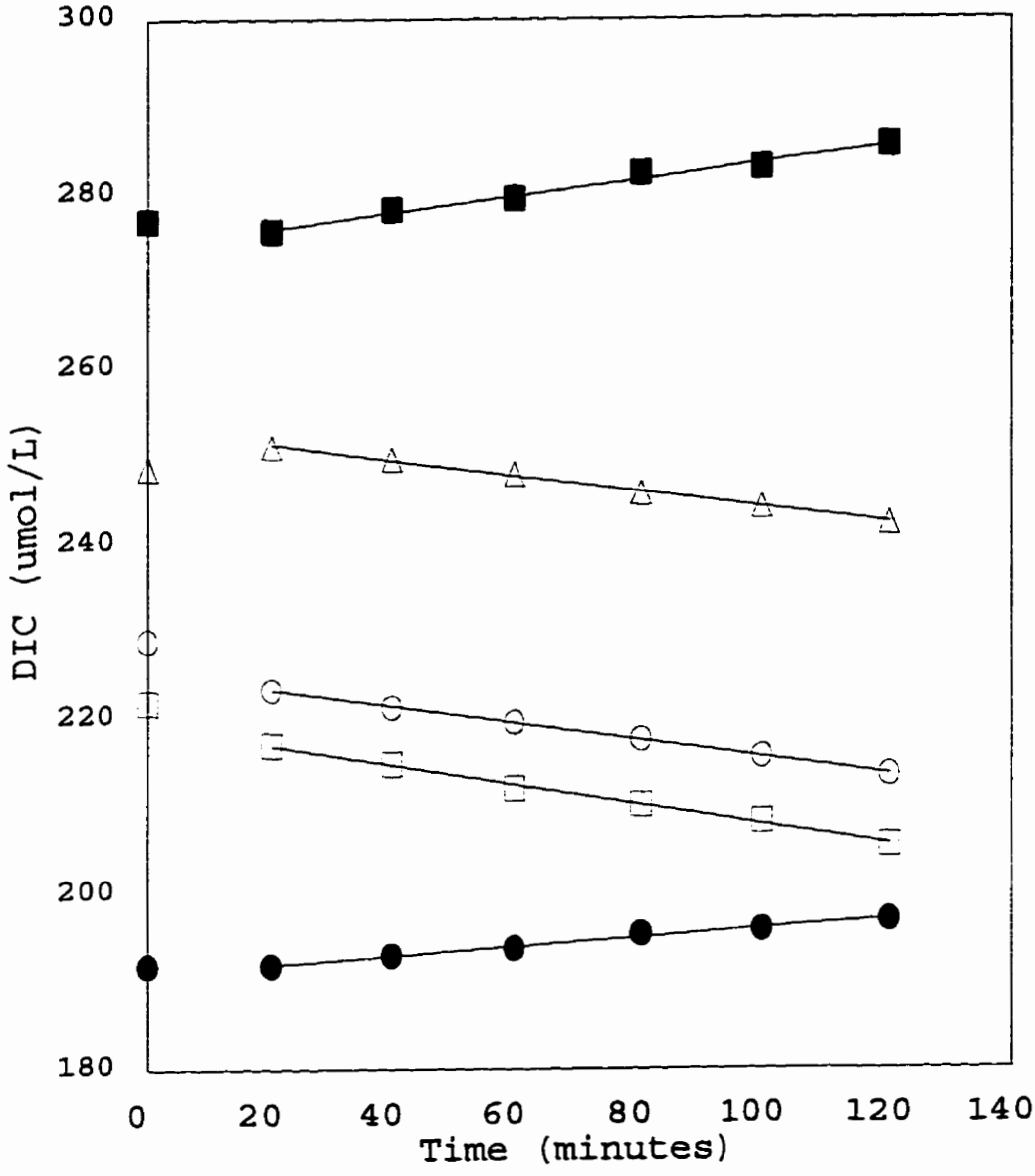

Appendix 6(f): Summary of incubation for chemostat 3NP(ii). Light bottle = LB; Dark bottle = DB: LB1(□), LB2(○), LB3(△), DB1 (■), and DB2(●).

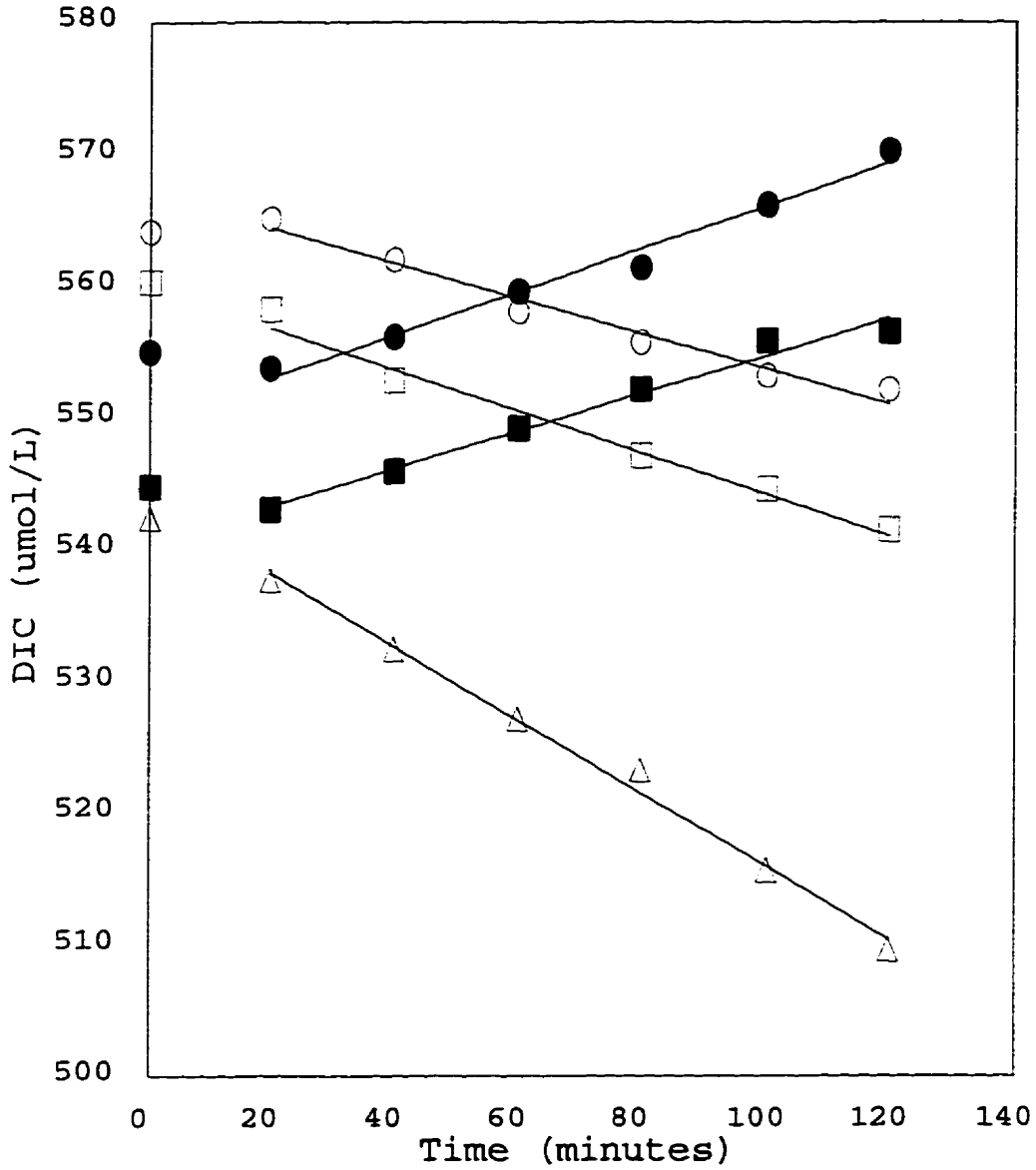

Appendix 6(g): Summary of incubation for chemostat 1P(i). Light bottle = LB; Dark bottle = DB: LB1(□), LB2(○), LB3(△), DB1 (■), and DB2(●).

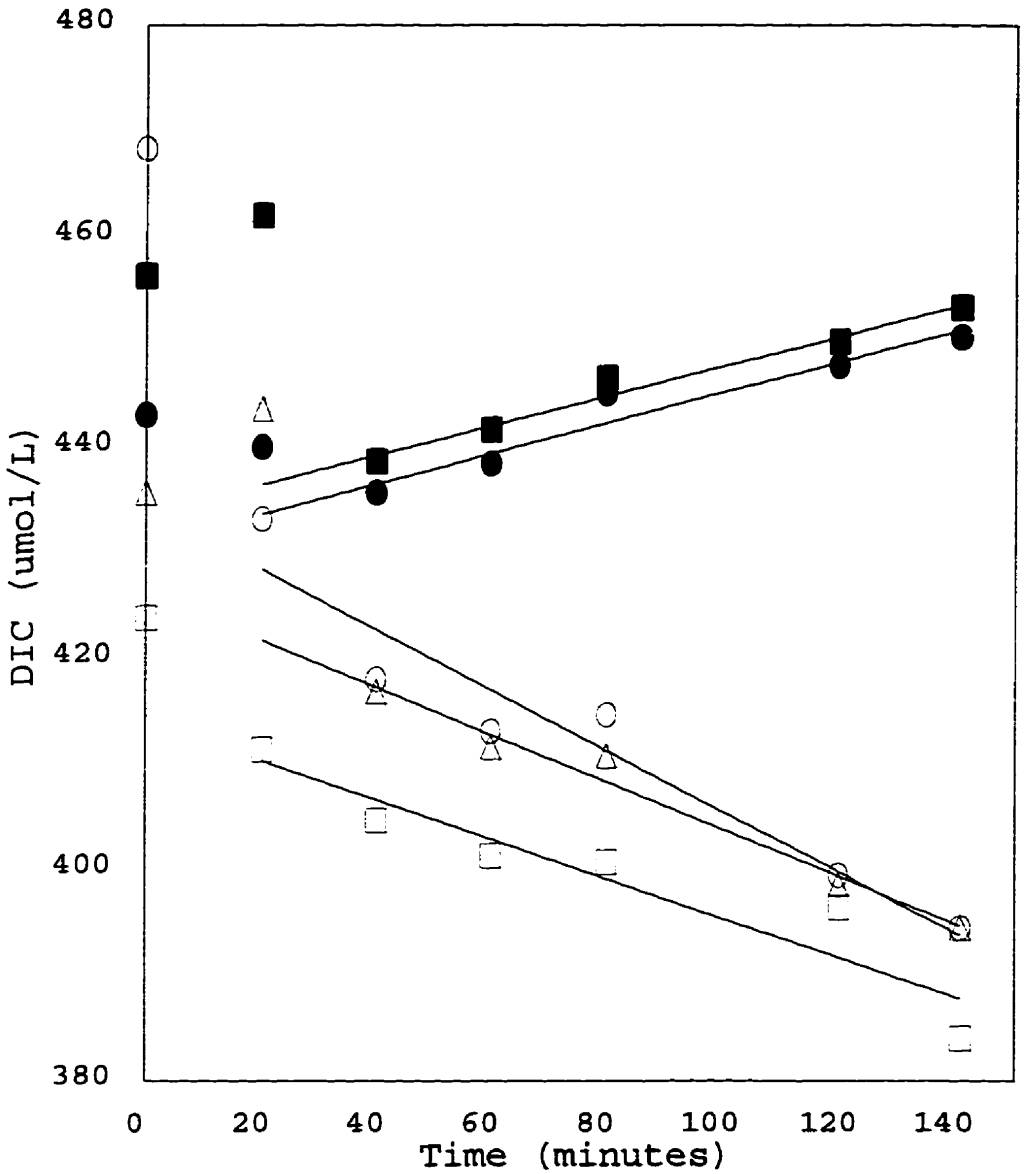

Appendix 6(h): Summary of incubation for chemostat 2P(i). Light bottle = LB; Dark bottle = DB: LB1(□), LB2(○), LB3(Δ), DB1 (■), and DB2(●).

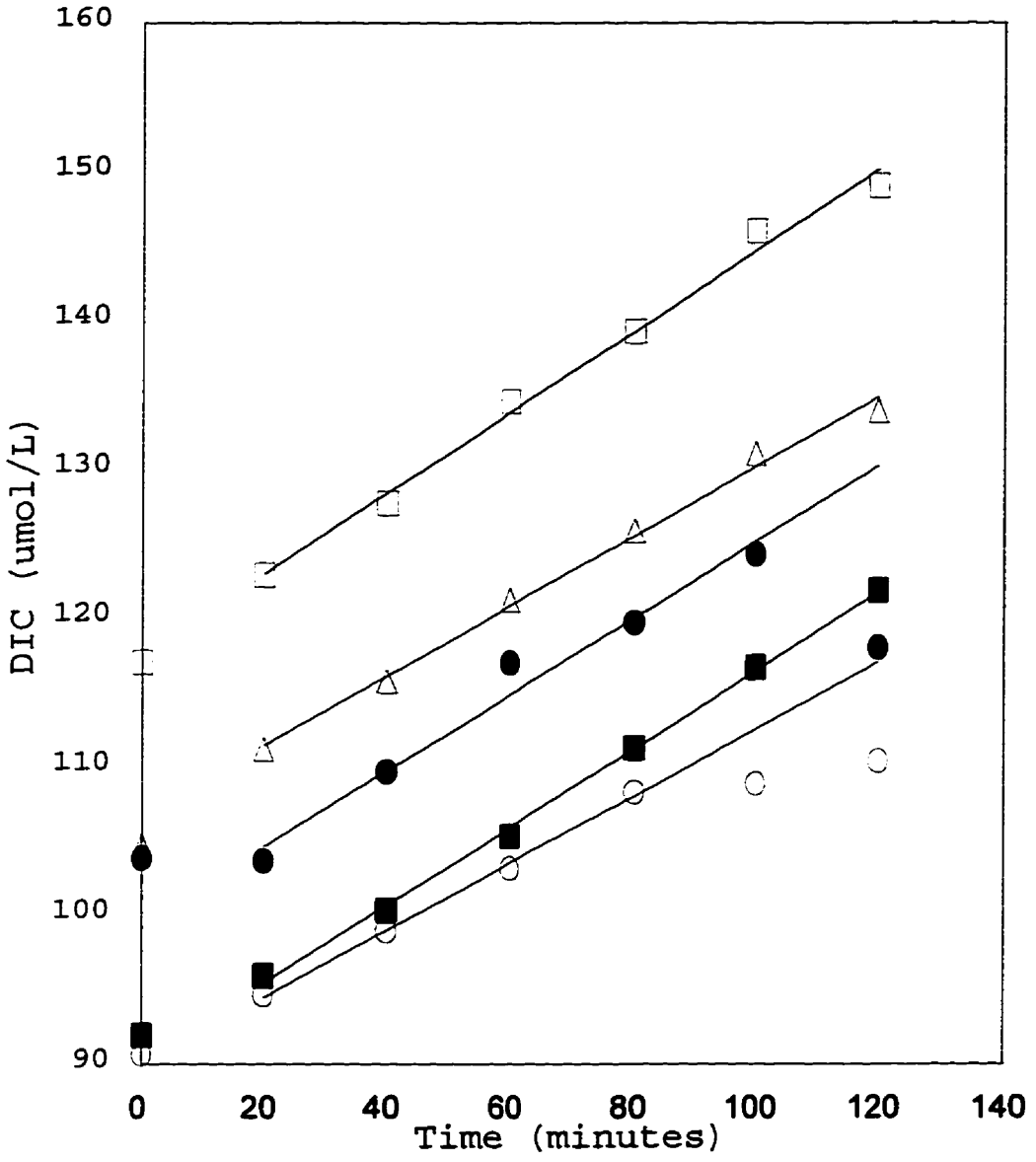

Appendix 6(i): Summary of incubation for chemostat 2P(ii). Light bottle = LB; Dark bottle = DB: LB1(□), LB2(○), LB3(△), DB1 (■), and DB2(●).

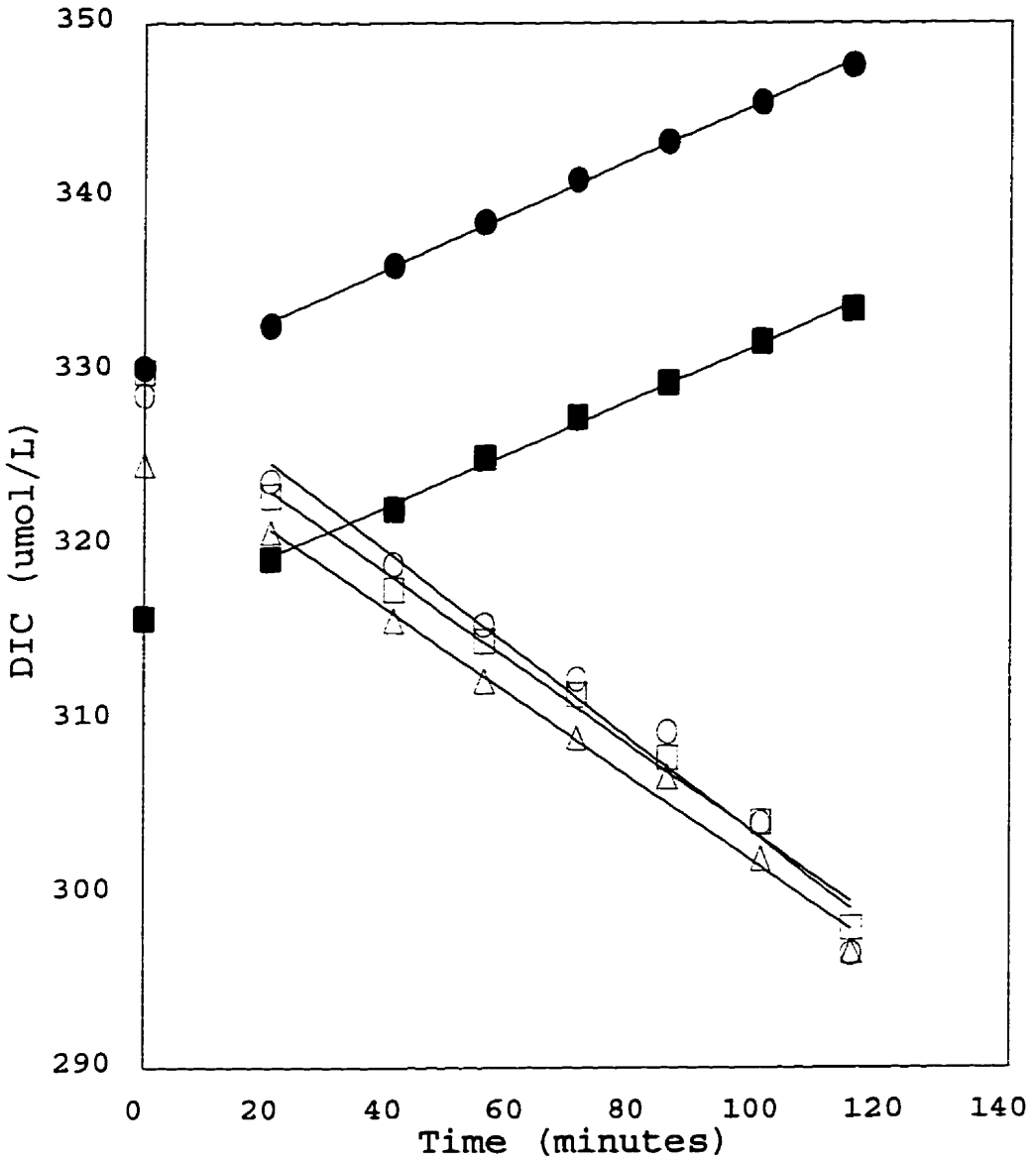

Appendix 6(j): Summary of incubation for chemostat 3P(i). Light bottle = LB; Dark bottle = DB: LB1(□), LB2(○), LB3(△), DB1 (■), and DB2(●).

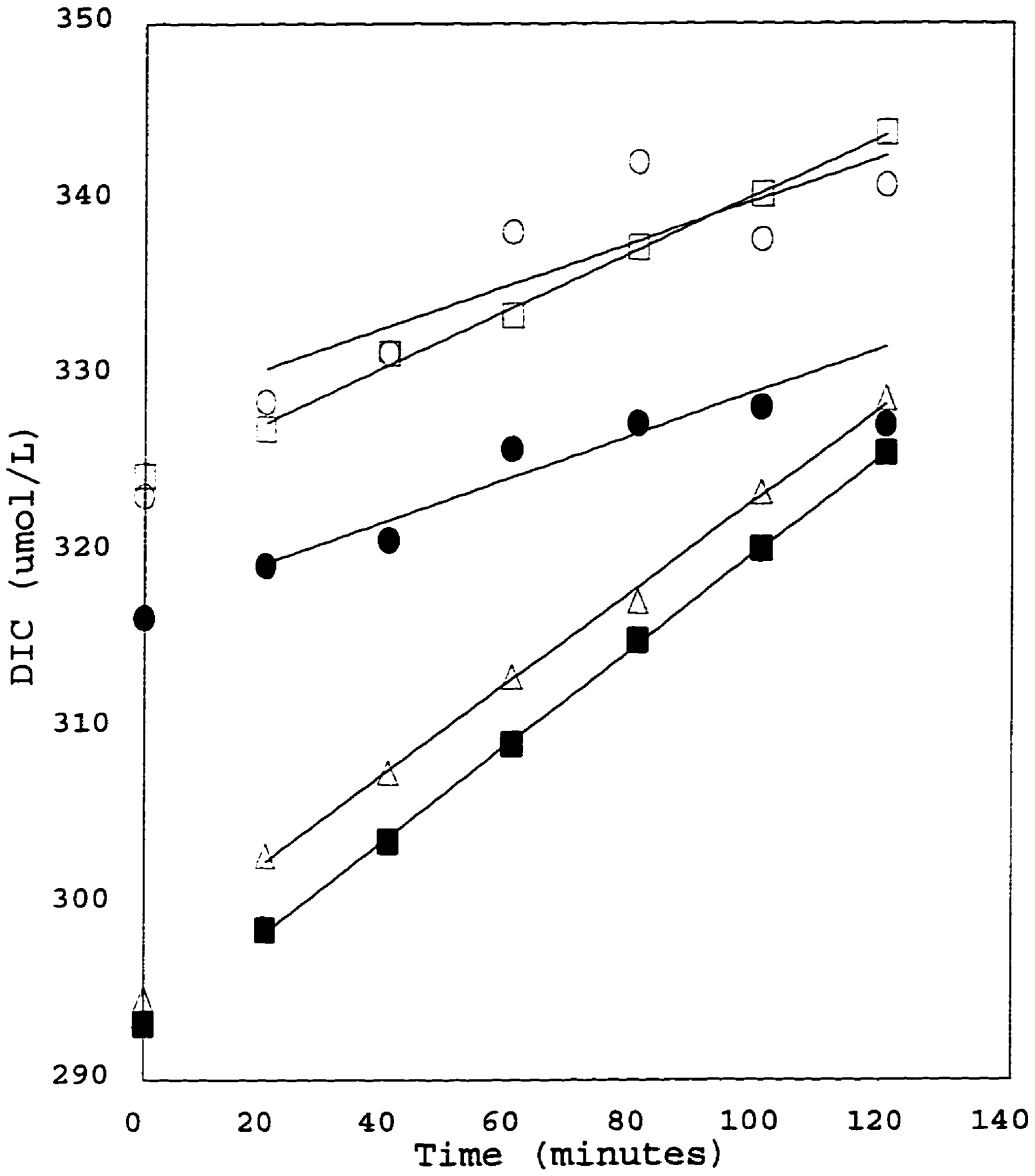

Appendix 6(k): Summary of incubation for chemostat 3P(ii). Light bottle = LB; Dark bottle = DB: LB1(□), LB2(○), LB3(△), DB1 (■), and DB2(●).

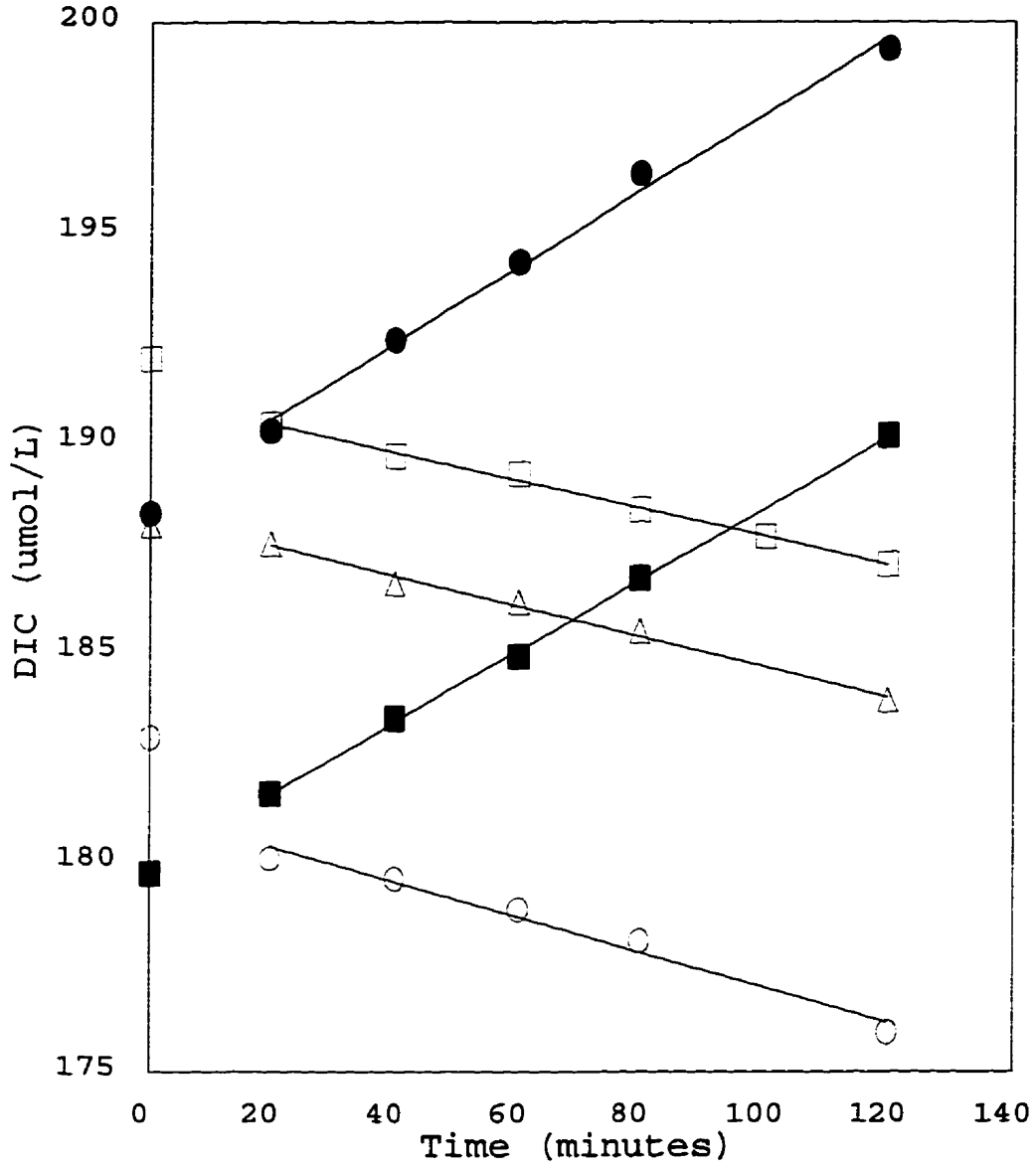

Appendix 6(l): Summary of incubation for chemostat 1N(i). Light bottle = LB; Dark bottle = DB: LB1(□), LB2(○), LB3(△), DB1 (■), and DB2(●).

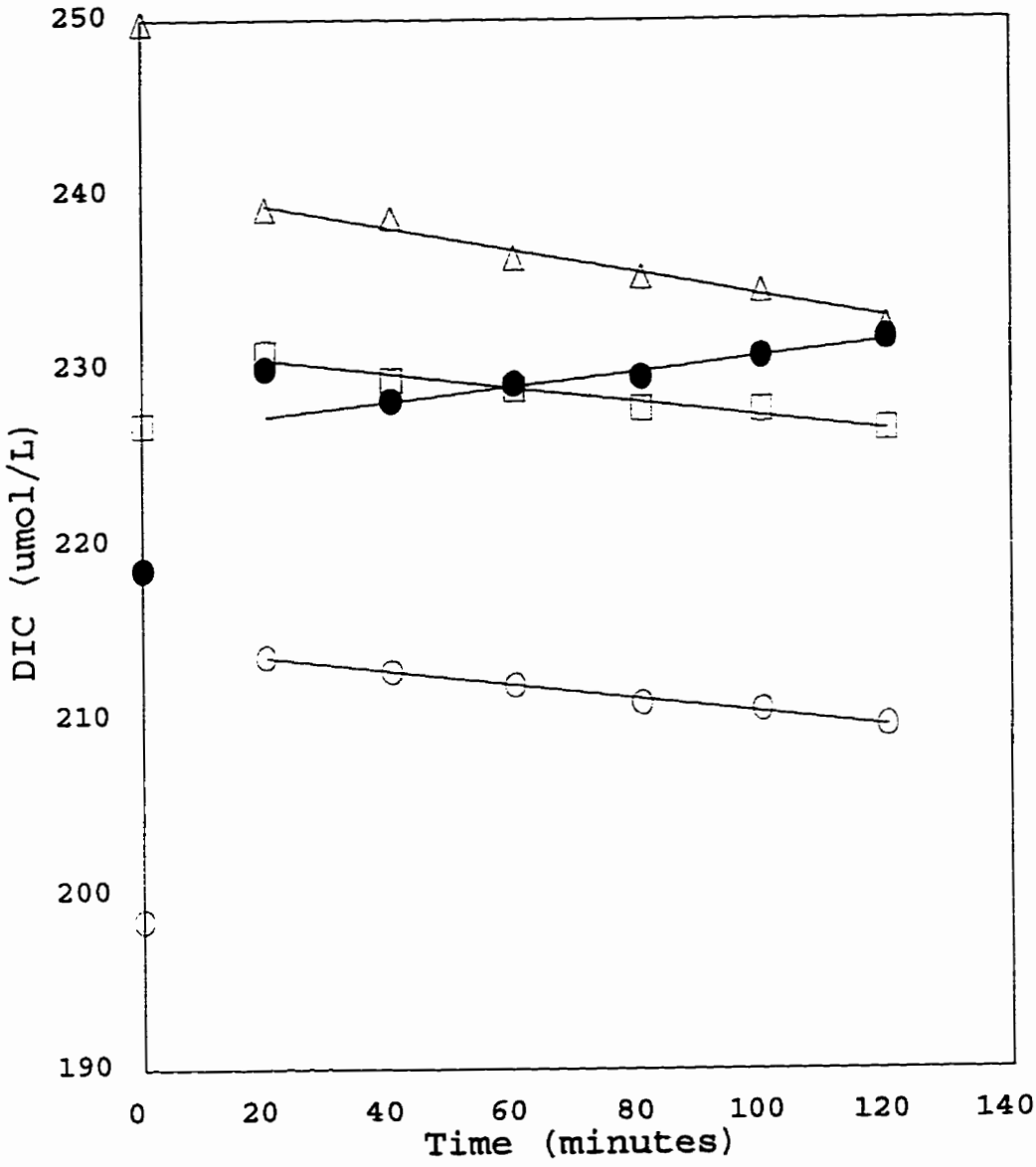

Appendix 6(m): Summary of incubation for chemostat 1N(ii). Light bottle = LB; Dark bottle = DB: LB1(□), LB2(○), LB3(△), and DB2(●).

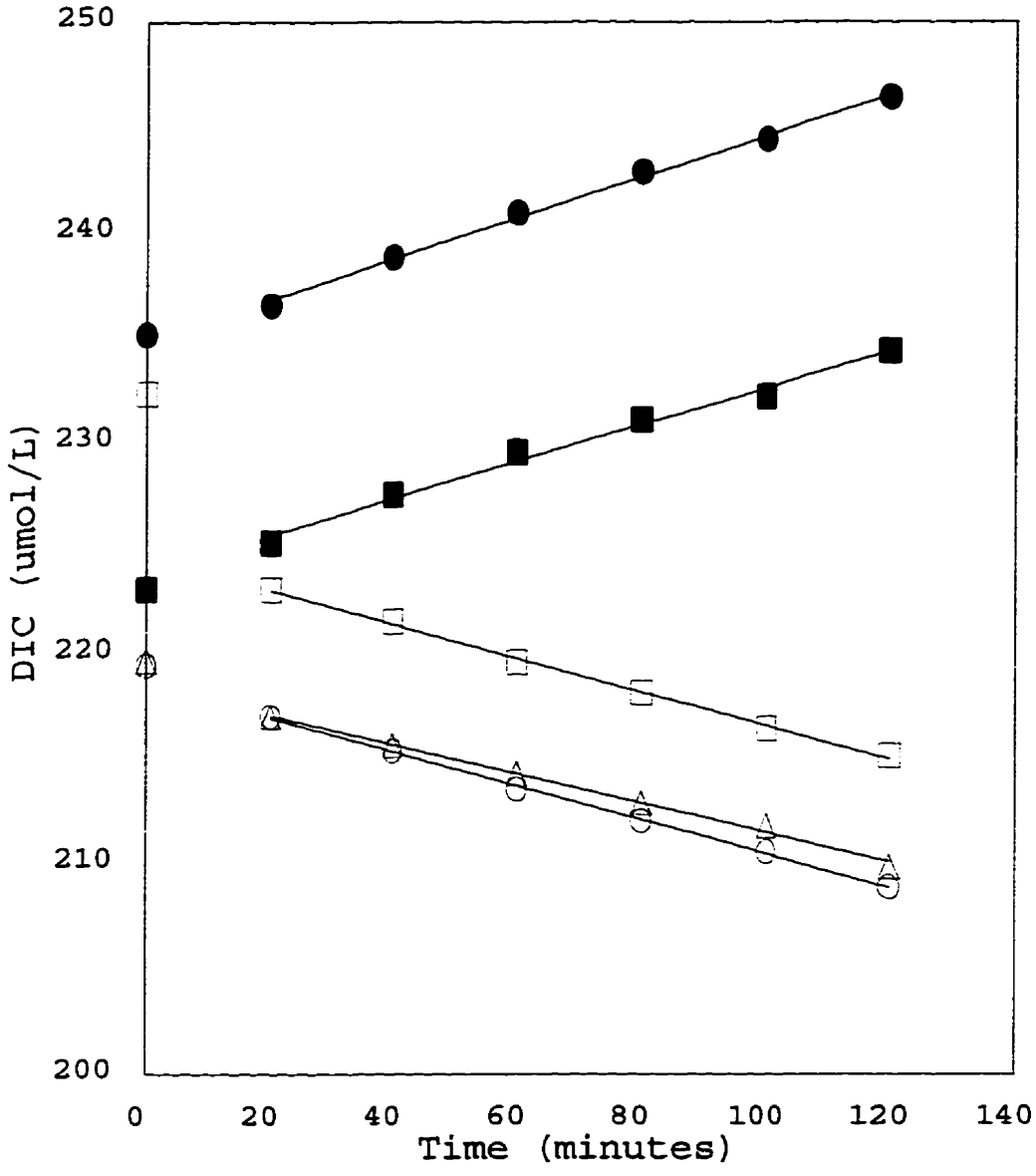

Appendix 6(n): Summary of incubation for chemostat 2N(i). Light bottle = LB; Dark bottle = DB: LB1(□), LB2(○), LB3(△), DB1 (■), and DB2(●).

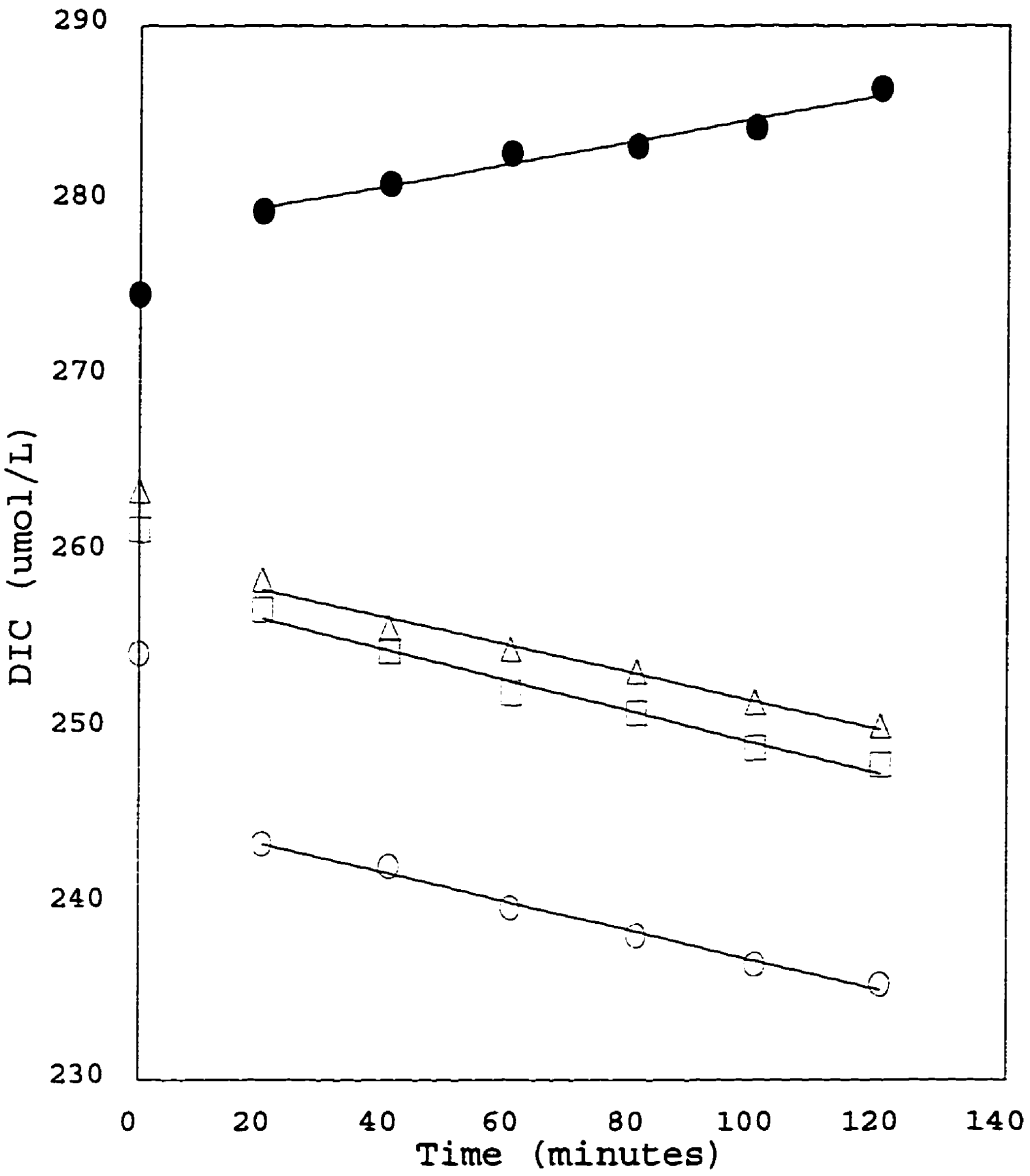

Appendix 6(o): Summary of incubation for chemostat 2N(ii). Light bottle = LB; Dark bottle = DB: LB1(□), LB2(○), LB3(△), and DB2(●).

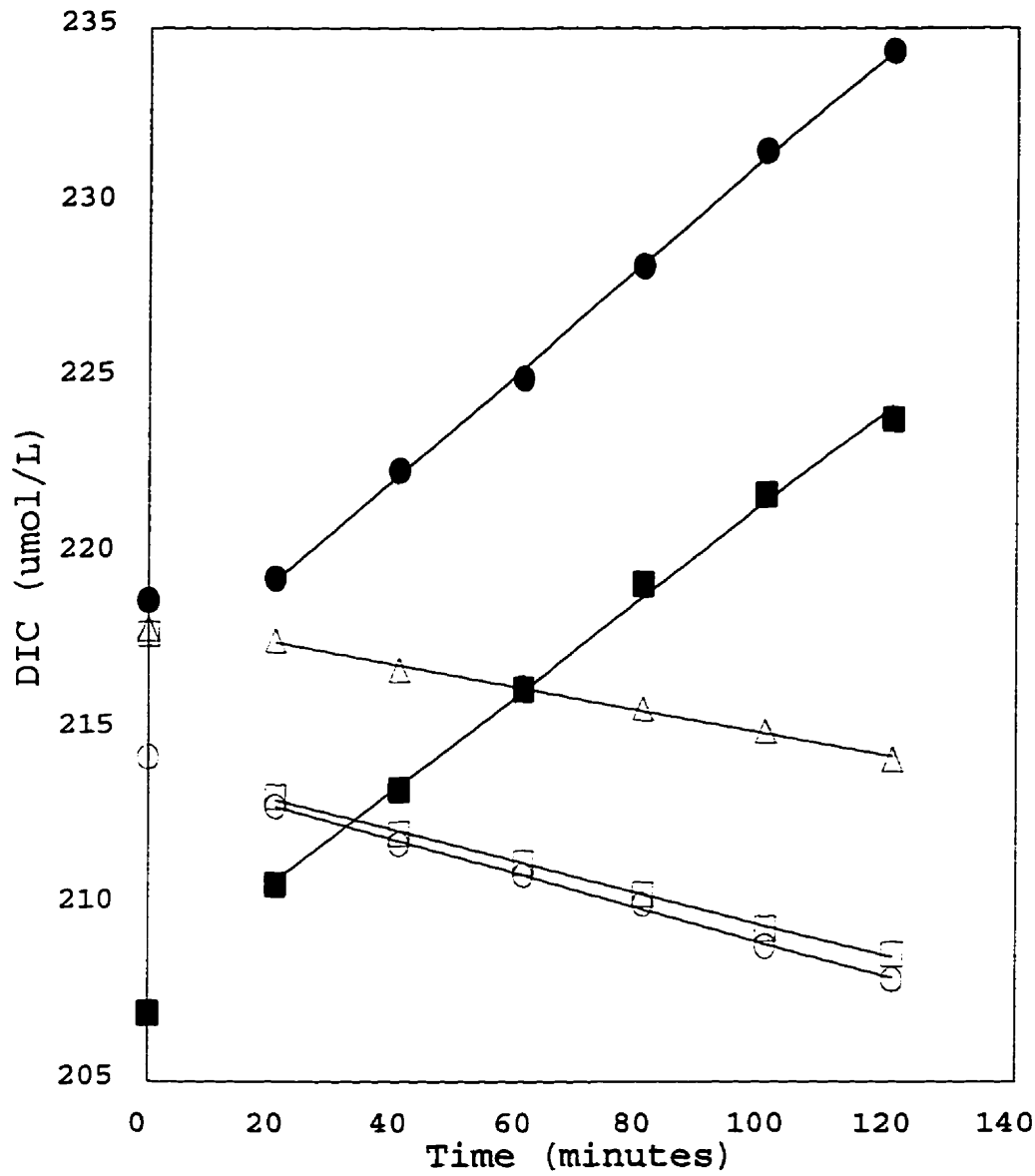

Appendix 6(p): Summary of incubation for chemostat 3N(i). Light bottle = LB; Dark bottle = DB: LB1(□), LB2(○), LB3(△), DB1 (■), and DB2(●).

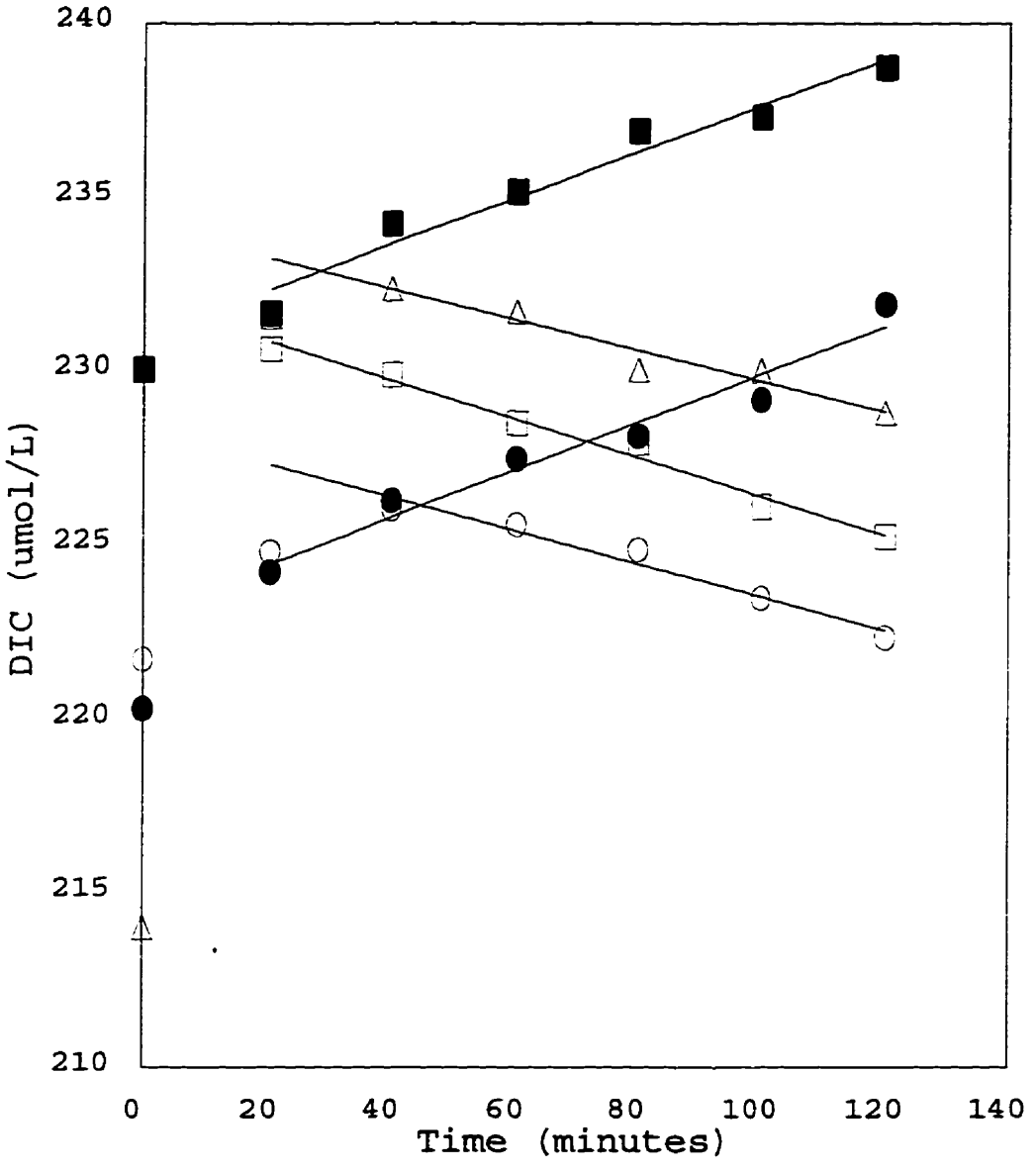

Appendix 6(q): Summary of incubation for chemostat 3N(ii). Light bottle = LB; Dark bottle = DB: LB1(□), LB2(○), LB3(△), DB1 (■), and DB2(●).

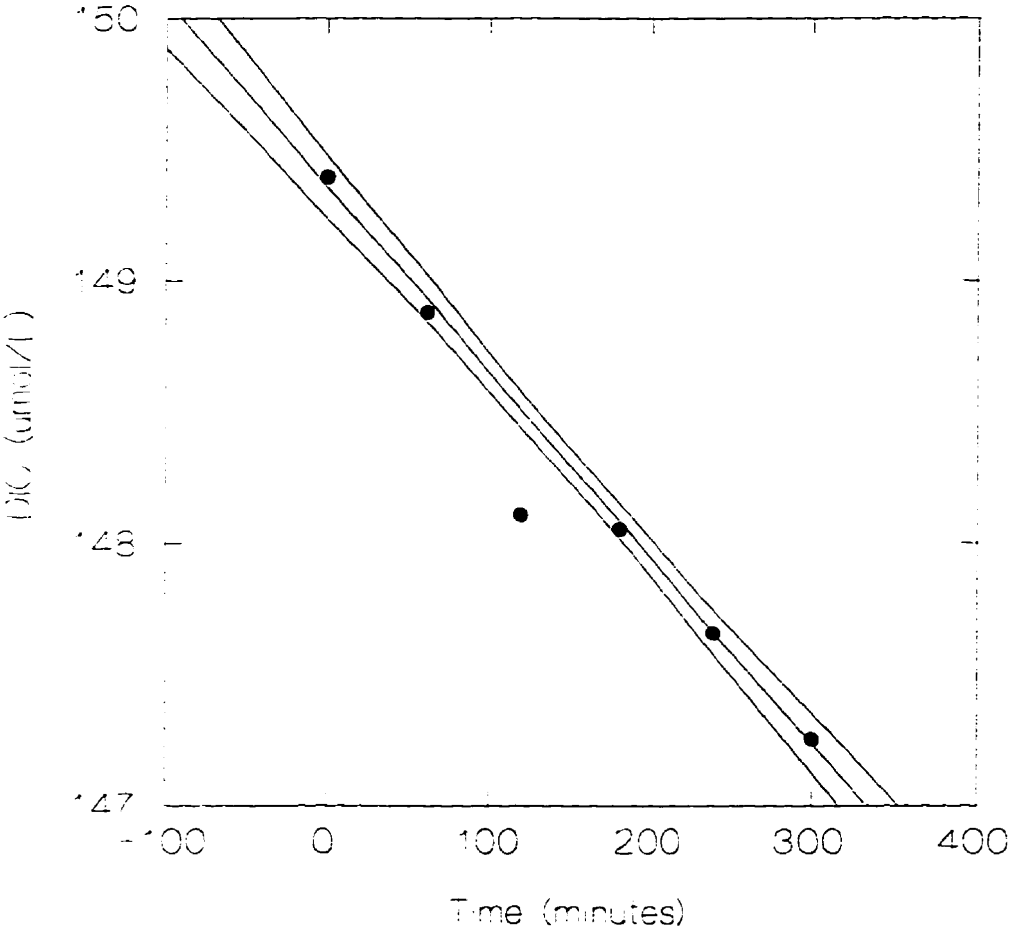

Appendix 7(a): Regression analysis with 95% confidence interval for the bottle exposed to 598 μmol/m^2/s. Lake 240 September 6, 1995. Point at time = 120 excluded from regression analysis.

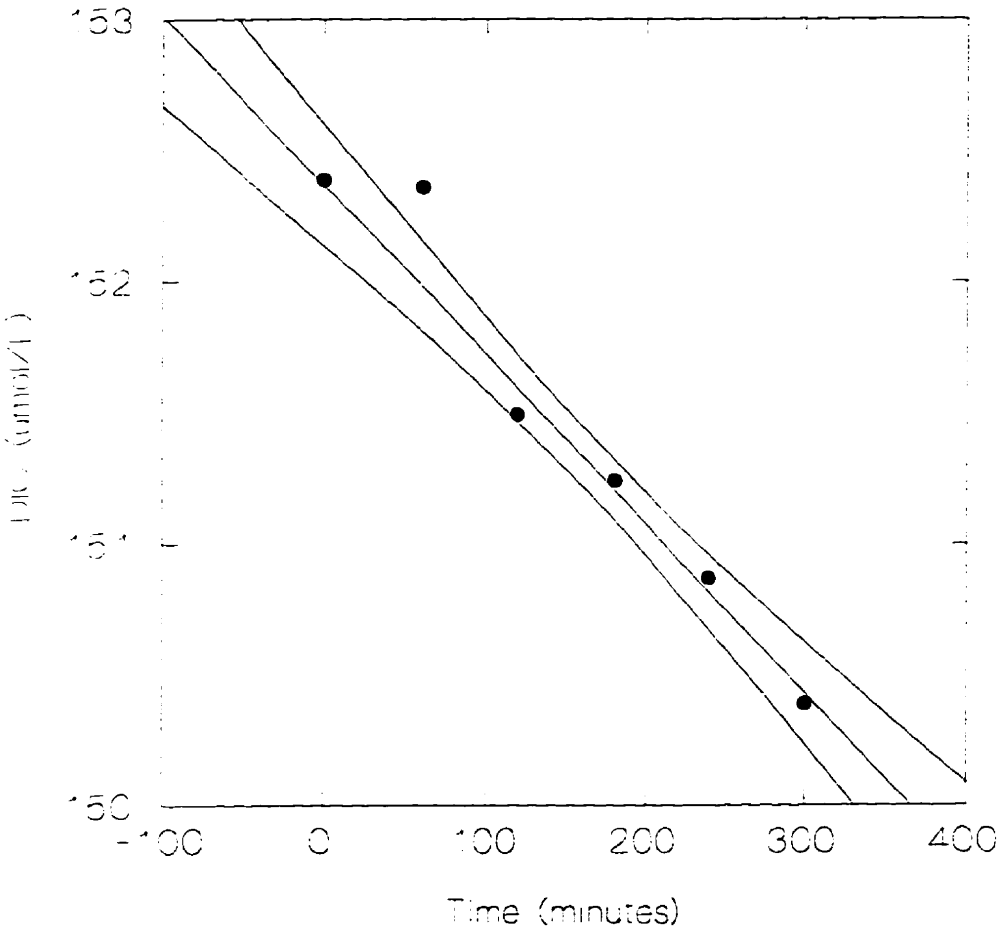

Appendix 7(b): Regression analysis with 95% confidence interval for the bottle exposed to 332 μmol/m^2/s. Lake 240 September 6, 1995. Point at time = 60 excluded from regression analysis.

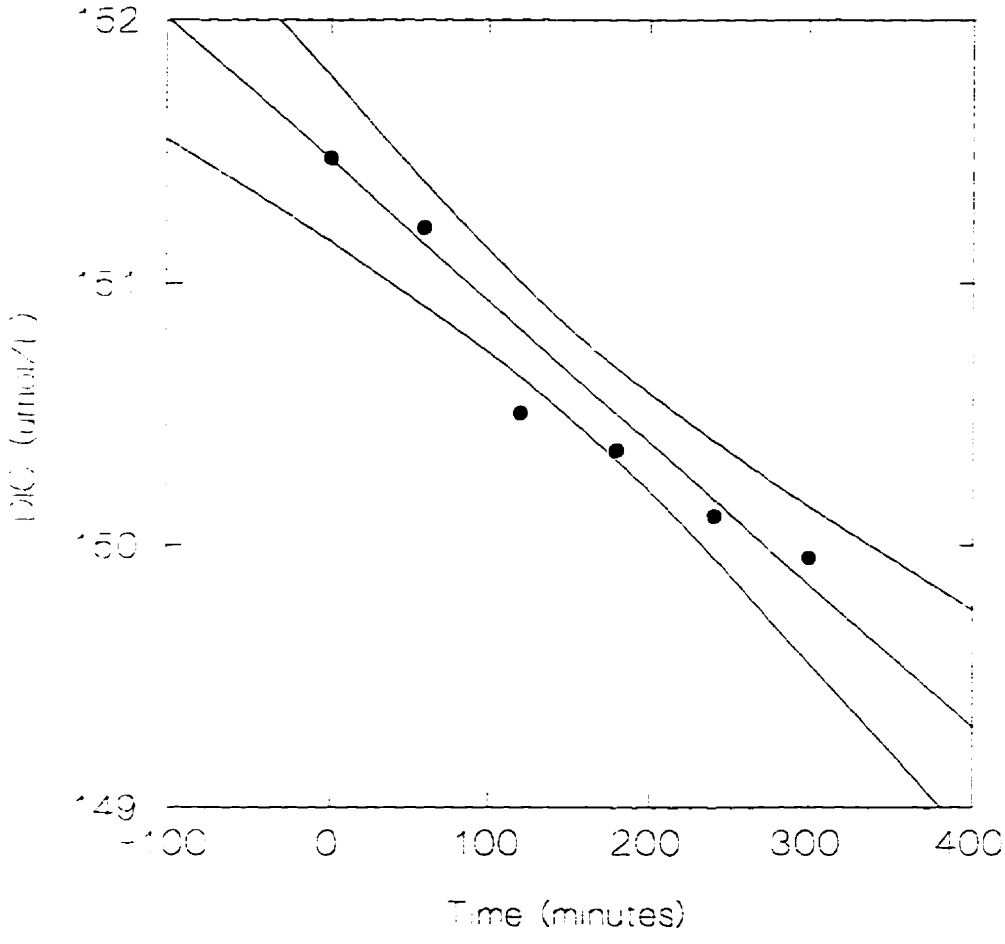

Appendix 7(c): Regression analysis with 95% confidence interval for the bottle exposed to 174 μmol/m²/s. Lake 240 September 6, 1995. Point at time = 120 excluded from regression analysis.

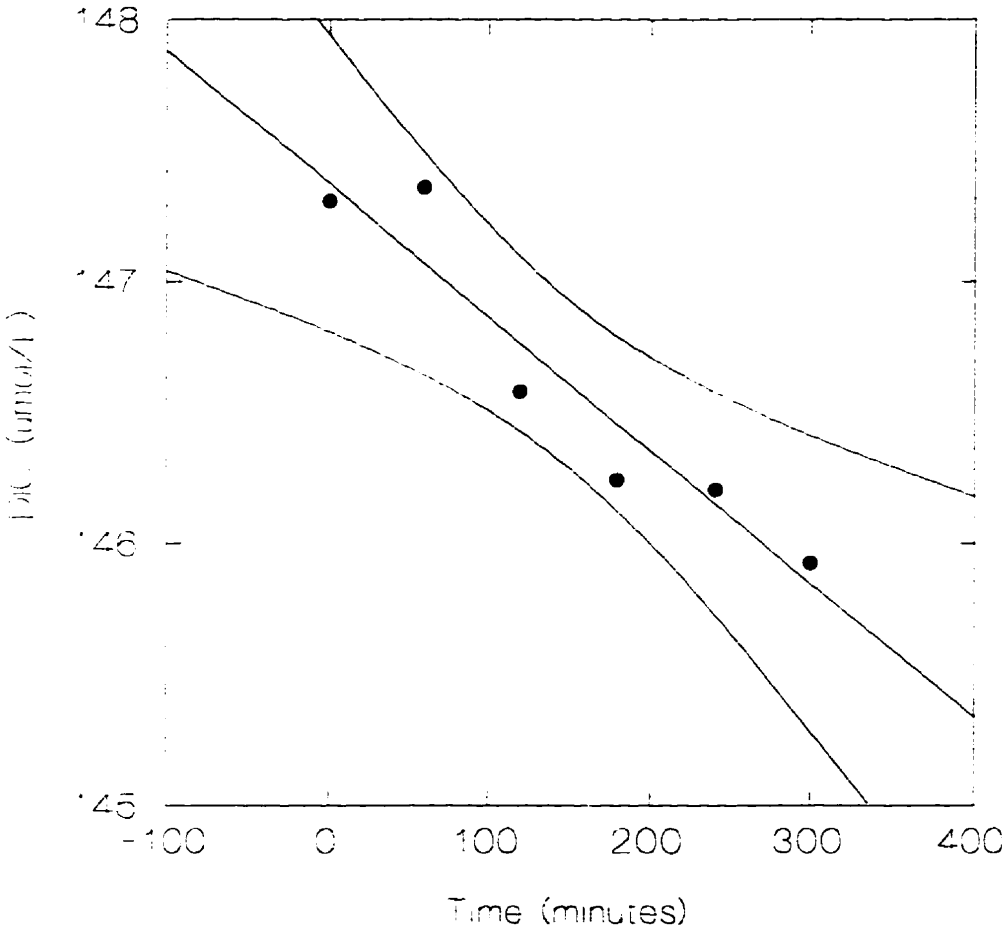

Appendix 7(d): Regression analysis with 95% confidence interval for the bottle exposed to 106 μmol/m^2/s. Lake 240 September 6, 1995. All points included in regression analysis.

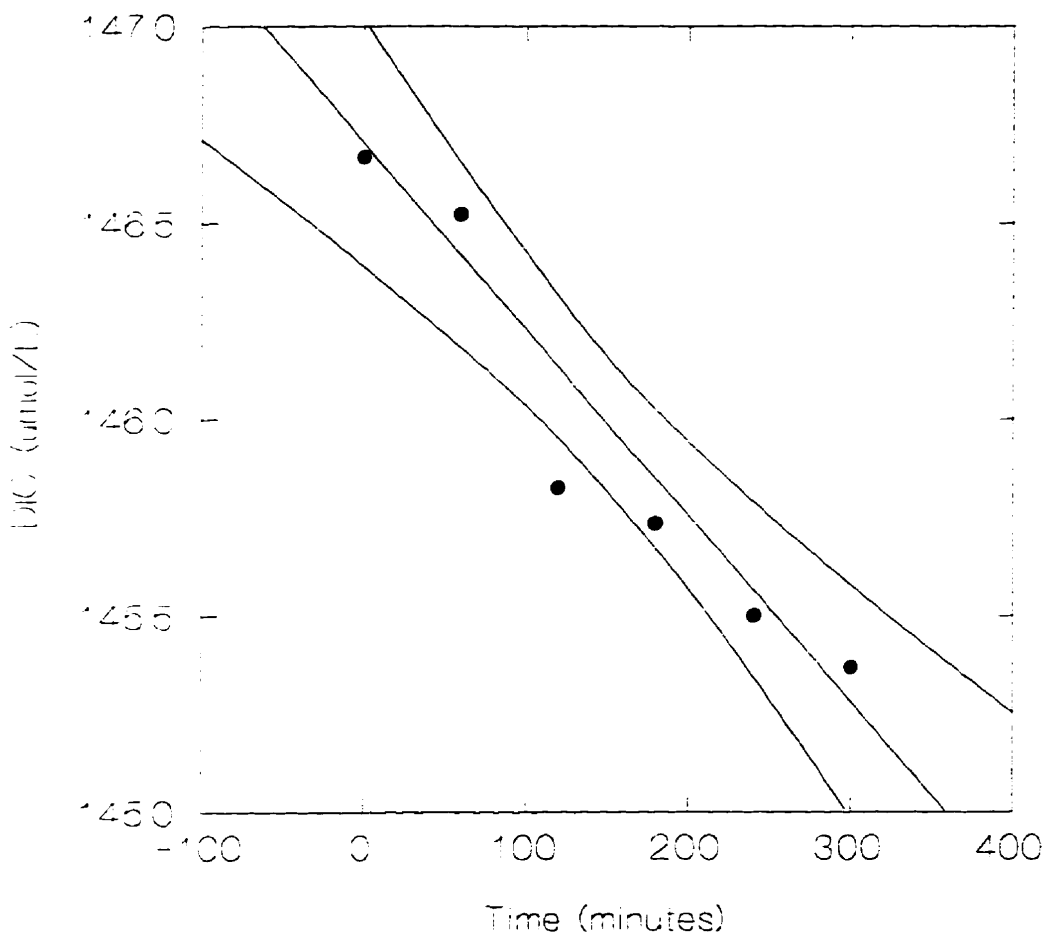

Appendix 7(e): Regression analysis with 95% confidence interval for the bottle exposed to 71 μmol/m^2/s. Lake 240 September 6, 1995. Point at time = 120 excluded from regression analysis.

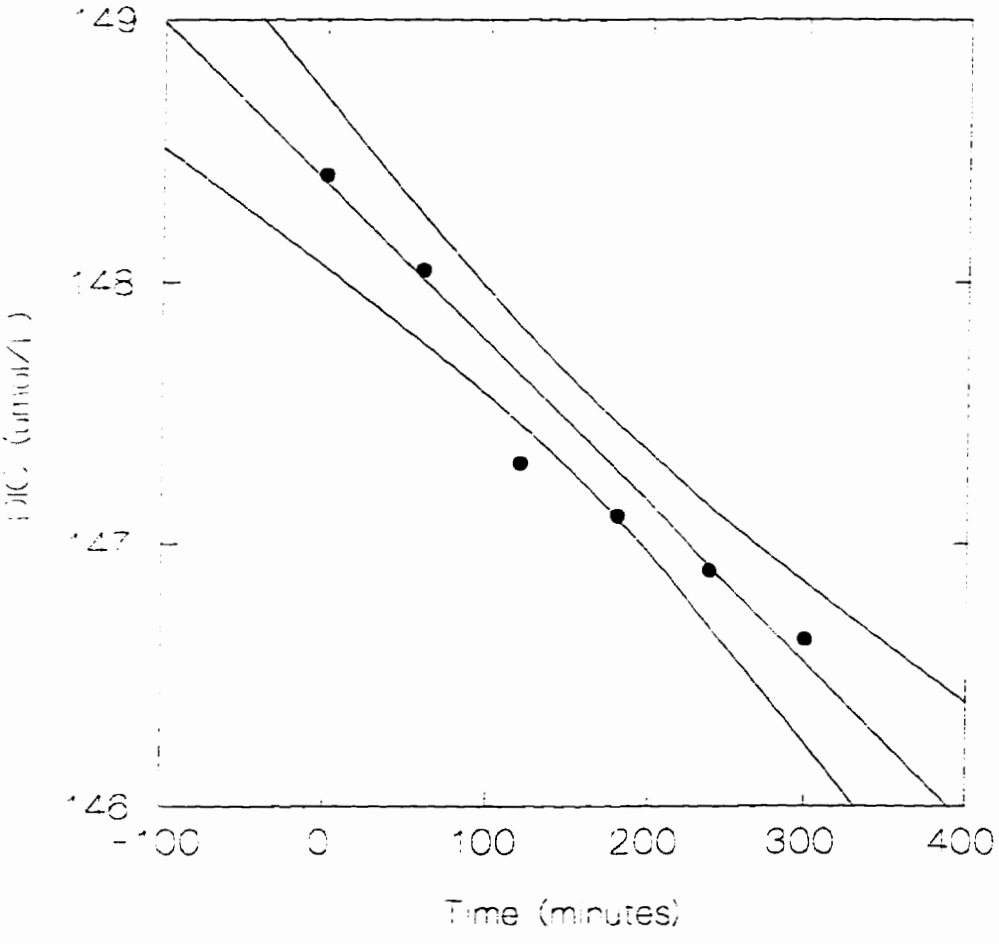

Appendix 7(f): Regression analysis with 95% confidence interval for the bottle exposed to 47 μmol/m^2/s. Lake 240 September 6, 1995. Point at time = 120 excluded from regression analysis.

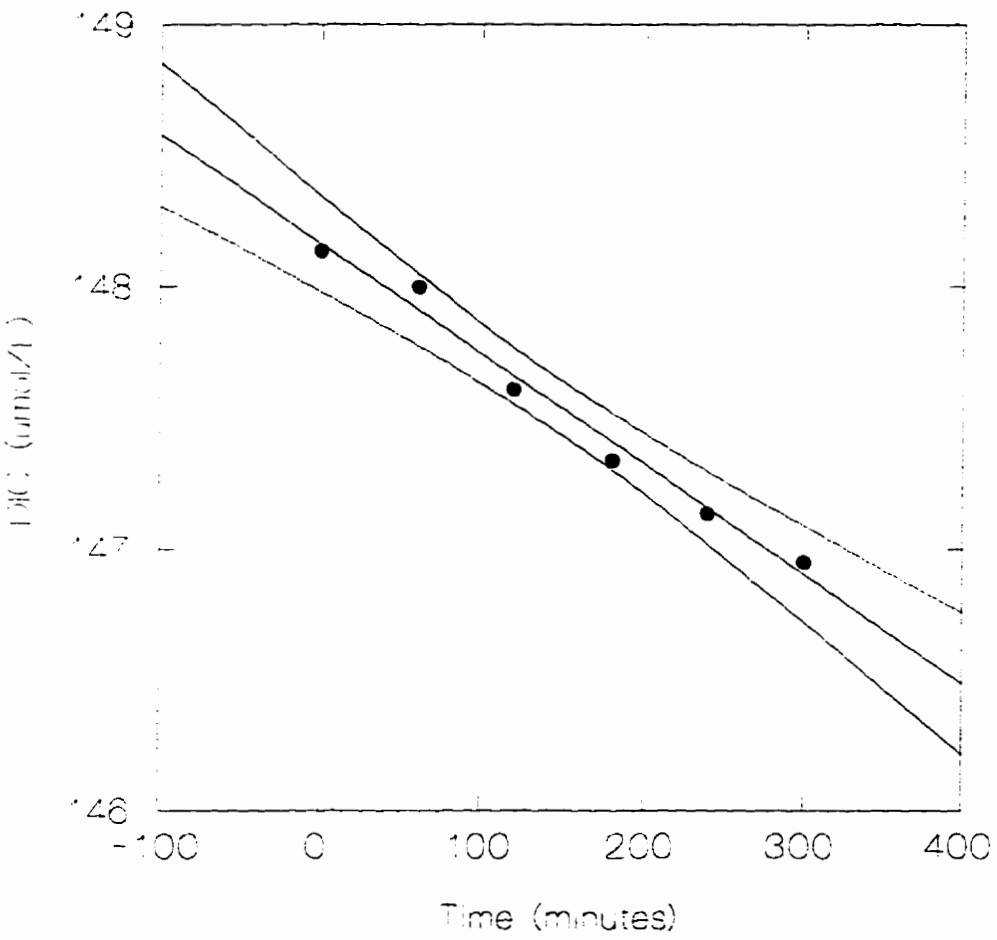

Appendix 7(g): Regression analysis with 95% confidence interval for the bottle exposed to 33 $\mu mol/m^2/s$. Lake 240 September 6, 1995. All points included in regression analysis.

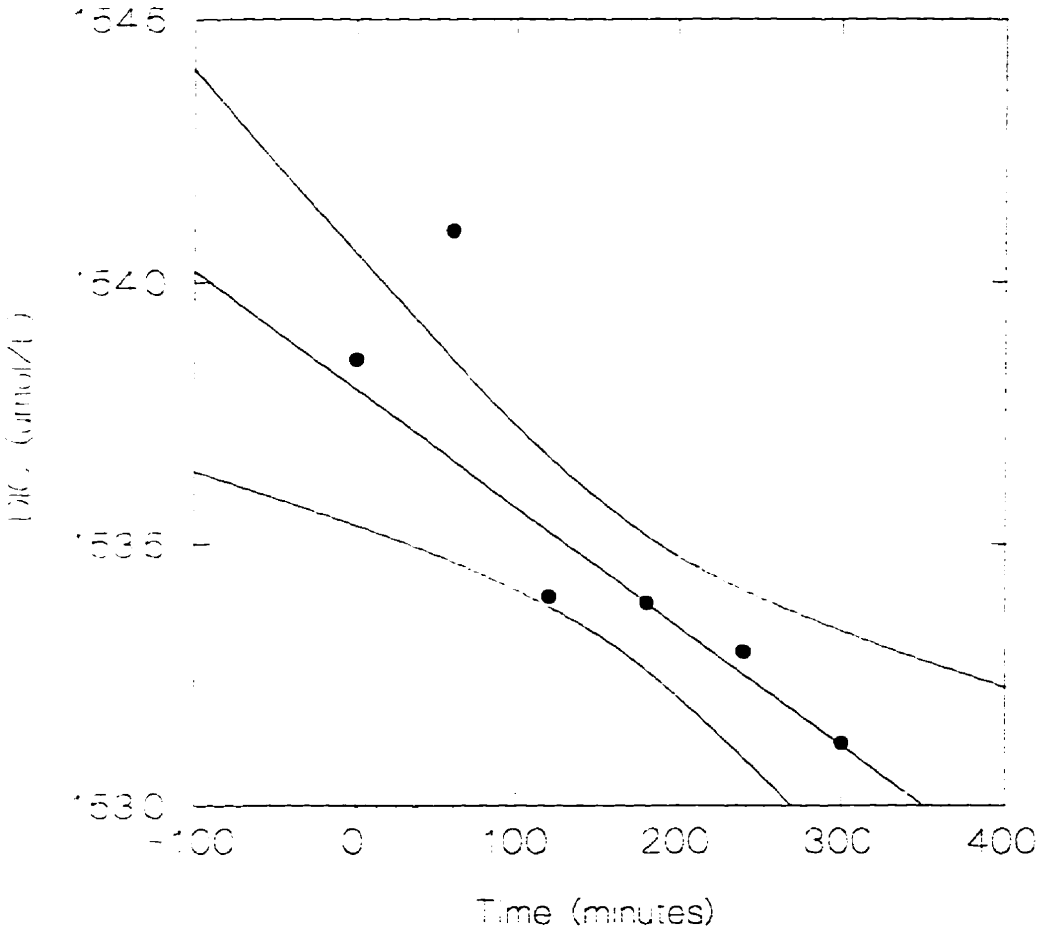

Appendix 7(h): Regression analysis with 95% confidence interval for the bottle exposed to 23 μmol/m^2/s. Lake 240 September 6, 1995. Point at time = 60 excluded from regression analysis.

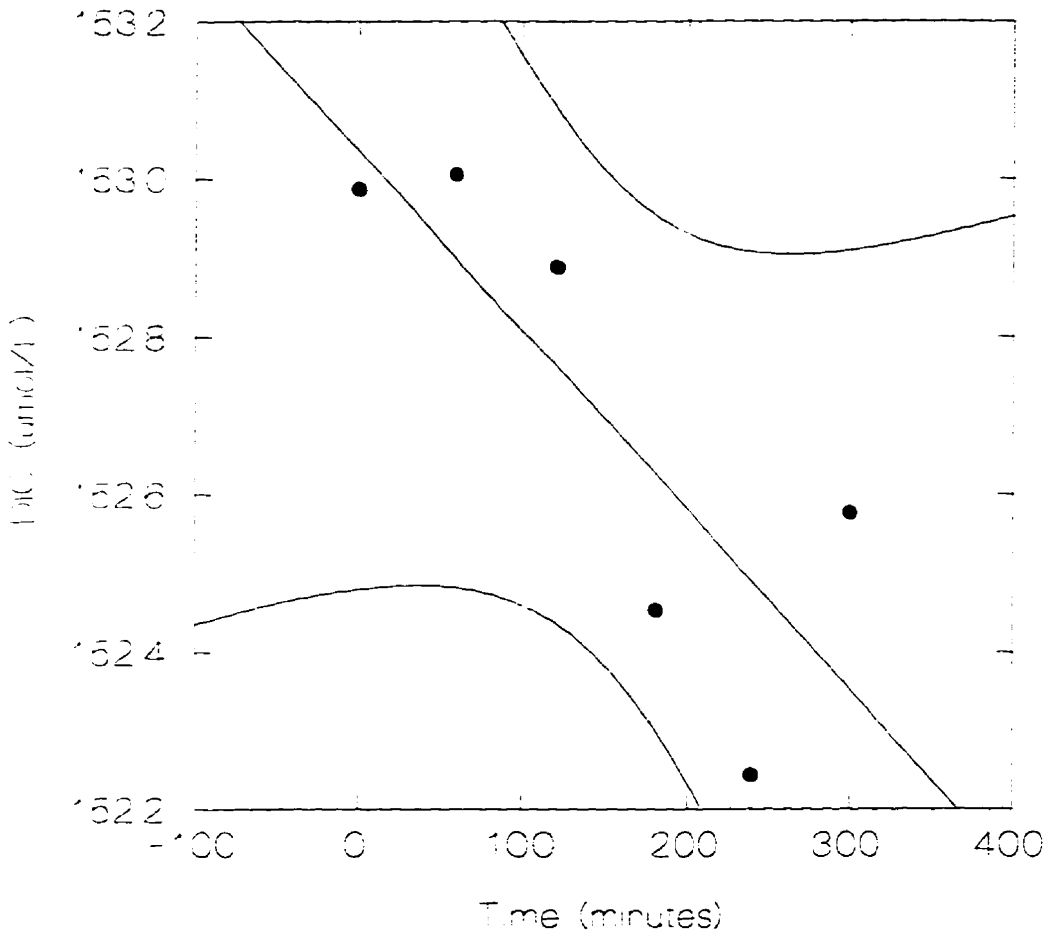

Appendix 7(i): Regression analysis with 95% confidence interval for the bottle exposed to 17 μmol/m^2/s. Lake 240 September 6, 1995. All points included in regression analysis.

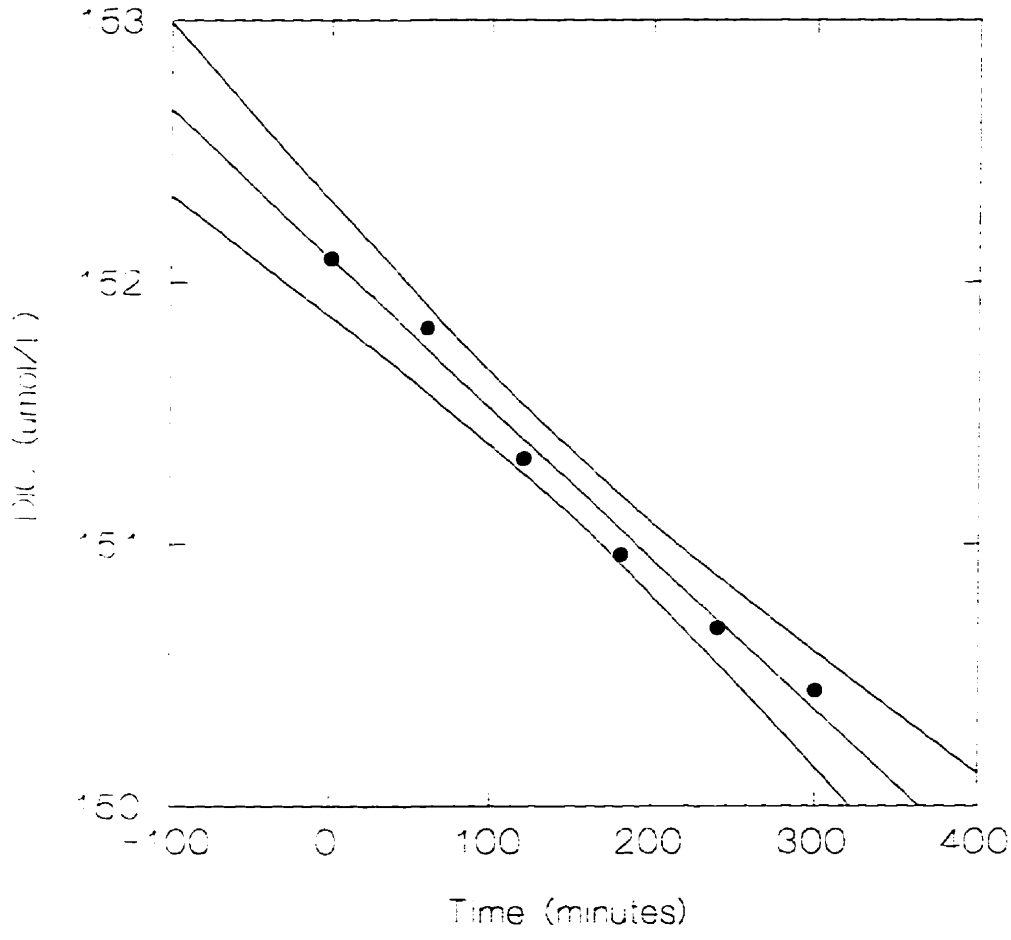

Appendix 7(j): Regression analysis with 95% confidence interval for the dark bottle. Lake 240 September 6, 1995. All points included in regression analysis.

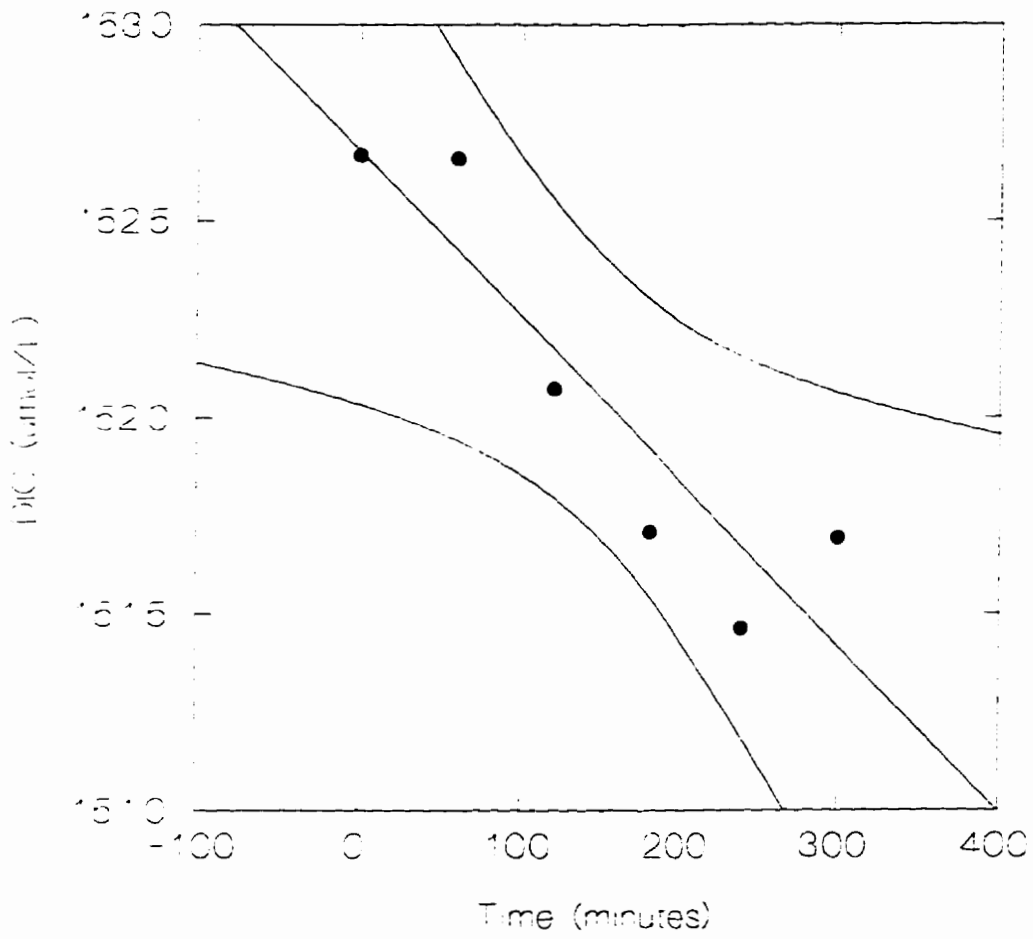

Appendix 7(k): Regression analysis with 95% confidence interval for the dark bottle. Lake 240 September 6, 1995. All points included in regression analysis.

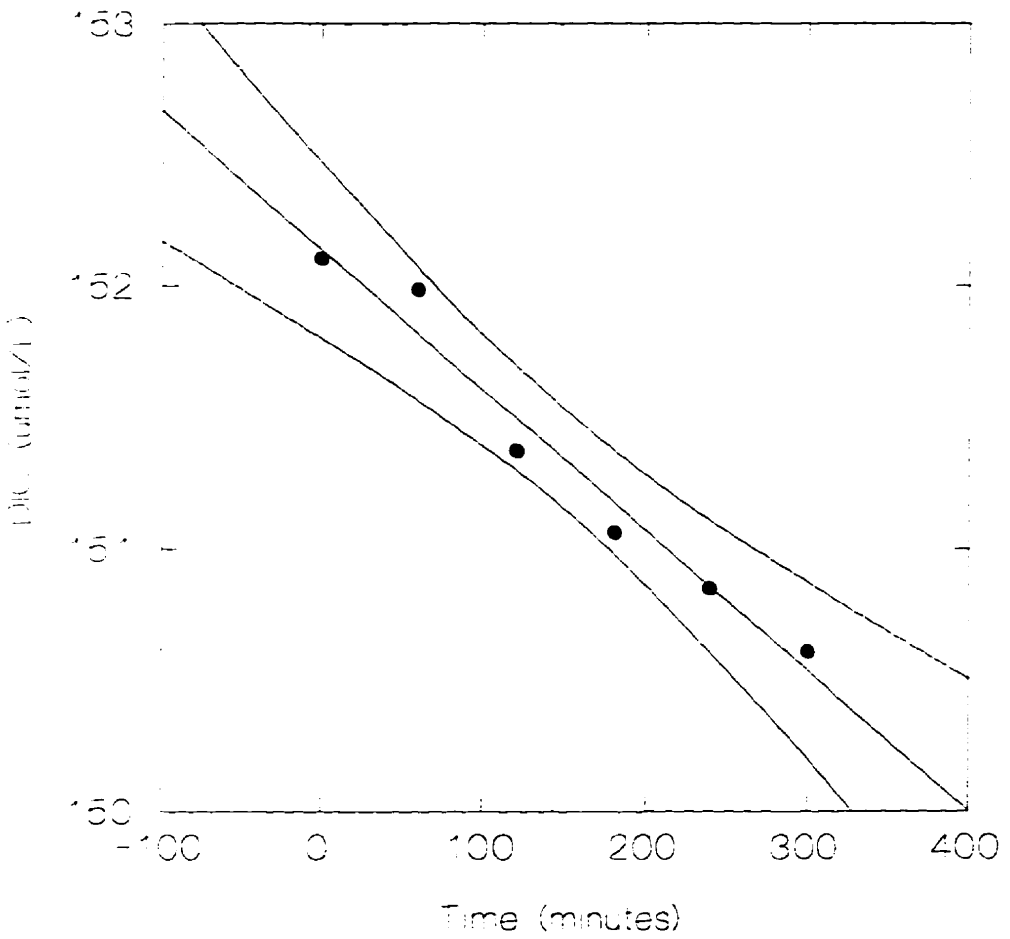

Appendix 7(1): Regression analysis with 95% confidence interval for the dark bottle. Lake 240 September 6, 1995. All points included in regression analysis.

Appendix 8(a): Linear regression r-squared and significance values (P) for L227, August 23, 1995 field incubation. Chlorophyll a concentration = 63.2μg/L. Dark respiration (mgC/m³/h.): -8.8, -5.5, and -7.5.

Light (μmol/m²/s)	R-Squared	P	Photosynthetic Rate (mgC/m/h.)
598	0.990	<0.001	74.7
399	0.984	<0.001	101.4
233	0.991	<0.001	88.0
141	0.978	<0.001	80.8
90	0.976	<0.001	59.7
58	0.810	0.014	9.1
42	0.950	0.001	20.6
28	0.924	0.002	12.0
22	0.933	<0.001	6.1
Dark	0.978	<0.001	-8.8
Dark	0.853	0.008	-5.5
Dark	0.920	0.002	-7.5

Appendix 8(b): Linear regression r-squared and significance values (P) for L240, August 25, 1995 field incubation. Chlorophyll a concentration = 2.31μg/L. Dark respiration ($mgC/m^3/h.$): -2.1, 1.8, and 1.5.

Light ($\mu mol/m^2/s$)	R-Squared	P	Photosynthetic Rate (mgC/m/h.)
498	0.871	0.020	1.7
299	0.831	0.031	3.7
183	0.269	0.481	0.2
116	0.898	0.052	1.6
76	0.691	0.196	1.2
53	0.329	0.234	2.3
36	0.512	0.110	-1.4
26	0.915	0.011	-3.1
22	0.930	0.008	-4.4
Dark	0.540	0.096	-2.1
Dark	0.795	0.042	-1.8
Dark	0.799	0.016	-1.5

Appendix 8(c): Linear regression r-squared and significance values (P) for L240, September 6, 1995 field incubation. Chlorophyll a concentration = 1.77μg/L. Dark respiration (mgC/m³/h.): 4.1, 3.0, and 3.8.

Light (μmol/m²/s)	R-Squared	P	Photosynthetic Rate (mgC/m/h.)
598	0.998	<0.001	5.1
332	0.993	<0.001	4.7
174	0.980	0.001	3.8
106	0.903	0.004	3.7
71	0.974	0.002	3.4
47	0.983	0.001	4.4
33	0.984	<0.001	3.0
23	0.931	0.008	1.6
17	0.657	0.050	1.6
Dark	0.987	<0.001	4.1
Dark	0.830	0.012	3.0
Dark	0.966	<0.001	3.8

Appendix 8(d): Linear regression r-squared and significance values (P) for L302s, August 19, 1995 field incubation. Chlorophyll a concentration = 2.55μg/L. Dark respiration (mgC/m³/h.): -0.4, -1.4, and -2.4.

Light (μmol/m²/s)	R-Squared	P	Photosynthetic Rate (mgC/m/h.)
747	0.994	<0.001	11.2
482	0.999	<0.001	6.9
332	0.959	0.001	5.8
257	0.982	<0.001	4.0
191	0.972	<0.001	2.7
147	0.791	0.018	2.6
97	0.921	0.002	2.3
70	0.056	0.668	0.2
48	0.926	0.009	-3.0
Dark	0.716	0.071	-0.4
Dark	0.897	0.004	-1.4
Dark	0.972	0.002	-2.4

Appendix 8(e): Linear regression r-squared and significance values (P) for L302s, August 24, 1995 field incubation. Chlorophyll a concentration = 4.42μg/L. Dark respiration (mgC/m³/h.): 1.6 5.5, and 7.3.

Light (μmol/m²/s)	R-Squared	P	Photosynthetic Rate (mgC/m/h.)
581	0.983	<0.001	21.9
349	0.994	<0.001	19.3
208	0.984	<0.001	15.5
125	0.978	<0.001	13.4
78	0.981	<0.001	12.6
55	0.973	<0.001	10.1
37	0.935	0.002	9.4
28	0.888	0.016	2.5
22	0.732	0.065	6.7
Dark	0.471	0.132	1.6
Dark	0.924	0.002	5.5
Dark	0.973	<0.001	7.3

Appendix 8(f): Linear regression r-squared and significance values (P) for L302s, September 2, 1995 field incubation. Chlorophyll a concentration = 3.01μg/L. Dark respiration (mgC/m³/h.): -1.5, -3.7, and 0.1.

Light (μmol/m²/s)	R-Squared	P	Photosynthetic Rate (mgC/m/h.)
615	0.959	<0.001	4.6
365	0.995	<0.001	7.8
199	0.978	<0.001	3.8
118	0.998	<0.001	2.8
70	0.922	0.009	-1.6
51	0.900	0.004	-2.5
33	0.997	<0.001	-4.0
21	0.682	0.043	-1.2
17	0.945	0.001	-3.9
Dark	0.766	0.022	-1.5
Dark	0.961	0.001	-3.7
Dark	0.004	0.908	0.1

Appendix 8(g): Linear regression r-squared and significance values (P) for L302s, September 7, 1995 field incubation. Chlorophyll a concentration = 7.27μg/L. Dark respiration (mgC/m³/h.): 0.6, 1.2, and 0.7.

Light (μmol/m²/s)	R-Squared	P	Photosynthetic Rate (mgC/m/h.)
581	0.973	<0.001	16.0
316	0.985	<0.001	18.4
191	0.979	<0.001	11.7
116	0.947	0.005	6.8
73	0.978	0.001	5.8
48	0.938	0.007	4.1
34	0.954	0.004	3.5
24	0.746	0.059	2.5
17	0.442	0.221	1.5
Dark	0.155	0.440	0.6
Dark	0.400	0.252	1.2
Dark	0.153	0.515	0.7

Appendix 8(h): Linear regression r-squared and significance values (P) for L303, August 31, 1995 field incubation. Chlorophyll a concentration = 5.61μg/L. Dark respiration (mgC/m³/h.): 4.1, 5.8, and 4.1.

Light (μmol/m²/s)	R-Squared	P	Photosynthetic Rate (mgC/m/h.)
664	0.981	<0.001	23.1
365	0.976	<0.001	22.0
191	0.947	0.001	17.7
128	0.917	0.003	13.9
87	0.893	0.004	11.8
55	0.854	0.008	11.0
38	0.869	0.007	8.7
28	0.785	0.019	8.6
22	0.854	0.025	7.4
Dark	0.796	0.042	7.2
Dark	0.668	0.047	5.8
Dark	0.490	0.121	4.1

Appendix 8(i): Linear regression r-squared and significance values (P) for L303, August 31(pressurized), 1995 field incubation. Chlorophyll a concentration = 5.61μg/L. Dark respiration (mgC/m³/h.): 4.2, 7.5, and 3.8.

Light (μmol/m²/s)	R-Squared	P	Photosynthetic Rate (mgC/m/h.)
664	0.996	<0.001	12.4
365	0.980	<0.001	13.2
191	0.875	0.006	10.9
128	0.985	<0.001	8.4
81	0.951	0.001	6.0
55	0.934	0.002	4.6
38	0.742	0.028	5.9
28	0.905	0.004	6.6
22	0.922	0.002	5.5
Dark	0.822	0.013	4.2
Dark	0.950	0.001	7.5
Dark	0.795	0.017	3.8

Appendix 8(j): Linear regression r-squared and significance values (P) for L303, September 7, 1995 field incubation. Chlorophyll a concentration = 6.46μg/L. Dark respiration (mgC/m³/h.): 1.3, -0.1, and 0.3.

Light (μmol/m²/s)	R-Squared	P	Photosynthetic Rate (mgC/m/h.)
631	0.987	<0.001	14.4
332	0.992	<0.001	14.7
186	0.993	<0.001	10.9
116	0.969	<0.001	7.5
71	0.970	0.002	4.6
45	0.967	0.003	3.6
34	0.864	0.022	1.4
25	0.480	0.195	0.8
18	0.663	0.094	0.7
Dark	0.568	0.083	1.3
Dark	0.015	0.846	-0.1
Dark	0.152	0.512	0.3

Appendix 8(k): Linear regression r-squared and significance values (P) for L303, September 11, 1995 field incubation. Chlorophyll a concentration = 5.36 g/L. Dark respiration ($mgC/m^3/h.$): 2.5, 1.7, and 0.2.

Light ($\mu mol/m^2/s$)	R-Squared	P	Photosynthetic Rate (mgC/m/h.)
532	0.976	<0.001	16.2
291	0.992	<0.001	12.7
166	0.977	<0.001	8.3
95	0.966	<0.001	6.3
63	0.954	0.001	5.6
40	0.940	0.001	4.5
30	0.938	0.001	3.7
22	0.899	0.004	3.4
17	0.827	0.012	3.1
Dark	0.820	0.013	1.6
Dark	0.837	0.011	2.5
Dark	0.845	0.010	1.7

Appendix 8(l): Linear regression r-squared and significance values (P) for L373, August 2, 1995 field incubation. Chlorophyll a concentration = 0.73μg/L. Dark respiration (mgC/m³/h.): -5.0, -4.4, and -3.8.

Light (μmol/m²/s)	R-Squared	P	Photosynthetic Rate (mgC/m/h.)
635	0.806	0.015	-3.6
359	0.906	0.003	-4.1
238	0.880	0.006	-4.2
174	0.857	0.008	-4.1
113	0.807	0.038	-2.6
86	0.877	0.006	-2.4
66	0.747	0.026	-4.8
47	0.925	0.002	-4.1
35	0.819	0.013	-3.7
Dark	0.891	0.005	-5.0
Dark	0.903	0.004	-4.4
Dark	0.898	0.004	-3.8

Appendix 8(m): Linear regression r-squared and significance values (P) for L979, September 2, 1995 field incubation. Chlorophyll a concentration = 14.0μg/L. Dark respiration (mgC/m³/h.): -0.8, -2.0, and -9.6.

Light (μmol/m²/s)	R-Squared	P	Photosynthetic Rate (mgC/m/h.)
747	0.883	0.015	54.4
365	0.791	0.003	61.4
208	0.886	0.006	27.9
118	0.706	0.008	13.2
68	0.963	0.038	9.2
51	0.530	0.006	-6.8
35	0.385	0.026	8.7
22	0.908	0.002	-3.6
17	0.596	0.013	-5.4
Dark	0.006	0.005	-0.8
Dark	0.047	0.004	-2.0
Dark	0.578	0.004	-9.6